Title	Possible influences of motion and attention to contribution of retinal adaptation effect in color constancy
Author(s)	WAN Lifang
Citation	, .
Date of issue	2018-03
URL	http://hdl.handle.net/10173/1877
Rights	
Text version	ETD
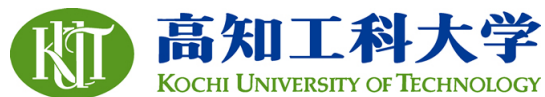
高知工科大学
KOCHI UNIVERSITY OF TECHNOLOGY

Possible influences of motion and attention to contribution of retinal adaptation effect in color constancy

by

WAN Lifang

Student ID Number: 1196019

A dissertation for the degree of Doctor of Engineering
in the Doctoral Program of Engineering Course,
Department of Engineering, Graduate School of Engineering,
Kochi University of Technology,
Kochi, Japan

Dissertation Assessment Committee:
      Supervisor: Keizo Shinomori
      Co-Supervisor: Shuoyu Wang
      Co-Supervisor: Hiroaki Shigemasu
      Mendori Takahiko
      Shinichi Yoshida

March 2018

ABSTRACT

Possible influences of motion and attention to contribution of retinal adaptation effect in color constancy

WAN Lifang
Doctoral Program of Engineering Course, Department of Engineering,
Graduate School of Engineering

Color constancy is the common phenomenon where the perceptual color of a surface does not change significantly by an illuminant changes. The adaptation of the photoreceptors at the retina and early part of neural pathways and cognitive mechanism occurring at a higher level are considered as two main factors contributing to the color constancy. The retinal adaptation effect is that since cones and early neural pathways are adapted by the color illumination, the matching in the color constancy will reflect the reduction of cone and/or neural responses. The illumination estimation effect is that the observer will estimate the color of the illumination and shows the color constancy in considering the reflectance of the colored surface (shown in the standard pattern in this study). It is not clear, however, how the utilization of these color constancy mechanisms depends on target motion and attention. This study aims to investigate about the possible influences of target motion and attention defined by a gaze-state to the color constancy. The color constancy was examined under three conditions in a haploscopic view on a monitor: target-static and target-motion and target-rotation conditions. In the motion conditions, color targets in both patterns moved from top to bottom with the speed of the 3 deg. /sec, or color targets rotated 10 times in one min. For attention modulation, we additionally used two observation conditions; the observers were asked to fixate their eye on the test target as an eye-fix condition or to explore the entire stimulus as an eye-free condition.

Since the color constancy would be analyzed not only in terms of cone excitations but also in terms of color-opponency, the illuminations in this study was set by chromatic shifts on red-green and blue-yellow color-opponent axes. The colors of red and green illuminants were shifted equally by the color difference of 53 ΔE^*_{uv} along (L-M) axis. The colors of blue and yellow illuminants were shifted by 45 ΔE^*_{uv} along [S-(L+M)] axis. The 5 deg.-square standard pattern illuminated by D65 (white) illumination (in simulation) and 5 deg.-square test pattern illuminated by one of color illuminations were presented side by side in the haploscopic view; both patterns consisted of a 1.2 deg.-square central color target having one of 12 colors as a surface property surrounded by background ellipses painted by other 8 colors. Six color-normal observers from 22 to 28 years old were asked to complete the task by making a simultaneous paper match on the color targets between the standard and test patterns under the D65 and color illuminations, respectively.

The results of this asymmetric color matching experiment indicated that the motion of the target could not improve the color constancy; rather the motion averagely decreased the color constancy. In the gaze-state, the free eye movement increased the color constancy. Each result could be explained by different situations of retinal adaptation effect and illumination estimation effect. In the motion and eye-fixation condition, foveal part of the retina was rather adapted to the mean chromaticity of the surround, so the retinal adaptation was stronger in this condition. The motion, however, made less attention to the color of the background; it could cause weaker effect of the illumination estimation. Conversely, in the static (no motion) condition, the attention to the background colors caused the illumination estimation effect stronger and the color constancy was improved. The result of this study is different with that of previous literature measured by achromatic adjustment experiment, in which the color constancy was influenced more by the cone adaptation and less by the illumination estimation. On the contrary, in this study, the result of the asymmetric color matching could be influenced by both illumination estimation and cone adaptation when the illumination estimation effect is stronger than the cone adaptation effect.

Keywords: color constancy, color, motion, attention, adaptation, illumination estimation

ACKNOWLEDGMENTS

Contents

List of Figures

List of Tables

Chapter1

General introduction

What is color constancy? Color constancy is the ability to perceive colors of objects, invariant to the color of the light source. Despite the paintings under greenish or white illuminants, you will find that the color of lemon is always yellow.

Figure 1. 1 The painting of lemon under greenish illuminant (left side), and the painting of lemon under white illuminant (right side), From Lecture of Hulbert(The color of Paintings in a Contemporary Light)

To investigate about color constancy, I will discuss about the human vision, different visual mechanisms and factors contribute to color constancy, four main research methods to measure the color constancy, computational models for color constancy, and my research motivations.

1.1 Human vision

1.1.1 The eyes and retina

Eyes are the windows of the heart, and eyes are important for vision, human use their eyes to collect light and feel the world. The light falls through the eyes, hit onto the retina and transfer to the brain, the retina consists of a set of important photoreceptors as rods and cones, as shown in Figure1.2. The cones are important for bright light conditions named photopic vision, there are three type of cones like L, M, S cone, response to different spectrum bands of visible light showed in figure1.3(b), and the rods are important for dark conditions named scotopic vision. The sensitivities of rods and cones are shown in Figure1.3(a). There are approximately 126 million photoreceptors inside the retina, most of the 6 million cones are located inside fovea.
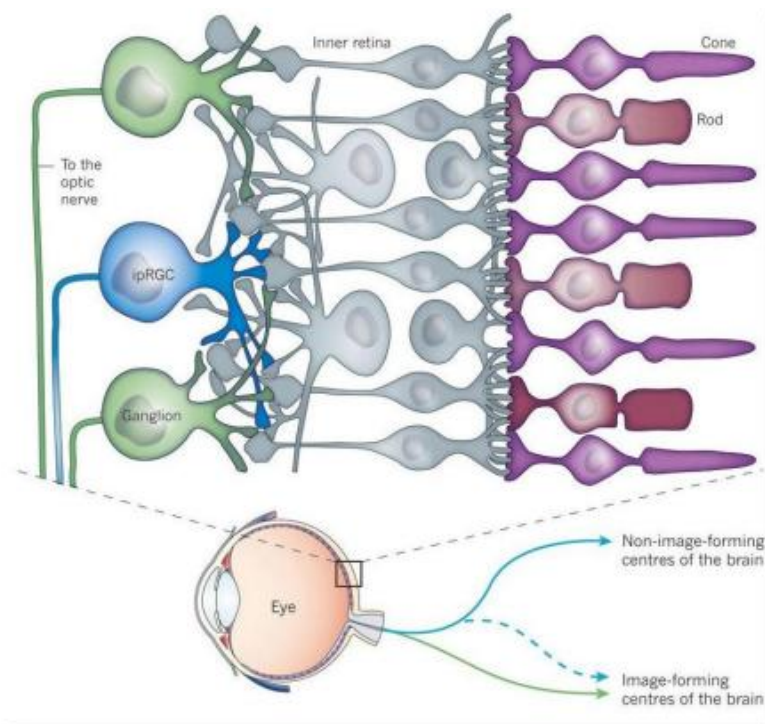
Figure 1. 2 Light passes through the ganglion layer and cells in the inner retina to the predominant photoreceptors in the eye –rods and cones. From Corie Lok(2011).
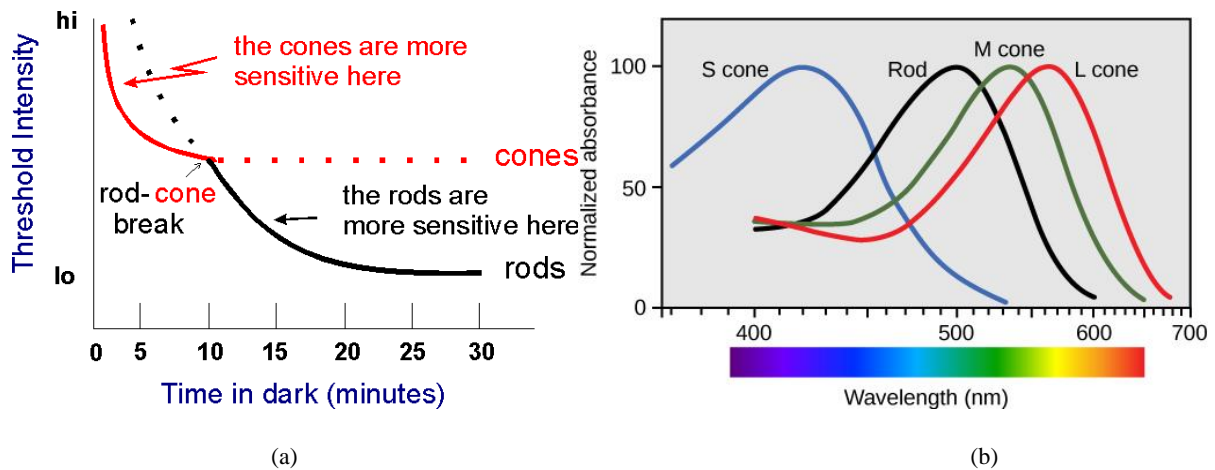
Figure 1. 3 (a). The threshold intensity of rod and cones as function of time in the dark. (b). wavelength responsiveness of short(S), medium(M), long(L)wavelength cones compared to that of rods.

The photoreceptors transmit the information of the visible light to the bipolar cells, and the bipolar cells form synaptic connections with the retinal ganglion cell. The retinal ganglion cells have their receptive fields which usually have a center and a surround that are in competition with each other, some cells show an on-center surround response while others show an off-center surround response, as showed in Figure1.4. Cells with a center-surround organization are mainly used for contour-enhancing. The on-off ganglion cells are sensitive to motion and many of these cells also show direction-sensitive response.
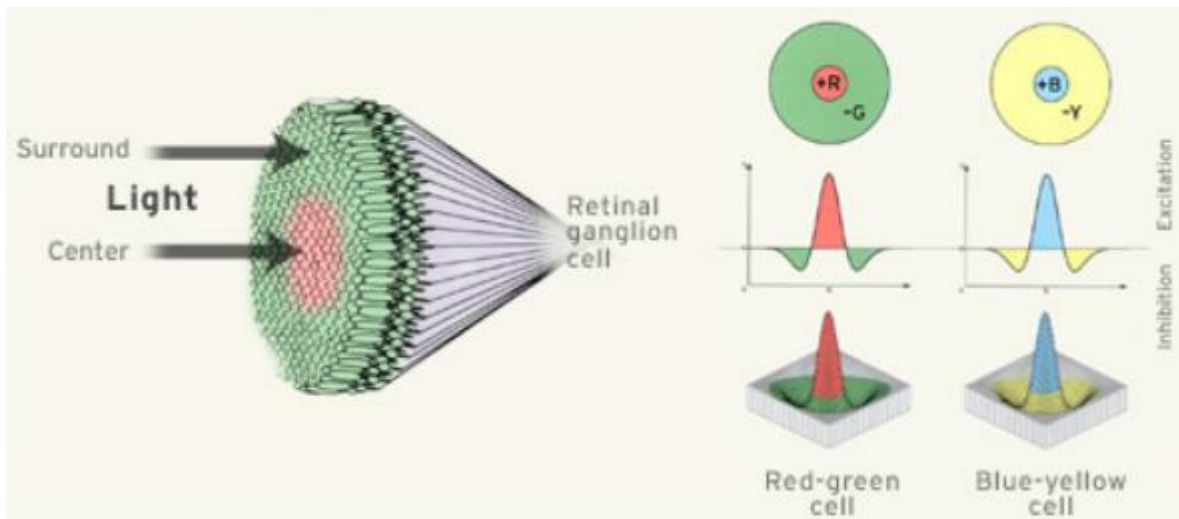
Figure 1. 4 The ganglion cells add and subtract signals from many cones. By comparing the response of the M and L cones, a ganglion cell determines the amount of green-or-red, blue-or-yellow. Moreover, they are excited in the middle of the field, and inhibited in the surrounding field, which makes them particularly sensitive to edges. from Xiao(2008)

1.1.2 Visual Cotex

The optic nerve leaves the eye at the blind spot and begins its journey to the main relay point in cotex ---the LGN, LGN has six layers, three from each eye. Layer1 and 2 are the magnocellular layers, and layers 3,4,5,6 are known as parvocellular layers, show in figure1.5. In Schiller et al.'s experiment, monkeys lesioned in the parvocellular layers have impaired color discrimination, magnocellular lesions impair motion. There are other cells mainly situated between the layers known as the koniocellular cells(K cell). P pathway is based on a green-red comparison, carry information about finer features and color. K pathway is based on a blue-yellow comparison. M pathway is based on a black and white comparison, carries information about course features and color.
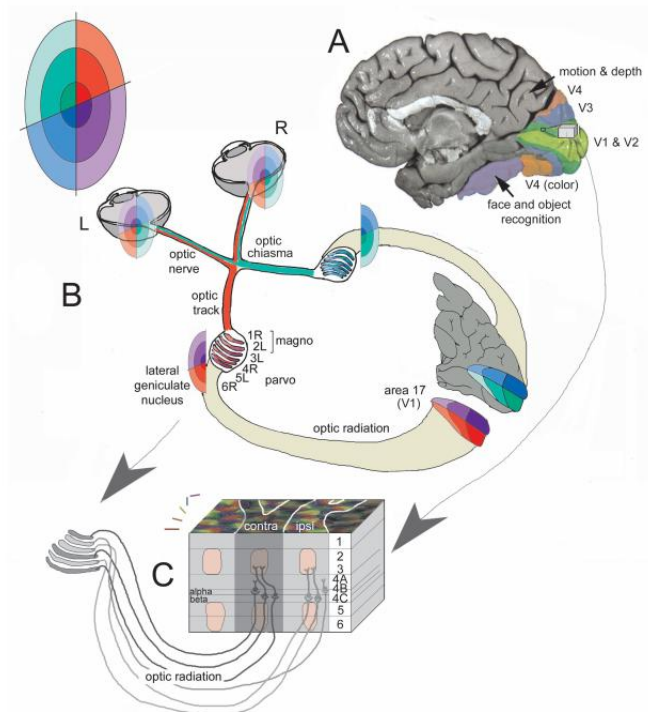
Figure 1. 5 Feed-forward projections from the eyes to the brain and topographic mapping(left).

The trichromatic model of Young and Helmholtz was explained as figure1.6 shows: the outputs from the red and green cones are combined to form a luminance channel. The red-green system compares the output from the red and green cones. The blue-yellow system compares the output of the blue cones with the combined output of the red and green systems.
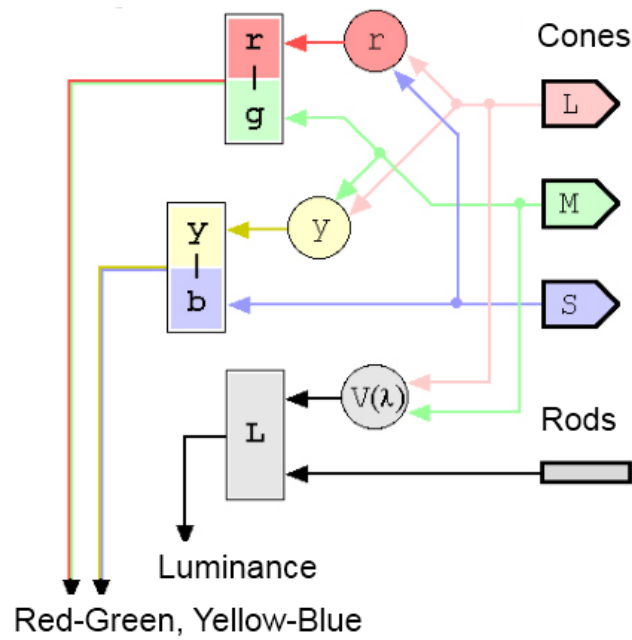
(a)
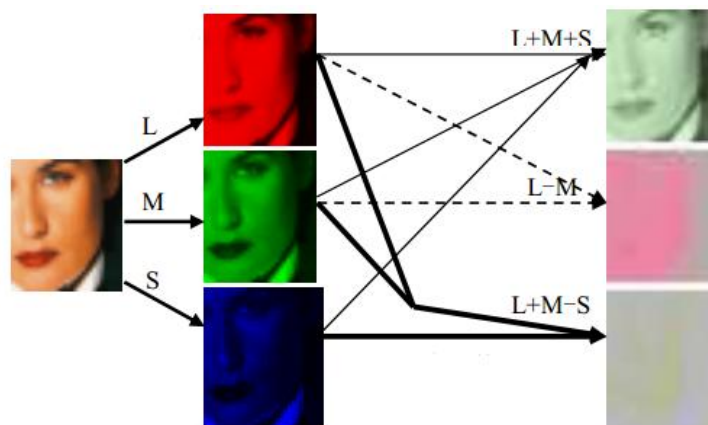
(b)

Figure 1. 6 (a)(b) Three channels in visual system,from Liao(2009)

Processing of visual information is done in separate cortical areas, show in figure1.7. Each aspect of the visual information, such as the shape of an object, its color and direction of motion, is processed in separate visual areas. Color is primarily processed in the blobs of V1, in the thin stripes of V2, and in the V4 complex, while motion is primarily processed in layer 4B of V1, in the thick stripes of V2 and in the V5/MT. On the other hand, dually selective neurons for color and motion direction were found in V1 and more frequently in V2 .Color produce the perception of hue and saturation in V4, motion produce the perception of motion direction and speed in MT. Color, motion, shape, texture is segregated in the cortex. Color could produce the perception of shape and motion could also produce the perception of shape, and the active area of this two kinds of shape

discrimination did not overlap in the cortex (controversial now). Orientation (shape) seems produced in the pale area which is between thin and thick area in V2, mentioned in An (2012).
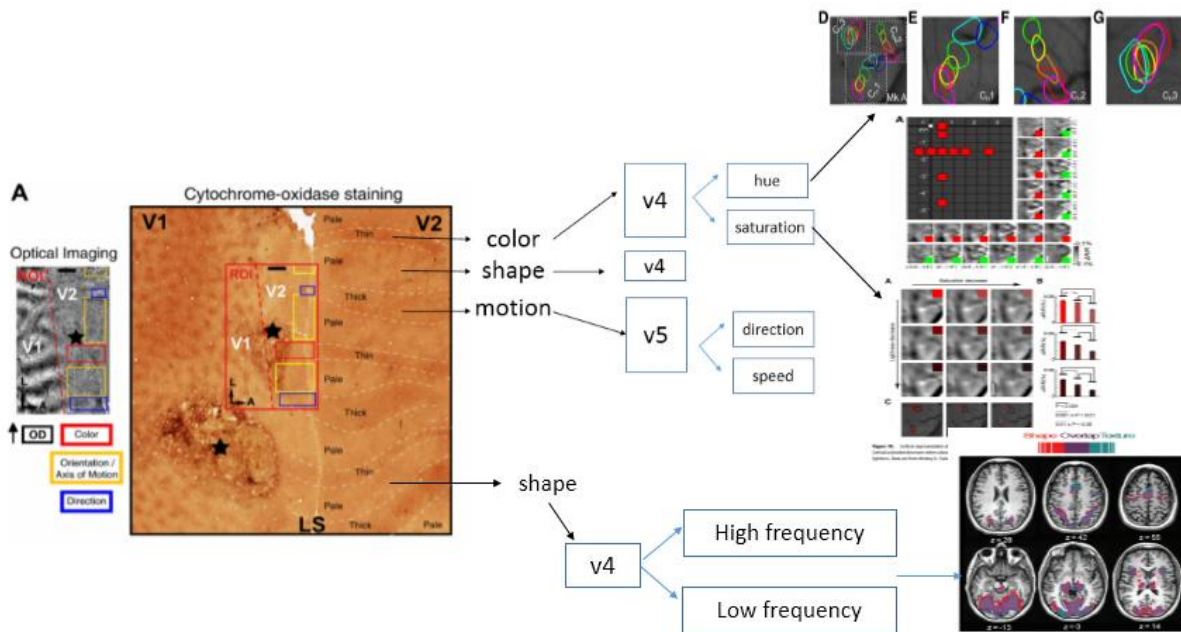
Figure 1. 7 Color ,shape, motion response to construct for V1,V2,V4 maps for macaque, figure are collected from An(2012),. from Ming Li,2014, from C.Cavina-Pratesi(2009)

As in the LGN, the single- and double opponent receptive field models in V1 cortex came from experiments with grating patterns was firstly tested by Johnson (2001) and Thorell (1984). There were single-opponent cells which were sensitive for the color in V1, and they had low-pass spatial frequency responses to equiluminant red–green grating patterns— like the single-opponent LGN cells studied by De Valois and Pease (1971). However, unlike the LGN cells, they are not sensitive to achromatic patterns of higher spatial frequency. The V1 single-opponent cells, like LGN single-opponent cells, had nearly equal but opposite inputs from L and M-cones, and some received S-cone input (Johnson et al., 2004). Most double-opponent cells were orientation-selective for both achromatic and chromatic stimuli (Johnson et al., 2008). There were a few color-preferring double-opponent cells that responded weakly to achromatic stimuli (Johnson et al., 2004, 2008). The hypotheses that edge-responsive with double-opponent, and area responsive with single-opponent seems reasonable, and still need to be proved by additional experiments (Robert Shapley et al.,2011).

Figure1.8, Figure1.9 shows Models of double-opponent and single-opponent V1 neurons and their spatial-frequency tuning for cone-isolating gratings reported by Johnson (2008). A is proposed sensitivity profile for an orientation-selective double-opponent simple cell, the spatial receptive field map is made of subregions and the L- and M-cones signals within each subregion are opposite

compare with their surrounding signals, but their strength are not precisely balanced with the surrounding. And their spatial symmetry is also different from a center-surround cell, it is asymmetric or odd-symmetric spatial receptive fields. The left part of diagram shows the organization of the two-dimensional receptive field, and the right diagram shows the hypothetical spatial sensitivity profile. The classical model of a hypothetical double-opponent neuron that receives both excitation and inhibition from each cone input showed in figure B. Originally, the strength of center and surrounding signals exactly balanced as shown. C is Single-opponent red– green sensitive neurons which receive inputs from L-and M-cones that are opposite in sign, but signals from each cone type are all the same sign. The figure C shows the two-dimensional maps and spatial profiles for one type of single-opponent neuron. Many parvocellular LGN neurons and single-opponent V1 cells are like those single-opponent and concentric cells.
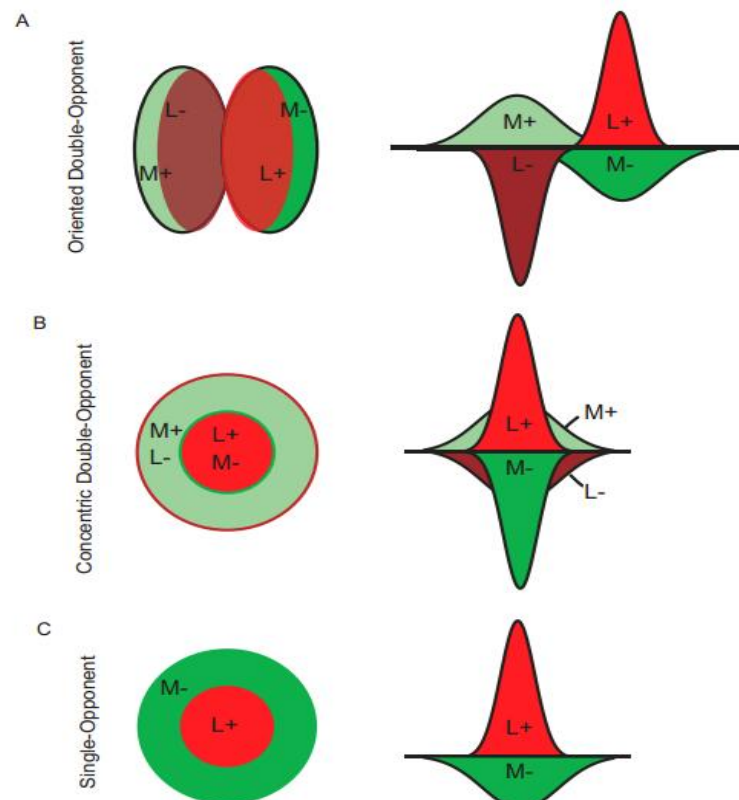
Figure 1. 8 Models of double-opponent and single-opponent V1 neurons, from Johnson(2008).

(a)   (b)
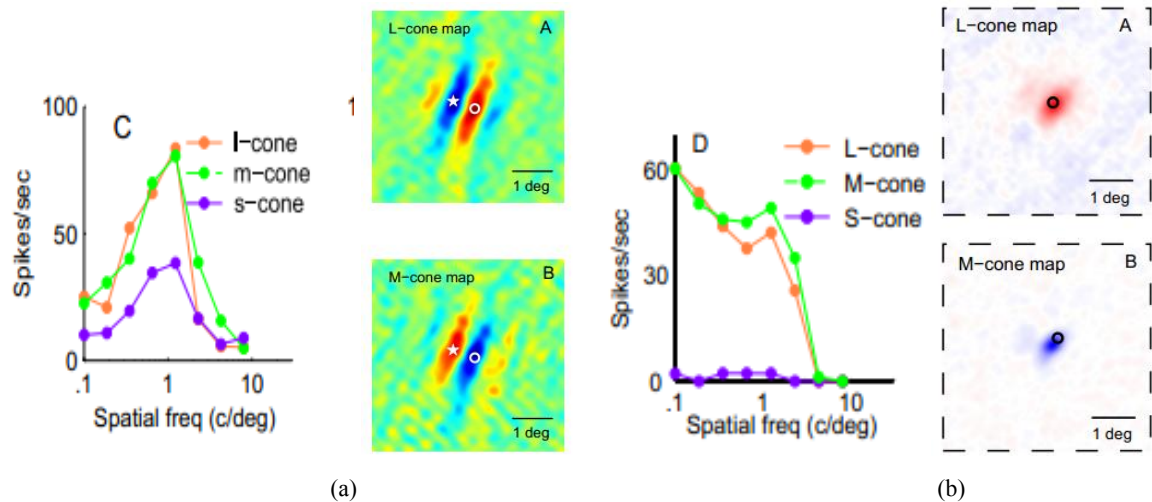
Figure 1. 9 The figure show the experiment result of Johnson (2008) (a). Spatial-frequency tuning for cone-isolating gratings, band-pass (double-opponent cell examples: a complex cell from layer 2/3)   (b). Spatial-frequency tuning for cone-isolating gratings, low-pass (V1 single-opponent neuron from layer 6)

Double-opponency model for color constancy could be explained by these single and double opponent cells. We will discuss double-opponency model later.

Color produce the perception of hue and saturation in V4, the perceptual color map in macaque visual area V4 has been drew (Ming Li,2014) as Figure 1.10, and Figure 1.11 shows. If the illumination change, the position of the color response area in the cortex may change to a relative area.
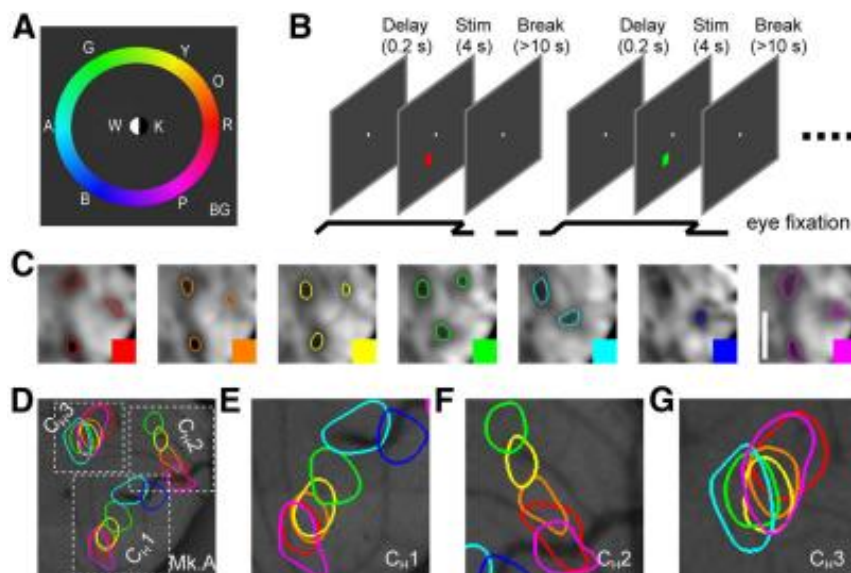
Figure 1. 10 Hue map in V4(macaque) from Ming Li,2014
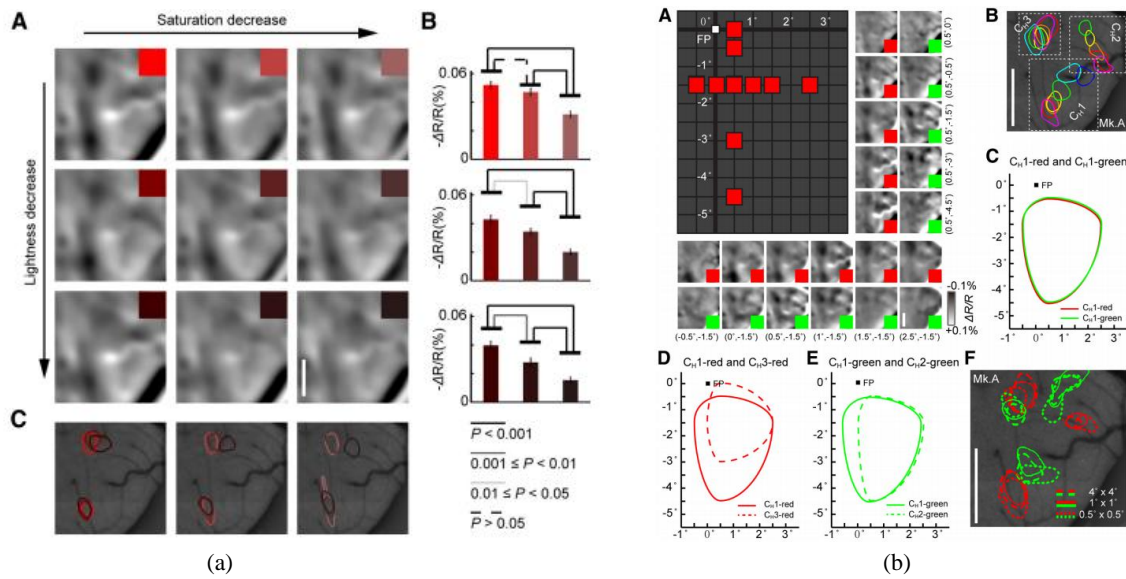
Figure 1. 11 (a) Saturation map in V4(macaque), (b) Retinotopy of the hue map in V4 from Ming Li,2014

When the illumination changes, V1, V2, V3 will respond to the new light but V4 cell dose not which exhibits color constancy. Interestingly, a region anterior to area V4 called V8 is clearly activated more by the colored grating than by the black and white one. So a question is left there, whether V4 and V8 is the really important area for color vision.

1.2 Visual mechanisms and factors contribute to color constancy

There are several visual mechanisms and factors contribute to color constancy. However, the cone adaptation of the photoreceptors at the retina and cognitive mechanism occurring at a higher level are considered as two main factors contributing to the color constancy.

(1) Time-course of chromatic adaptation

Werner, Sharpe, and Zrenner (2000) investigated the time-course of chromatic adaptation using adaptation patterns of different spatial complexities (articulated and uniform, equivalent in size, average chromaticity and luminance). the fit exponential function was explained to the time-courses, . the adaptation effect have significant difference acoording to their different time constants. It suggested three processes with different time-constants, wavelength and spatial sensitivity (see Figure1.12):

(a)   (b)
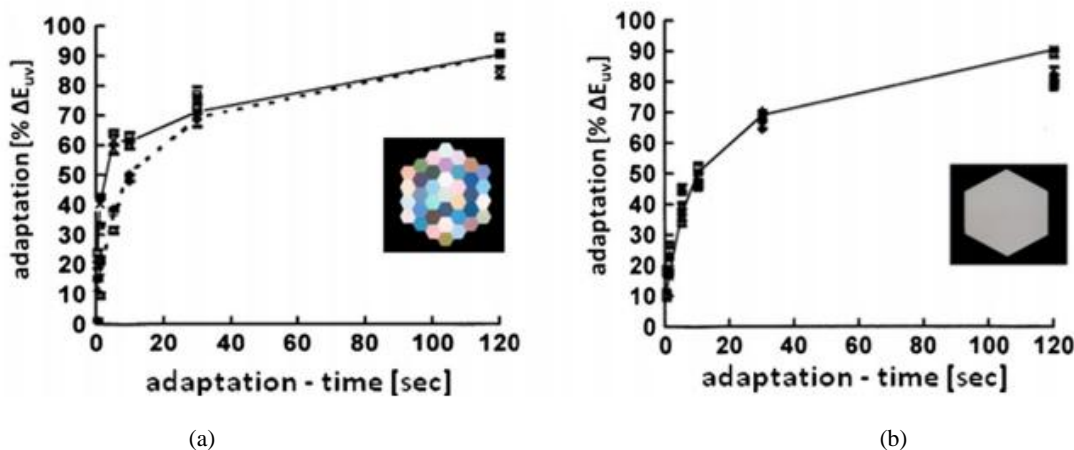
Figure 1. 12 (a) and (b) time-courses measured by Werner, Sharpe, and Zrenner (2000), using an articulated (a) or uniform (b) background. Adaptation times were 200 ms to 120 s. Size of displays: 15.4* 13.2 deg , test-patch 2.4 *2.2deg ; luminance: 19.3 cd/m2. In (a), the dotted line refers to shortwavelength (blue) and longwavelength (red) adapting lights, the solid line shows adaptation to middle-wavelength (green, yellow) light; in (b) the time-courses are identical for all adapting lights.

Chromatic adaptation works at multiple time-scales, ranging from almost instantaneous to minutes, which means it happens all the time, but the accumulation strength may has some differences; the sensitivity of the chromatic system are presetted by the very long-term processes, which is then modulated by fast and intermediate adaptation to the present set of stimuli. Adaptation response is in high level at the beginning of the time interval and then go to stable (for example, after 40 seconds the data of adaptation response is more stable than in first 20 seconds, show in figure1.12).

(2) Spatial properties of chromatic adaptation

Chromatic adaptation to middle wavelength light was found to be most pronounced if the spatial frequency and orientation of the adapting background and test-field matched, referenced in review of Werner(2014). Figure1.13 shows that the adaptation response result to different spatial and orientation seemed as a function of a band-pass filter, Spatially selective adaptation in doube-opponent cells is therefore a potential neural correlate for the observed tuning in chromatic adaptation. Johnson(2001) found that the multi-plexing neurons has been a important reason for the spatio-chromatic co-processing function, the oriented double-opponent cells in V1 and higher cortical areas are response to the colour-form contingencies, and some cells has band-pass characteristic, supported by Johnson(2008),Gheiratmant, Meese,& Mullen(2013).

(a)	(b)
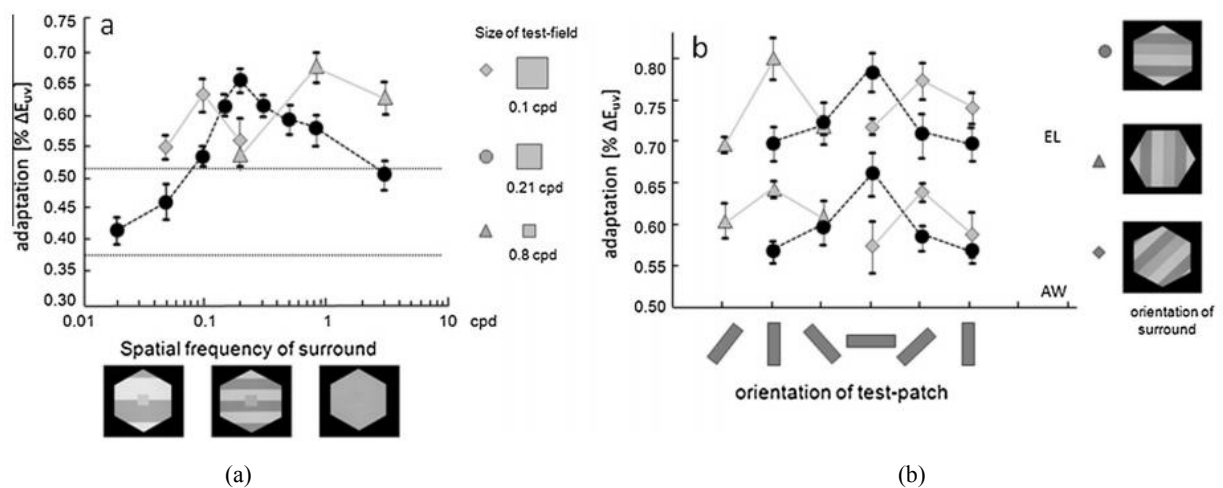
Figure 1. 13 Spatial tuning in chromatic adaptation measured by Werner(2003). (a) Shows colour constancy performance as a function of the spatial frequency of the background (0.02–3 cpd); different symbols refer to different sizes of the test-patch (0.1–0.8 cpd). (b) Shows colour constancy performance as a function of the orientation of the background, different symbols refer to different orientations of the test-patch (figure modified after Werner, 2003). The test-patterns appeared achromatic under the standard condition ($u0= 0.197, v0= 0.468$) and consisted of luminance contrast only (Lmin = 10.3 cd/m2, Lmax = 28.3 cd/m2, Lmean= 19.3 cd/m2); chromatic adaptation was measured for a 5 s green adapting light;

(3) Color contrast influences color constancy

Color contrast and induction is one important reason for color appearance as showed in figure1.14.
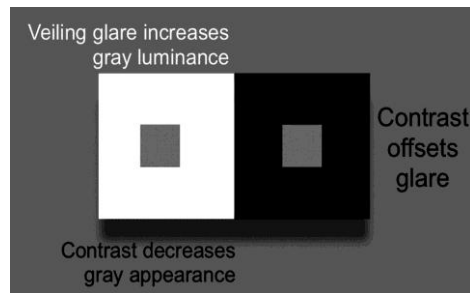
Figure 1. 14 Two opposing spatial mechanisms control the appearance of gray patches.

Figure1.15 shows the stimulus parameters and protocol for the basic 2AFC task in Hurlbert's experiment (2004). Hurlbert reported that the induction of the moving target is stronger than that in the stationary condition. She also found that the strength of contrast induction was weakened in the order of blue > yellow > red > green substantially, and the induction of a blue-yellow texture is stronger than a red-green texture, show in Figure 1.16.
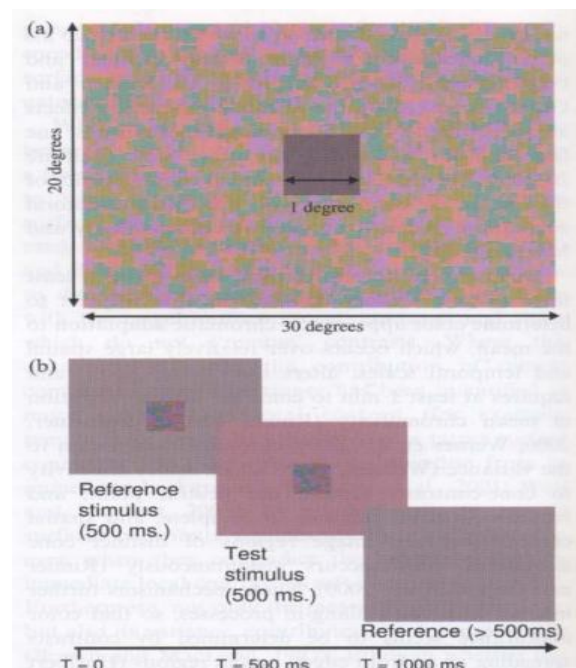
Figure 1. 15 (a) and (b) Stimulus parameters and protocol for the basic 2AFC task in Hurlbert's experiment(2014). The basic stimulus (Ia) consists of a `target'square, its luminance is set 8% dimmer than the background level of 15 cd/m 2. The background in this example is made of the ` Mondrian' texture. Fig.(b) shows the time- course of a single trial. During the first stage, presented for 500ms, the observer memorizes the color of a neutrally colored target (Reference), set against a neutrally colored background. The background color is then shifted isoluminantly along the LM-axis by a fixed amount, and a concomitant variable color shift is

introduced to the target (Test). The experimental task is to decide, during the 500ms for which this stimulus is presented, whether the new target viewed against the shifted background appears reddish or greenish.

(a)　　　　　　　　　　　　　　　　　(b)
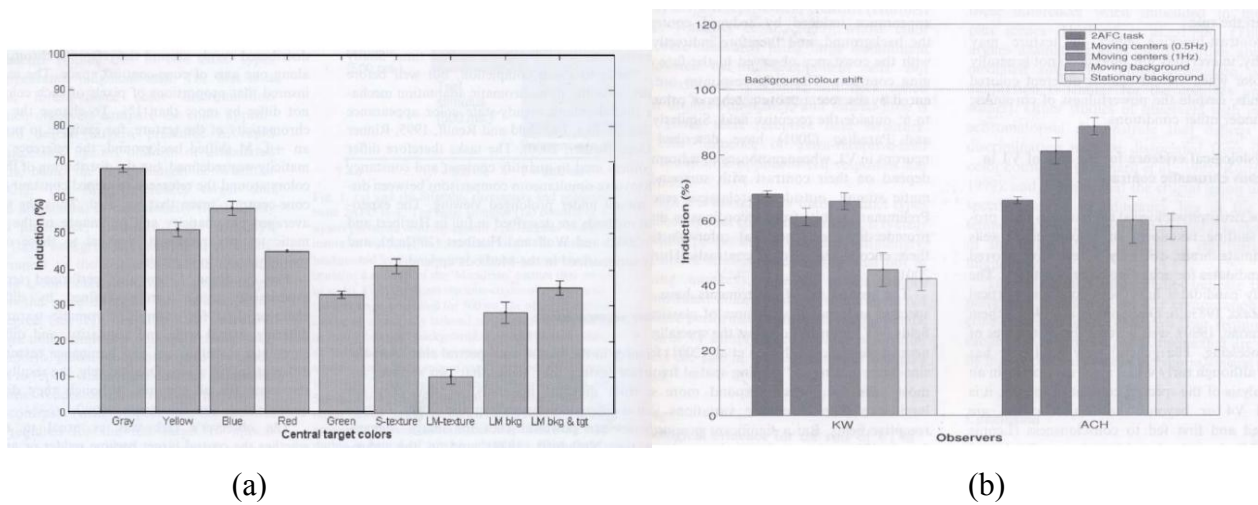
Figure 1. 16 Induction response measured by Hurlbert(2004) (a) The strength of contrast induction under different stimulus configurations for a single observer (KW) . Induction is strongest for a uniform gray target viewed against a uniform background. It is weaker for blue, yellow, red or green targets in order, but in each case still stronger than when the same individual colors are combined to make a blue and yellow texture (S -texture condition) or a red and green texture (LM - texture condition) for which induction is weakened substantially, and induction of S-texture is much more stronger than LM- texture. The bar labeled LM bkg shows that induction is intermediate in strength for a uniform neutral target against a textured background. (b) A comparison of the strength of contrast induction as measured by a variety of techniques. A value of 100% would indicate that the target square must always have the same chromaticity as its immediate background in order to appear neutral. A value of 50% indicates that the target appears neutral when its chromaticity is halfway between that of the immediate background and the neutral point. The strength of induction is comparable in basic 2AFC experiment and in the `moving- center ' experiments. The result shows that the induction of the moving target is stronger than the stationary target.

(4) Feedback from horizontal cells (HC) mediates color induction.

Efficiency of color induction in the cone output and optic nerve decreased significantly with the inhibition of HC-cone feedback, HC-cone feedback in mediating color induction, and therefore, likely also in mediating color constancy, reported by Shai Sabbah (2013).

(5) High level cortical processing.

Kulikowski (2012) found that Von Kries rule was limited for explaining color and lightness constancy, suggesting that cortical mechanisms must underlie color constancy. Sobagaki(1974) argued that lightness constancy was found, irrespective of the change of chromatic adaptation. It implies that von Kries cone adaptation is not the only factor contributing to color constancy, color constancy also involves high level cognitive mechanisms. Goddard (2010) found that the increased after effect in the constant scene condition cannot be wholly attributed to adaptation of receptors and neural mechanisms responsive to raw quantal catch, the existence of adaptable mechanisms

responsive to surface color, most likely located in early visual cortex. Allen (2012) investigated that color constancy is related with working memory, they have divided the observers into to two groups according to their ability of working memory which is to maintain a desired representation while suppressing irrelevant information and they found that lowWM observers showed significantly better simultaneous color constancy than HighWM observers in the complex-background condition, it is in fact involve to attention mechanism which we will discuss in details later. Olkkonen (2008) said that visual identity of an object has a measurable effect on color perception, and that this effect is robust under illuminant changes, indicating its potential significance as an additional mechanism for color constancy, the achromatic color match result is show in figure1.17 . Dose it looks like that the memory of color also has opposite adaptation effect?

(a)   (b)
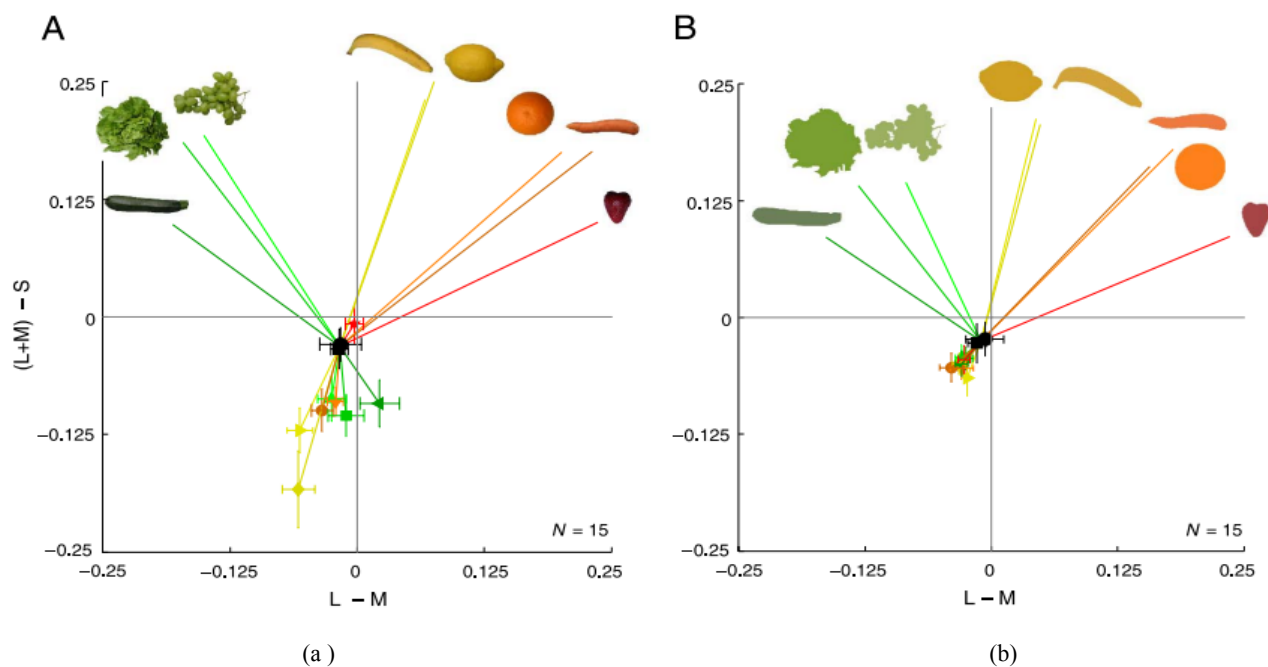
Figure 1. 17 The achromatic color match result measured by Olkkonen,2008. (a) Mean achromatic settings for fruit photographs. Achromatic settings for the uniform disc and the noise disc are denoted with the black circle and square, respectively. Lines are drawn from the disc settings to the typical settings for each fruit; the data points for the typical settings fall outside the scale of the plot. Achromatic settings for fruit outline shapes are plotted similarly in (b).

(6) Color constancy in 3D scene

Some research found that the color constancy based on three-dimensional scenes or objects is better than that based on flat surfaces. Hedrich (2009) found that color constancy was better when the target color was learned in a cue-rich 3D scene than in a 2D palette. Delahunt and Brainard (2004a) investigated that three-dimensional scenes contain many additional cues for illuminant estimation compared to computer simulations of flat surfaces, such as shadow, light reflection from atmosphere, light reflection from surfaces (Delahunt and Brainard,2004b), peripheral illumination (Hansen et

al.2007), specular highlight (Yang and Maloney2001; Yang and Shevell2003) and visual appearance of an real object (Olkkonen et al.2008).

(7) Color constancy in natural scenes

In natural viewing conditions, visual systems encounter illumination changes at several spatial and temporal scales which is metioned in the review of Werner (2014): (1) short-term illumination changes due to the changes in the spectral and intensity of the illumination in the scene; (2)slow and long-lasting changes of the overall illumination occur in the course of the day, due to atmospheric changes or the place changes; (3) long-lasting changes in the environment occur from seasonal changes or the effect of aging on the optical media in the eye. David H. Foster (2015)investigated about the illumination in natural environments varies through the day, figure1.18 shows the spatial ratios of cone excitations across different times of day. They found that within sampling constraints, ratios of cone excitations, and also of opponent-color combinations, provide an approximately invariant signal for stable surface-color inferences, despite spectral and geometric variations in scene illumination. The main reason of this result may cause by the adaptation effect which purpose is mainly to dragged the color back to the area which is near to the white point on the daylight locus, it seems like a balance processing for human to maintain the constant perception to the natural world.
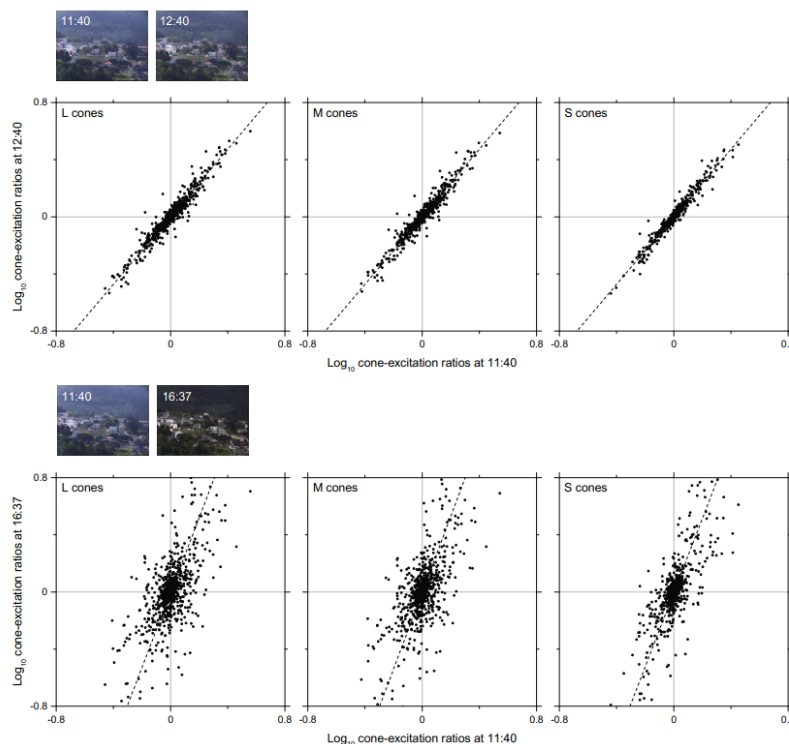
Figure 1. 18 Scatter plots of spatial ratios of cone excitations across different times of day for the Nogueiró scene, measured by Foster(2015). In the top row, data are shown for successive times of 11:40 and 12:40. For each pair of randomly chosen points in the scene, the logarithm of the ratio at one time is plotted against the logarithm of the ratio at another time for L, M, and S cone excitations. For clarity, just 1000 data points from the 10,000 available are plotted. The spacings of points in each sample pair were drawn randomly from the logarithmic scale 1, 2, 4, ..., 256 pixels, and their orientations randomly from the circle. Image sizes were 1344

*1024 pixels, corresponding approximately to 6.9*5.3deg. The dashed lines represent orthogonal linear regressions. In the bottom row, corresponding data are shown for more widely separated times of 11:40 and 16:37.

(8) Statistic information from scenes contribute to constancy

The effects of image surfaces on color constancy were investigated by several experiments. One hypothesis is that the constancy of spatial cone-excitation ratios of images surfaces contributes to the color constancy (Foster et al.2006, 2015; Foster and Nascimento1994; Nascimento et al.2002). This hypothesis seems mainly caused by adaptation effect in my opinion. The other famous hypothesis is that observers estimate illuminant by exploiting luminance-redness statistic information from scenes (Golz2008; Golz and MacLeod2002) or by referring to bright colors in scene (Uchikawa et al.2012). Kuriki(2006), Martinovic (2011) argued that luminance information in scenes has a strong effect on color constancy. Golz and MacLeod (2002) found that the observer could discriminate the redness of objects which were making up the scene and the redness of the light source which illuminated the scene, by comparing the statistics result of mean redness and luminance-redness correlation, it also bring me a question, how about the result of blueness mean or correlation? Later, Golz (2008) found that in the region of 4.3 degree, the illuminant estimation based on luminance-redness correlation, not chromatic contrast at borders, mainly contributed to color constancy. It looks like that 4.3 degree area is the area that adaptation effect influences in my opinion.

(a)   (b)
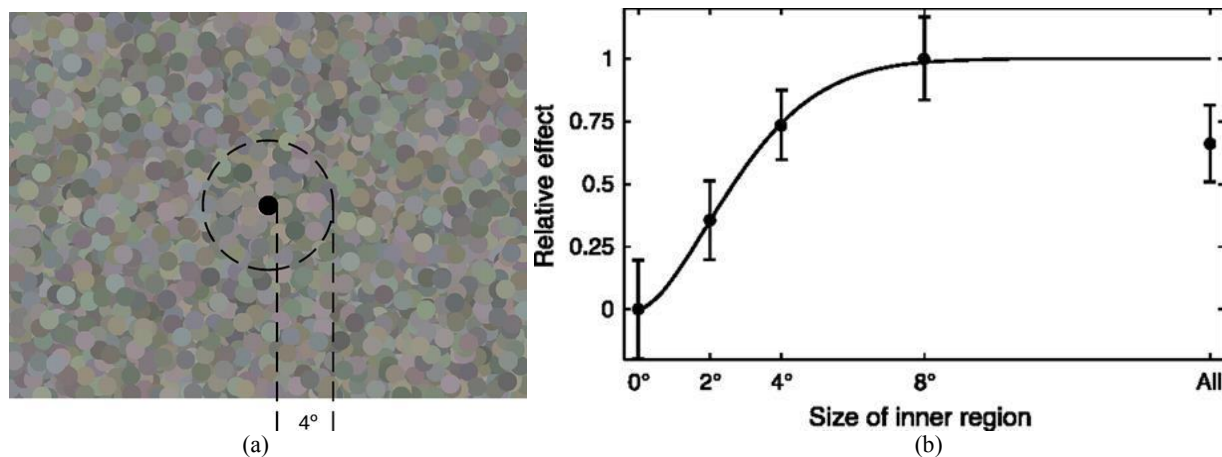
Figure 1. 19 Stimuli and test result from Golz's experiment (2008) (a). Example of stimuli used in the experiment. The dashed elements were not displayed in the experiment but are used here to indicate the inner region of the surround (dashed circle) in which a higher luminance-redness correlation was present than in the remaining outer region of the surround. The size of this inner region is manipulated in the experiment. The central test field is indicated here by black marking. This image is an example for the condition with a size of the inner region of 4- deg. (b). Mean relative effects results for the average observer. Error bars represent ±1 *SEM* averaged across subjects. The vertical straight line indicates the size of the inner region for which 75% of the maximum effect of the luminance-redness correlation is obtained (estimated from the fit) (Jürgen Golz,2008).

Uchikawa (2012) found that the luminance balance of surfaces with no chromaticity shift had clear effects on the observers' matches. Morimoto(2016) investigated about the effects of surrounding stimulus properties on color constancy based on luminance balance, they find that unlike chromaticity-based color constancy, chromatic variation does not influence the effect of luminance balance. It is shown that luminance- balance-based estimation of an illuminant performs better for scenes with reddish or bluish surfaces. This suggests that the visual system exploits the optimal color distribution for illuminant estimation

(a)   (b)
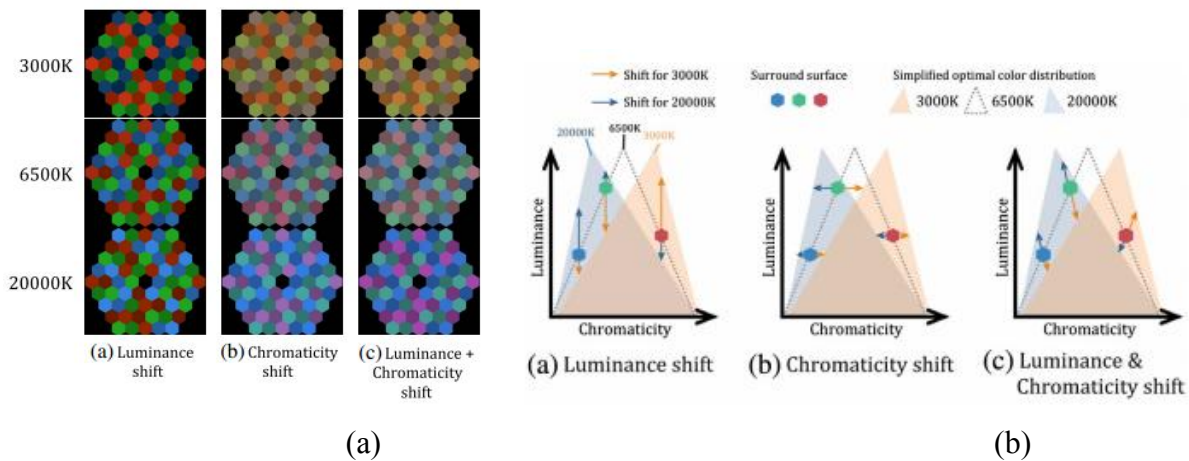
Figure 1. 20 Stumli used in Morimoto's experiment (2016)and simplified illustration of each shift condition. (a)Surrounding stimuli employed in Morimoto's Experiment. Each row and column indicates different color temperature and shift conditions, respectively.(b) Simplified illustration of each shift condition. Hexagons and triangles show scene surfaces and optimal color distribution under three illuminants, respectively.

(a)   (b)
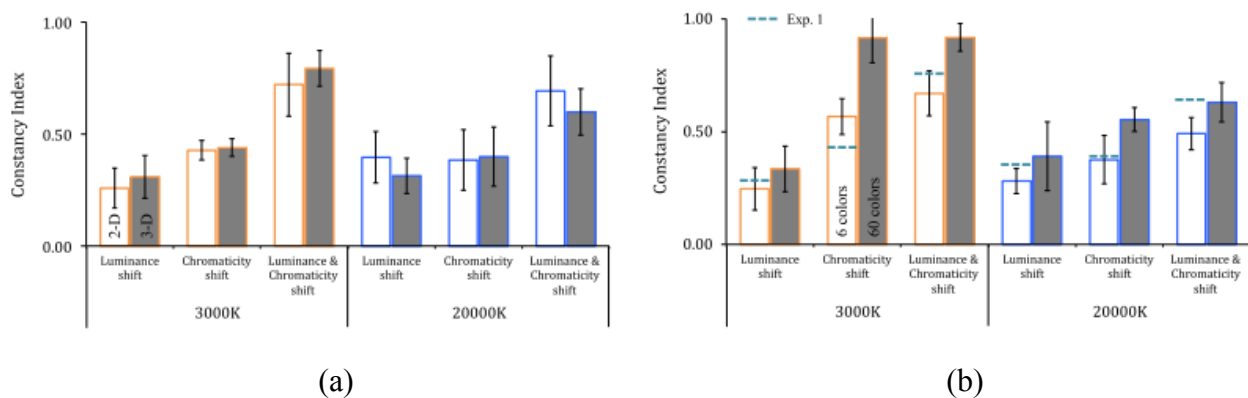
Figure 1. 21 (a) Averaged constancy indices across four observers in Morimoto's experiment (2016). Higher values indicate better color constancy. The error bar indicates ± S.E. across four observers. The left and right bars indicate 2D and 3D conditions, respectively. (b)Averaged constancy indices across four observers. The left and right bars indicate 6 colors and 60 colors in the background. The error bar indicates ±S.E. across four observers. The blue dashed lines are the constancy index from Experiment result showed by the left figure (a) for comparison (2D and 3D conditions were averaged)

(9) Color constancy under different uniform illuminant conditions.

Some scientists expect that the color constancy under illuminant changes on daylight locus should be better than that off-daylight locus, because we usually live under daylight illumination. Surprisingly, it was found that the color constancy under illuminant changes on daylight locus is not better than that under illuminant changes off daylight locus (Delahunt and Brainard2004b; Hedrich et al.2009), on the contrary, the color constancy under blue and green illuminants is better than that under red and yellow illuminants (Delahunt and Brainard2004b), the result is showed in figure1.23. In Delahunt's experiment (2004), observers viewed scenes displayed on a CRT-based stereoscope and adjusted a test patch embedded in the scene until it appeared achromatic, stimuli showed in figure 1.22. Two of these changes (Blue and Yellow) were consistent with the statistics of daylight, whereas two (Green and Red) were not. The results indicate that constancy was least across the Red change, as one would expect for the statistics of natural daylight. Constancy for the Green direction, however, exceeded that for the Yellow illuminant change and was comparable to that for the Blue.

(a)Valid-cue experiment　　　　　　(b)Invalid-cue experiment
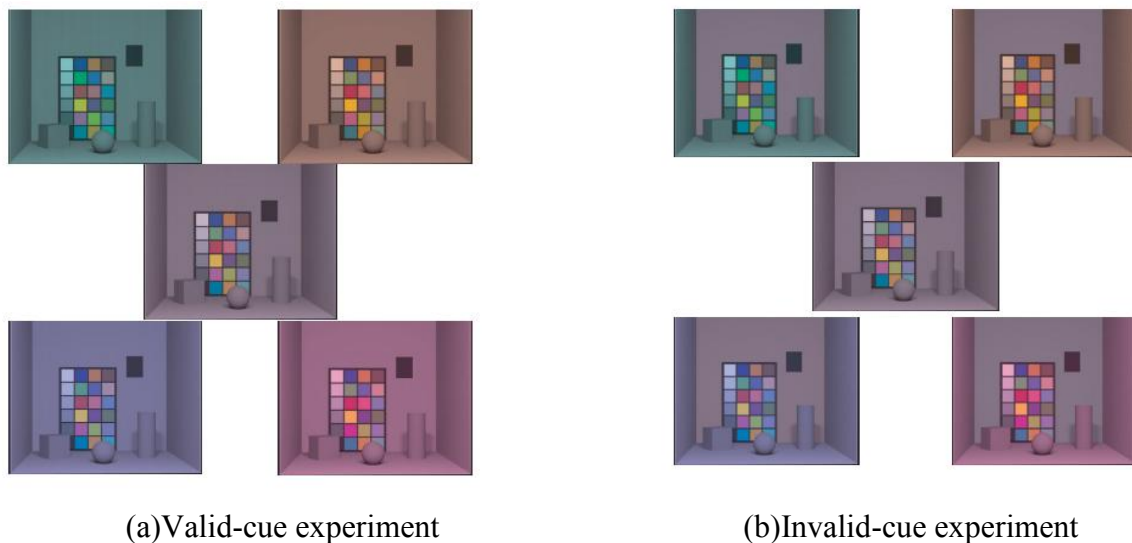
Figure 1. 22 Stimuli used in Delahunt's experiments(2004) (a) Valid-cue experiment of the stereo image pairs. Each image in the pair was synthesized from a three-dimensional scene description using the RADIANCE rendering software (Larson & Shakespeare, 1998). Scene objects were Lambertian. There was a single light source that produced moderately diffuse illumination. For the image pair shown, the Neutral experimental illuminant (see below) was used. The test patch is shown as the dark square toward the upper right of the images. To simulate binocular disparity, the left- and right-eye images were rendered for different view-points. The stereo pair in the figure is arranged so that it can be cross-fused. (b) Invalid-cue experiment, invalid-cue experiment was a replication of Valid-cue experiment with one important change: for each experimental illuminant, the simulated reflectance of the back-ground surface in the scene changed so as to equate the chromaticity and luminance of the light reaching the observer from that region of the image.

(a)   (b)
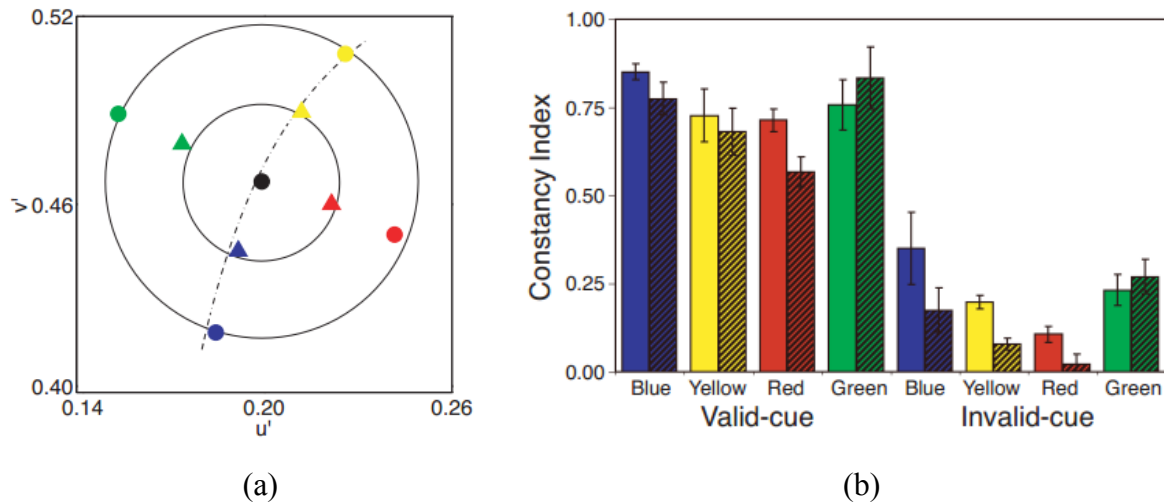
Figure 1. 23 Illumination set in the experiment and the constancy index measure by Delahunt (2004) (a) The experimental illuminant chromaticities are illustrated in CIE u'v' coordinates. The closed circles show the illuminants at the perceptual distance of 60 Δ E* units and the triangles show the illuminants at the perceptual distance of 30 Δ E* units. The symbols are color coded so that the Blue illuminants are shown in blue, etc. Both sets of illuminants (60 Δ E* and 30 Δ E*) are approximately equally distant from the Neutral illuminant in the u'v' representation. The blackbody locus is shown by the dashed black curve. (b) The mean constancy indices obtained in experiment are shown. The plain bars are the indices for the 60 Δ E * illuminant changes, and the patterned bars are for 30 Δ E *. The error bars show ±SEM. The reduction of invalid-cue data is consistent with the notion that the local surround plays a large role in color constancy.

Their experiment result is quite different from experiment result of I and Pearce and Hurlbert (2014), we will discuss it later.

Figure 1.24 show the stimuli and scene backgrounds in Pearce's experiment(2014). As reported by Pearce and Hurlbert (2014), the ability to discriminate highly-chromatic illuminations may involve strong estimation effect, chromatic illumination discrimination ability of blue is poorest and green is best, showed in figure1.25.
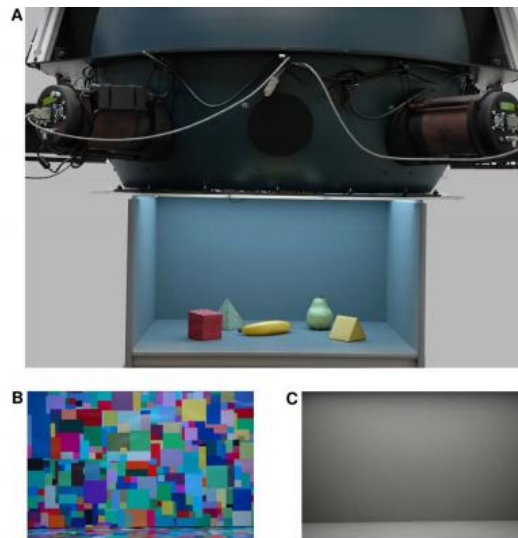
Figure 1. 24 Photographs of the illuminator equipment and the scene backgrounds in Pearce's experiment(2014) A. Photograph of illuminator and the viewing box (with front wall removed) under extreme blue illumination, with fake pear, banana and chromatically matched novel objects. B. The Mondrian background used for the variegated scene condition, under D67 illumination. C. The grey background used for the grey scene condition.

(a)   (b)
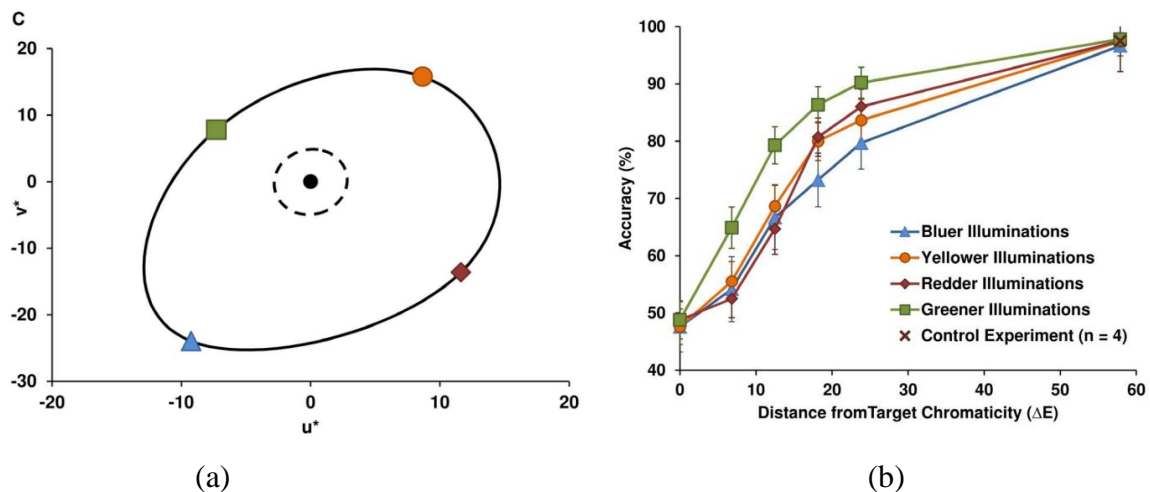
Figure 1. 25 Illumination set and test result in Pearce's experiment (2014). (a) Computed △Euv mean thresholds at 75% accuracy for each chromatic direction, plotted in CIE u*v* colour space, with a spline forming the just-noticeable-difference discrimination contour (bold line) from D67 (black marker); just-noticeable-difference MacAdam ellipse boundary for D65 (dashed line) plotted around D67 point. (b)Mean accuracy across all conditions and participants for each chromatic direction as a function of perceptual distance from the target chromaticity △Euv.

(10) Color constancy under different nonuniform illuminant conditions.

John J. McCann' experiments (2014) measured color constancy under nearly uniform illumination and compared it with the result of that under non-uniform illuminations which had sharp shadows created distinctive edges, they measured color constancy by a simultaneously 3-D Mondrian experiment. The observers were asked to measure changes in appearances of individual color facets compared to a ground of

same set of truth color sample showed in front of the 3-D Mondrians, and quantify the degree of color constancy in more real-life illuminations. The Mondrian in their experiment are shown in Figure 1.26(a). The LDR illumination experiment stimuli showed in Figure 1.26(b) is an uniform illumination and observers reported that many facets with the same paint have a better color constancy. The HDR illumination used in figure1.26(c) contained two different white lights illuminated the 3-D Mondrian from different directions with sharp shadows, and the observers showed poorer color constancy. It implies that color appearance correlates with the edges in the retinal image, not with the reflectance of each painted surface.
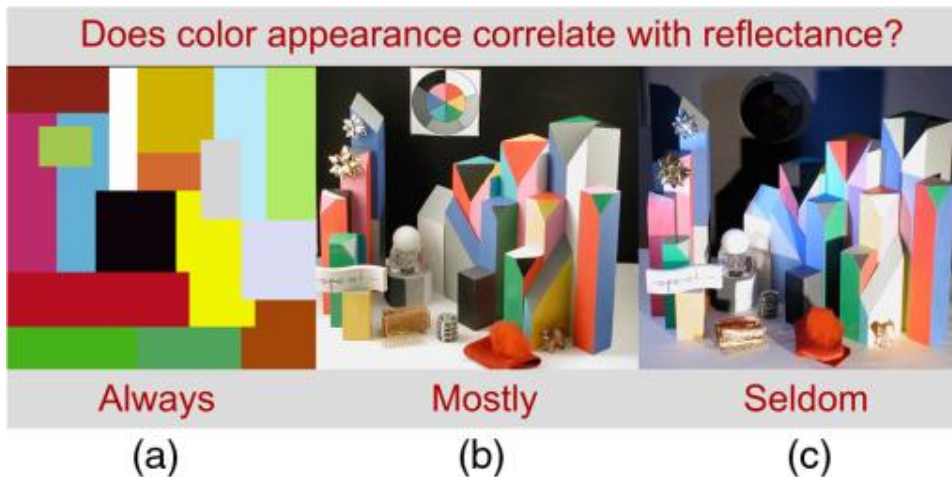
Figure 1. 26 Illustrations of the three different Color Mondrian experiments measured by John J. McCann (2014). (a) 17-Area 2-D (flat) Mondrian in uniform illumination. (b) 3-D Mondrians in LDR, partially uniform illumination. Better color constancy were reported by observers. (c) 3-D Mondrians in HDR (sharp shadows) illumination, poor color constancy were reported by observers.

(11) Effects of attention

Most observations suggest that attention alters the sensitivity of neurons without affecting their stimulus preferences. Only some neurons in V1 are modulated by attention; others ignore it and some respond exclusively when the stimulus is attended. The influence of attention increases with cortical hierarchy, perhaps also with increasing feature specificity of the cells. Attention may also change the synchrony of neuronal signals in the visual cortex.

J.Suchow have shown that motion could cause failure to detect changes of color and size, except in the case that the observer attended to the objects and noticed the objects' changes (2011). The stimuli showed in figure1.27.
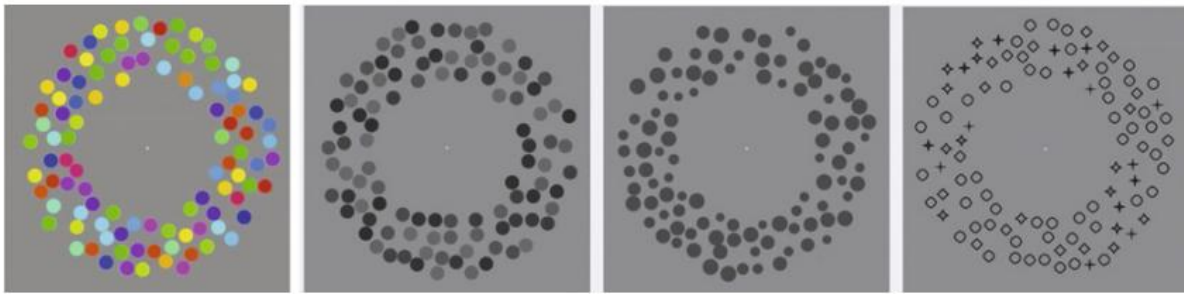
Figure 1. 27 Motion Silences Awarenes s of Changes in Hue, Luminance, Size, and Shape,from experiment of J.Suchow(2011). One hundred dots are arranged in a ring around a central fixation mark. During the experiment, each dot changes rapidly in (left to right) hue, luminance, size, or shape . When the ring is briskly rotated about its center, the dots appear to stop changing—this is silencing. See movies from website: http://www.sciencedirect.com/science/article/pii/S0960982210016507

Golz (2010) found that the viewing behavior also has influences on color constancy; the exploration in the visual field increases the color constancy compared to fixating to the test field.
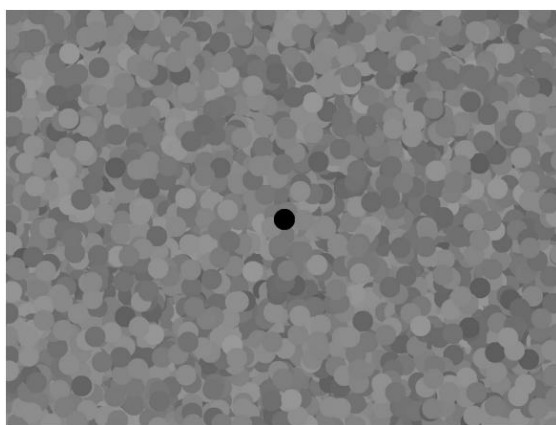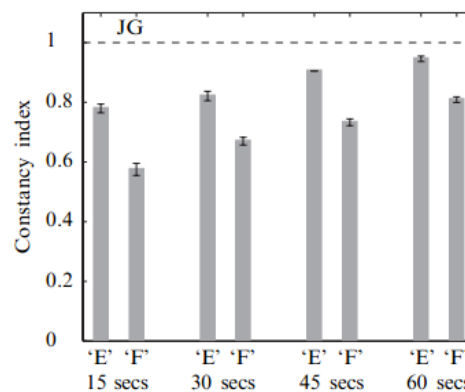
(a)   (b)

Figure 1. 28 (a)Grey-scale reproduction of the variegated type of stimuli used in the Golz' experiment(2010). The central test field is indicated here by the black circle. (b) Results for four different trial durations. Error bars represent ±1 SEM. Note:`E' = `Explore', `F'= `Fixate'.

(12) Effects of motion

Werner's researches investigate that the color constancy improves with an object motion (2007). In their experiments, the color constancy was tested under the situation that observers fixed eyes on stable objects, or pursued to track moving objects with no consideration about attention. However, attention and consciousness also have different effects on the retinal adaptation and they can subsequently influence to the color constancy.

(a)

(b)

(c)

(d)
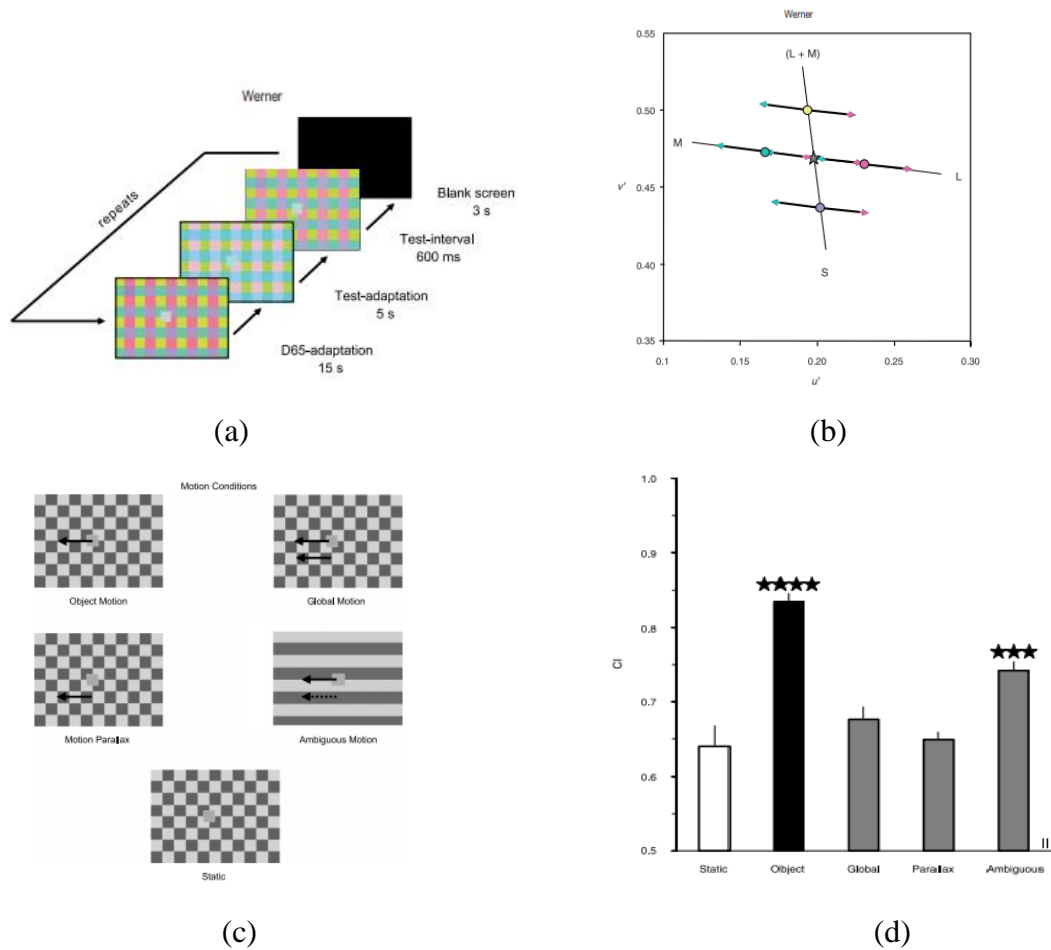
Figure 1. 29 (a)Experimental sequence in Werner's achromatic adjustment experiments (2007). The experimental sequence commenced with 15 s adaptation to the pattern in standard condition (D65，adaptation), followed by 5 s adaptation to the pattern in " Red " or " Green" condition (test adaptation, here: green) and the 600-ms test interval. After the presentation of a 3-s black screen, the sequence was repeated.(b) CIE 1976 UCS diagram illustrating the u', v' coordinates of the heterochromatic test pattern in the different illumination conditions: star refers to the color locus of D65 and of the test patch in standard condition; filled circles refer to the color loci of the background patches in standard condition; arrowheads indicate the shift of the color loci of test and background patches following the illumination changes toward " Green" and toward " Red," respectively. Thin black lines indicate the L/M and the S/ (L + M) axes. (c) illustrates the different motion conditions. Static: color constancy with static test patch; object motion: motion of the test patch relative to the static background; global motion: test patch and background move with identical speed and direction; motion parallax: background moves relative to the static test patch; ambiguous motion: test patch moves along a static horizontal grating. (d) Color constancy measured for different motion paradigms, the constancy indices of observers II, the inset on the left Error bars show ±1SEM.

1.3 Methods of color constancy experiment

Four main kinds of psychophysical methods have been used to measure color constancy: Asymmetric color matching, achromatic adjustment, color naming, discriminating illuminant changes from reflectance changes. By using different kinds of methods, observers performance in different ways, and these factors would influence the experiment result.

➢ **Asymmetric color matching**

Stimuli is compared under different viewing conditions, here different illuminants. Stimuli may be viewed simultaneously or successively or in an alternating sequence, binocularly or dichoptically.
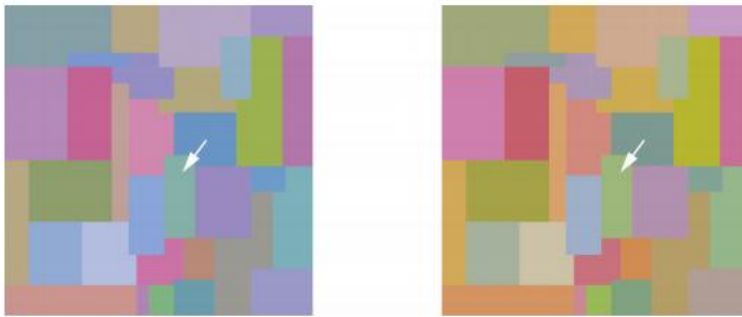
Figure 1. 30 Mondrian patterns used byArend and Reeves (1986) in simultaneous asymmetric color matching.

➢ **Achromatic adjustment**

The method of achromatic adjustment is normally applied in an undifferentiated way. A subject typically sets a test stimulus so that it appears ''achromatic'', i.e. somewhere on the continuum from gray to white (Fairchild & Lennie, 1992; Werner & Walraven, 1982; Werner 2007). but there are interpretational difficulties in that, depending on the criterion used by the subject, the achromatic setting provides only an estimate of the illumination spectrum at that point or region in the scene (Foster, 2003).

➢ **Color naming**

Unlike asymmetric color matching, color naming provides a direct method of measuring color constancy, since it concentrates on identification rather than equivalence.

➢ **Discriminating illuminant changes from reflectance changes**

If surface color is considered as a proxy for surface spectral reflectance, a more objectively oriented method of measuring color constancy is to ask subjects to distinguish between changes in illumination spectrum and in surface reflectance (or material) in a scene.

1.4 Previous Literature List based on four main methods of color constancy research:

Part1. Color constancy research about simultaneous asymmetric matching.

1. **Title:** Simultaneous color constancy.

Author: L. Arend, A. Reeves,1986, Journal of the Optical Society of America A – Optics Image Science and Vision, 3(1986), pp. 1743-1751

Illumination: Daylights, 4000, 6500, 10000 K, Spectral product

Background: 2D multielement, Mondrian display on Monitor

Paper match CI: 0.52,**Appearance match CI:** 0.2

Points of this research: Observers matched patches (simulated Munsell papers) in two simultaneously presented computer-controlled displays, the hue–saturation matches showed little color constancy. The data show that simultaneous mechanisms alone alter hues and saturations too little to produce hue constancy.

2. **Title:** Quantitative studies of color constancy

Author: K. Tiplitz Blackwell, G. Buchsbaum(1988), Journal of the Optical Society of America A – Optics Image Science and Vision, 5(1988), pp. 1772-1780

Illumination: Daylights, A, F2, B, D55, C, D65

Background: 2D patch in surround with **Appearance match CI:** 0.3

Background: 2D patch in far surround with **Appearance match CI:** 0.15

Points of this research: The center was presented with (1) no surround, (2) an adjacent chromatic surround, or (3) a chromatic surround separated from the center by an achromatic gap. When no surround is present, color constancy fails; When surrounds are present, some degree of color constancy is displayed. Color constancy is poor when chromatic induction is minimal, if the ratios of R, G, and B of the center to R, G, and B of the surround remain constant as the illuminant changes, color constancy results.

3. **Title:** Simultaneous color constancy: Papers with diverse Munsell values

Author: L.E. Arend Jr, A. Reeves, J. Schirillo, R.Goldstein, Journal of the Optical Society of America A – Optics Image Science and Vision, 8(1991), pp. 661-672

Illumination: Daylights, 4000, 6500, 10000 K, Spectral product

Background: 2D patch (annulus display), **Appearance match CI:** 0.11

Background: 2D patch (annulus display), **Paper match CI:** 0.35

Background: 2D patch (Mondrian display), **Appearance match CI:** 0.18

Background: 2D patch (Mondrian display), **Paper match CI:** 0.44

Points of this research: The paper matches were often approximately color constant. The hue-saturation matches were in the correct direction for constancy but were always closer to. a chromaticity match (no constancy) than to the chromaticity required for hue-saturation constancy.

4. **Title:** Naming versus matching in color constancy

Author: J.M. Troost, C.M.M. de Weert, Perception & Psychophysics, 50 (1991), pp. 591-602

Illumination: Daylights, 4000K, 6500K, 10000K, 25000K, von Kries shift

Background: 2D multielement(hexagon array),

Simultaneous asymmetric matching, Appearance match CI: 0.46, **Paper match CI:** 0.81

Successive asymmetric matching, Appearance match CI: 0.41, **Paper match CI:** 0.59

Color naming method, From 12 colors, CI: 0.65

Points of this research: In the object-matching condition of the successive experiment, an overestimation, instead of an underestimation, of the illuminant component. Because the results of matching experiments are difficult to interpret, mainly due to their sensitivity to instruction effects, we introduced another type of color-constancy task. In this task, subjects simply named the color of a simulated patch. It was found that, by applying such a task, a reliable measure of the degree of identification of object color can be obtained.

5. **Title:** Simultaneous colour constancy revisited: An analysis of viewing strategies

Author: F.W. Cornelissen, E. Brenner, Vision Research, 35 (1995), pp. 2431-2448

Illumination: Daylights, 4000K, 6500K, 10000K, von Kries shift

Background: 2D multielement (Mondrian display),

Appearance match CI: 0.18, **Paper match CI:** 0.37

Points of this research: Eye movement and adaptation data were combined to predict differences in colour matches. Two of the five subjects showed an instructional effect that was much larger than that predicted. Analysis of the eye movements, and an experiment with dynamic surrounding colours, reveal that several viewing strategies do not account for the influence of the instruction.

6. **Title:** Simultaneous color constancy: How surface color perception varies with the illuminant

Author: K.-H. Bäuml, Vision Research, 39 (1999), pp. 1531-1550

Illumination: Daylights, D65, two bluish, two yellowish illuminants,

Background: 2D multielement, Mondrian display on Monitor

Paper match CI: 0.79, **Appearance match CI:** 0.23

Points of this research: The surface matches showed a much higher level of constancy than the appearance matches. The adjustment in the surface matches was nearly complete in the L and M cone data, and deviations from perfect constancy were mainly due to failures in the adjustment of the S cone signals. Besides this difference in amount of adjustment, the appearance and surface matches showed two major similarities. First, both types of matches were well described by simple parametric models. In particular, a model based on the notion of von Kries adjustment provided a good, although not perfect, description of the data. Second, for both types of matches the illuminant adjustment was largely independent of the surface collection in the image. The two types of matches thus differed only quantitatively, there was no qualitative difference between them

7. **Title:** Colour constancy from temporal cues: Better matches with less variability under fast illuminant changes

Author: D.H. Foster, K. Amano, S.M.C.Nascimento, Vision Research, 41 (2001), pp. 285-293

Illumination: Daylights, 6700, 25000 K, Spectral product

Background: 2D multielement, square array on Monitor

Simultaneous asymmetric matching, Paper match CI: 0.6

Successive asymmetric matching, Paper match CI: 0.69

Points of this research: To test whether temporal transient cues could improve colour-constancy estimates, the degree of colour constancy was significantly higher with sequential stimulus presentation than with simultaneous presentation, The variance between observers was also markedly reduced with sequential stimulus presentation. The visual system appears to have mechanisms not requiring adaptation that can provide almost unbiased information about surface colour under changing illuminants

8. **Title:** Colour constancy under simultaneous changes in surface position and illuminant.

Author: K. Amano, D.H. Foster, Proceedings of the Royal Society of London. Series B: Biological Sciences, 271 (2004), pp. 2319-2326

Illumination: Daylights, 6700, 25000 K, Spectral product

Background: 2D multielement, square array on Monitor

Surround permutation Paper match CI: 0.75,

no permutation Paper match CI: 0.73,

Points of this research: Two kinds of constancy underlie the everyday perception of surface colour: constancy under changes in illuminant and constancy under changes in surface position. Classically, these two constancies seem to place conflicting demands on the visual system: to both take into account the region surrounding a surface and also discount it. It is shown here, however, that the ability of observers to make surface-colour matches across simultaneous changes in test-surface position and illuminant in computer-generated 'Mondrian' patterns is almost as good as across changes in illuminant alone. Performance was no poorer when the surfaces surrounding the test surface were permuted, or when information from a potential comparison surface, the one with the highest luminance, was suppressed. Computer simulations of cone-photoreceptor activity showed that a reliable cue for making surface-colour matches in all experimental conditions was provided by the ratios of cone excitations between the test surfaces and a spatial average over the whole pattern.

9. **Title:** Minimalist surface-colour matching.

Author: K. Amano, D.H. Foster, S.M.C.Nascimento, Perception, 34 (2005), pp. 1009-1013

Illumination: Daylights, 6700, 25000 K, Spectral product

Background: 2D multielement, square array, 49 surface, on Monitor**, Paper match CI:** 0.73,

Background: 2D 2surface, on Monitor, **Paper match CI:** 0.72

Points of this research: Some theories of surface-colour perception assume that observers estimate the illuminant on a scene so that its effects can be discounted. The patterns had either 49 surfaces or a minimal 2 surfaces. No significant effect of number was found, suggesting that illuminant estimates are unnecessary for surface-colour matching

Part2 Color constancy research about Successive asymmetric matching

10. Title: Limitations of surface-color and apparent-color constancy.

Author: I. Kuriki, K. Uchikawa, Journal of the Optical Society of America A – Optics Image Science and Vision, 13(1996), pp. 1622-1636

Illumination: Daylights, 1000, 1700, 2400, 3400, 6000, 30000 K, Physical reflection

Background: 2D multielement with gray background, illuminated surfaces

Successive asymmetric matching with adaptation, Appearance match CI: 0.56, **Paper match CI:** 0.69

Dichoptic successive asymmetric matching with adaptation, Appearance match CI: 0.72, **Paper match CI:** 0.77

Points of this research: With 15 min of preadaptation to the illuminant, Under 1,000-K illuminant the surface-color appearance became totally achromatic, and color constancy was completely lost. Even with brief adaptation to the illuminant, the contribution of the surrounding stimulus is large enough to achieve a fair degree of color constancy, but complete adaptation to the illuminant helps to achieve almost perfect color constancy.

11. Title: Colour constancy as a function of hue**.**

Author: J.J. Kulikowski, H. Vaitkevicius, Acta Psychologica, 97 (1997), pp. 25-35

Illumination: Colored lights, Physical reflection

Background: 2D patch with gray background , illuminated surfaces

Undifferentiated color match CI: 0.46-0.63

Points of this research: The effects of colour categories on colour constancy were studied under two illuminants and two neutral grey backgrounds using Munsell chips and colour matching. It was found

that the categorical colours: red, yellow, green and blue, which are processed by basic colour-opponent mechanisms, show relatively better colour constancy than intermediate colours. The dominant wavelength of these categorical colours are closely related to the typical hues obtained in experiments with narrow-band spectral hues.

12. Title: Color constancy under natural and artificial illumination.

Author: M.P. Lucassen, J. Walraven, Vision Research, 36 (1996), pp. 2699-2711

Background: 2D multielement, on Monitor

Haploscopic successive asymmetric matching with adaptation,

Illumination: Daylights, 4000, 6500, 25000K, Spectral product, **Appearance match CI:** 0.69,

Illumination: Metamers,(consisting two wavelengths) Spectral product, **Appearance match CI:** 0.47,

Points of this research: The results show the expected failure of color constancy under two-wavelengths illumination, and approximate color constancy under natural illumination. Quantitative predictions of the results were made on the basis of two different models, a computational model for recovering surface reflectance, and a model that assumes the color response to be determined by cone-specific contrast and absolute level of stimulation. The latter model was found to provide somewhat more accurate predictions, under all illuminant conditions.

13. Title: Measurement of color constancy by color memory matching.

Author: K. Uchikawa, I. Kuriki, Y. Tone, Optical Review, 5 (1998), pp. 59-63

Background: 2D multielement, with gray background, illuminated surfaces

Successive asymmetric memory matching with adaptation,

Illumination: Daylights, 1700, 3000, 6500, 30000K, Physical reflection, **Physical match CI:** 0.64,

Points of this research: The results show that, for most test colors, the distributions of selected colors in stages 1 to 4 were similar among all illuminants, and that the u'v' chromaticity distance between a test color under 6500 K and its matched color was quite short. These indicate that good color constancy was retained in memory color comparison.

14. Title: Response of the human visual system to variable illuminant conditions: An analysis of opponent-colour mechanisms in colour constancy.

Author: J.L. Nieves, A. García-Beltrán, J. Romero, Ophthalmic and Physiological Optics, 20(2000), pp. 44-58

Background: 2D multielement on Monitor

Successive asymmetric memory matching with adaptation,

Illumination: Daylights, Spectral product, **Paper match CI:** 0.44,

Points of this research: Data are presented showing that colour-vision mechanisms respond differently to illuminant changes when colour constancy is considered at both receptoral and post-receptoral levels. The L- and M-cones tend to adapt so as to support colour constancy, whereas S-cones are strongly influenced by the illuminant changes. In addition, the data suggest good approaches to colour constancy linked particularly to the yellow-blue mechanism.

15. Title: Almost complete colour constancy achieved with full-field adaptation.

Author:I.J. Murray, A. Daugirdiene, H.Vaitkevicius, J.J. Kulikowski, R.Stanikunas,Vision Research, 46 (2006), pp. 3067-3078

Background: 2D patch in 120deg on Monitor with gray background**,**

Successive asymmetric memory matching with adaptation,

Illumination: Daylights A, C, S, Spectral product, **undifferentiated color match CI:** 0.91,

Points of this research: Colour shifts were specified in terms of a modified Brunswik ratio (BR). Higher values of BR were associated with longer adaptation periods but only when the larger background was used. Supplementary experiments showed that the changes in colour appearance were related to a slight shift in the perceived colour of the background. The timing of the colour shifts are modelled in terms of cone opponent responses. High values of BR correspond to almost complete von Kries adaptation in all three cone types.

16. Title: Role of color memory in successive color constancy.

Author: Y.-Z. Ling, A. Hurlbert, Journal of the Optical Society of America A – Optics Image Science and Vision, 25(2008), pp. 1215-1226

Background: 2D patch with white background samples**,** illuminated surfaces

Successive asymmetric memory matching with adaptation,

Illumination: D65,D40,D14,Red,Green, Physical reflection, **Physical match CI:** 0.92,

Points of this research: They find significant effects of the illumination, reference surface, and their interaction on the matching error. They characterize the matching error in the absence of illumination change as the "pure color memory shift" and introduce a new index for successive color constancy that compares this shift against the matching error under changing illumination. The index also incorporates the vector direction of the matching errors in chromaticity space, unlike the traditional constancy index. With this index, they find that color constancy is nearly perfect.

17. Title: Color constancy improves for real 3D objects.

Author: M. Hedrich, M. Bloj, A.I. Ruppertsberg, Journal of vision, 9(4)(2009)16,1-16

Successive asymmetric memory matching with adaptation,

Illumination: D1, Tun, D2, Lily, Physical reflection,

Background: 2D multielement, illuminated surfaces, **Paper match BR:** 0.58,

Background: 3D tableau, illuminated surfaces, **Paper match BR:** 0.79,

Points of this research: Color constancy was better when the target color was learned as a 3D object in a cue-rich 3D scene than in a 2D setup. This improvement was independent of the target color and the illuminant change. Normalizing individual color constancy hit rates by the corresponding color memory hit rates yields a color constancy index, which is indicative of observers' true ability to compensate for illuminant changes.

Part3 Color constancy research about Color naming

18. Title: How much does illuminant color affect unattributed colors?

Author: L. Arend, Journal of the Optical Society of America A – Optics Image Science and Vision, 10(1993), pp. 2134-2147

Illumination: Daylights, 4000, 6500, 10000 K, Spectral product

From unique hues and gray,

Background: 2D multielement, on Monitor **, CI:** 0.66,

Background: 2D patch with gray surround, on Monitor **, CI:** 0.70,

Background: 2D patch in void, on Monitor **, CI:** 0.63,

Points of this research: The chromaticities of those same reflectances under 4000 and 10,000 K are theoretical points representing illumination-invariant appearance of the light coming from the surfaces. Even for this small range of illuminants the adaptive shifts were too small for invariance, i.e., the appearance of the light was different even after full adaptation. This result sharpens the question of the basis for humans' concept of color as a stable property of surfaces.

19. Title: Colour constancy in context: Roles for local adaptation and levels of reference

Author: H. Smithson, Q. Zaidi, Journal of Vision, 4 (2004), pp. 693-710

Illumination: Daylights, sunlight, skylight, red-blue bias, green-yellow bias, Spectral product

From 4 colors,

Background: 2D multielement with global illuminant, on Monitor, **BR:**0.83

Background: 2D multielement with test illuminant, on Monitor, **BR:** 0.86,

Points of this research: The chromatic bias of the background had only a small effect on the classification of test materials. The results suggest that mechanisms that preserve information across successive test-presentations (e.g. spatially local adaptation with a time course of a few seconds, and perceptual adjustments to levels of reference) are key determinants of the stability of colour appearance.

20. Title: Color constancy and hue scaling

Author: S. Schultz, K. Doerschner, L.T. Maloney, Journal of Vision, 6 (2006), pp. 1102-1116

Illumination: Daylights, red,yellow,green,blue, Spectral product

From 4 colors, 7 numbers

Background: 3D tableau, on stereo Monitor **, CI:** 0.70,

Points of this research: Results show that subjects had nearly stable hue scalings for a given test surface across different illuminants. The results show that hue scaling is a useful technique to investigate color constancy in a more phenomenological sense. Furthermore, the results from the blocked control experiment underline the important role of slow chromatic adaptation for color

constancy.

21. Title: Effects of spatial and temporal context on color categories and color constancy.

Author: Hansen, T., Walter, S., & Gegenfurtner, K. R. (2007)., *Journal of Vision*, *7*(4): 2, 1–15.

Illumination: neutral, reddishi, bluish-greenish, yellow-greenish, purplish, Chromatic shift

From 8 colors

Background: 2D patch with full context, on Monitor, **BR:** 0.99,

Background: 2D patch in far surround, on Monitor, **BR:** 0.49,

Points of this research: This research studied color constancy in a color-naming task under different conditions of surround illumination and patch size. Boundaries between color categories were largely stable within and across observers under neutral illumination. Under changing illumination, there were small but systematic variations in the color category boundaries. Color category boundaries tended to rotate away from the illumination color. This variation was largest under full context conditions where highest degrees of color constancy were obtained.

22. Title: Categorical color constancy for simulated surfaces.

Author: Olkkonen, M., Hansen, T., & Gegenfurtner, K. R. (2009), *Journal of Vision*, *9*(12): 6, 1–18.

Illumination: D65, reddishi, bluish-greenish, yellow-greenish, purplish, Spectral product

Background: 2D patch in background, on Monitor, **From 8 colors, BR:** 0.75,

Background: 2D patch in background, on Monitor, **Gray, BR:** 0.94,

Background: 2D fruit images, on Monitor, **Typical color, BR:** 0.76,

Points of this research: The transformations in category boundaries caused by illuminant changes were generally small and could be explained well with simple linear models. Finally, an analysis of the pattern of naming consistency across color space revealed that largely the same hues were named consistently across illuminants and across observers even after correcting for category size effects. This indicates a possible relationship between perceptual color constancy and the ability to consistently communicate colors.

Part4 Color constancy research about Achromatic adjustment

23. Title: Color constancy in the nearly natural image: 2. Achromatic loci.

Author: D.H. Brainard, Journal of the Optical Society of America A – Optics Image Science and Vision, 15(1998), pp. 307-325

Illumination: Colored lights, Physical reflection

Background: 3D room, illuminated surfaces, **Achromatic adjustment, BR:** 0.85,

Points of this research: An analysis of the achromatic settings reveals that observers show good color constancy when the illumination is varied. Changing the background surface against which the test patch is seen, on the other hand, has a relatively small effect on the achromatic loci. The results thus indicate that constancy is not achieved by a simple comparison between the test surface and its local surround.

24. Title: Mechanisms of color constancy under nearly natural viewing

Author: J.M. Kraft, D.H. Brainard, Proceedings of the National Academy of Sciences of the United States of America,96 (1999), pp. 307-312

Illumination: Colored lights, Physical reflection

Background: 3D tableau, illuminated surfaces, **Achromatic adjustment, BR:** 0.83,

Points of this research: The results rule out all three classic hypotheses and thus suggest that there is more to constancy than can be easily explained by the action of simple visual mechanisms.

25. Title: Stereo disparity improves color constancy

Author: J.N. Yang, S.K. Shevell, Vision Research, 42 (2002), pp. 1979-1989

Illumination: Daylights, Spectral product

Background: 3D tableau, Stereo monitor, **Achromatic adjustment, BR:** 0.45,

Background: 3D tableau, no stereo, Stereo monitor, **Achromatic adjustment, BR:** 0.32,

Background: 3D tableau, no specular reflection, Stereo monitor, **Achromatic adjustment, BR:** 0.28,

Points of this research: Binocular disparity was found to improve color constancy. No significant change in constancy was found due to the geometrical distortion of specular highlights that occurs without stereo disparity, suggesting that constancy depends on other features of the percept affected

by disparity. The results are discussed in terms of illuminant estimation in surface color perception

26. Title: Surface-illuminant ambiguity and color constancy: Effects of scene complexity and depth cues

Author: J.M. Kraft, S.I. Maloney, D.H. Brainard, Perception, 31 (2002), pp. 247-263

Illumination: Colored lights, Physical reflection

Background: 3D tableau, complex, illuminated surfaces, **Achromatic adjustment, BR:** 0.86,

Background: 3D tableau, simple, illuminated surfaces, **Achromatic adjustment, BR:** 0.87,

Points of this research: Two experiments were conducted to study how scene complexity and cues to depth affect human color constancy. In the valid-cue condition, many cues provided valid information about the illuminant change. In the invalidcue condition, some image cues provided invalid information. Four broad conclusions are drawn from the data: (a) constancy is generally better in the valid-cue condition than in the invalid-cue condition; (b) for the stimulus configuration used, increasing image complexity has little effect in the valid-cue condition but leads to increased constancy in the invalid-cue condition; (c) for the stimulus configuration used, reducing cues to depth has little effect for either constancy condition; and (d) there is moderate individual variation in the degree of constancy exhibited, particularly in the degree to which the complexity manipulation affects performance.

27. Title: Does human color constancy incorporate the statistical regularity of natural daylight?

Author: P.B. Delahunt, D.H. Brainard, Journal of Vision, 4 (2004), pp. 57-81

Illumination: Daylights, red, green, blue, yellow, Spectral product

Background: 3D tableau, Stereo monitor, **Achromatic adjustment, BR:** 0.73,

Points of this research: Two of these changes (Blue and Yellow) were consistent with the statistics of daylight, whereas two (Green and Red) were not. The results indicate that constancy was least across the Red change, as one would expect for the statistics of natural daylight. Constancy for the Green direction, however, exceeded that for the Yellow illuminant change and was comparable to that for the Blue. This result is difficult to reconcile with the hypothesis that mechanisms of human constancy incorporate the statistics of daylights. Some possible reasons for the discrepancy are discussed.

28. Title: The influence of depth segmentation on colour constancy

Author: A. Werner, Perception, 35 (2006), pp. 1171-1184

Illumination: Daylights, Colored lights, Chromatic shift

Background: 2D multielement, Stereo monitor, **Achromatic adjustment, BR:** 0.69,

Background: 2D multielement, test in depth, Stereo monitor, **Achromatic adjustment, BR:** 0.61,

Points of this research: It is concluded that depth segmentation supports colour constancy in scenes with inconsistent illumination changes. Processes of depth segmentation are implemented at an early sensory stage of colour constancy, and they define visual regions within which the effects of illuminant changes are discounted for separately.

29. Title: Color constancy improves, when an object moves: High-level motion influences color perception.

Author: Werner, A. (2007), *Journal of Vision*, *7*(14): 19, 1–14

Illumination: Daylights, Colored lights, Chromatic shift

Background: 2D multielement, moving test, on monitor, **Achromatic adjustment, BR:** 0.82,

Background: 2D multielement, static test, on monitor, **Achromatic adjustment, BR:** 0.63,

Points of this research: human color constancy is influenced by motion and improves when a color surface moves.

30. Title: Color constancy: Influence of viewing behavior on grey settings

Author: Jürgen Golz, Perception, Vol 39, Issue 5, 2010

Illumination: 7000K, red, green, blue, yellow, Chromatic shift

Background: 2D multielement, fixation, on monitor, **Achromatic adjustment**,

Background: 2D multielement, explore, on monitor, **Achromatic adjustment**,

Points of this research: In variegated surrounds (but not in uniform surrounds) there is a robust effect of viewing condition for all subjects and all surround chromaticities tested, in that exploration increases colour constancy compared to fixating the test field. Values of a colour constancy index are increased by as much as 20% with an average across all subjects and surrounds of 12.6%.

31. Title: Effects of surrounding stimulus properties on color constancy based on luminance balance

Author: Takuma Morimoto, Kazuho Fukuda, Keiji Uchikawa, Journal of the optical society of America A. Vol.33, Issue 3, pp.A214-A227(2016)

Illumination: 3000K, 6000K, 20000K, Red-blue, Green-yellow, Chromatic shift

Background: 2D multielement, on monitor, **Achromatic adjustment**,

Points of this research: Experimental results replicate the previous finding; i.e., luminance balance makes a small, but significant, contribution to illuminant estimation. Stimulus dimensionality affects neither the degree of color constancy nor the effect of luminance balance. Unlike chromaticity-based color constancy, chromatic variation does not influence the effect of luminance balance. It is shown that luminance-balance-based estimation of an illuminant performs better for scenes with reddish or bluish surfaces. This suggests that the visual system exploits the optimal color distribution for illuminant estimation.

Part4.Color constancy research about illuminant reflectance change judgment.

32. Title: Effect of scene complexity on colour constancy with real three-dimensional scenes and objects

Author: S.M.C. Nascimento, V.M.N. de Almeida,P.T. Fiadeiro, D.H. Foster, Perception, 34 (2005), pp. 947-950

Illumination: Daylights, Physical reflection

Background: 3D object, uniform surround, illuminated surfaces, **Same material CI:** 0.80,

Background: 3D object, complex surround, illuminated surfaces, **Same material CI:** 0.79,

Points of this research: The extent of colour constancy achieved varied little with either scene structure or test-object colour, suggesting a dominant role of local cues in determining surface-colour judgments.

33. Title: Color constancy in natural scenes with and without an explicit illuminant cue

Author: K. Amano, D.H. Foster, S.M.C.Nascimento, Visual Neuroscience, 23 (2006), pp. 351-356

Illumination: Daylights, Spectral product

Background: 2D natural scenes on monitor, illuminated surfaces, **Same material CI:** 0.71,

Points of this research: Judging surface color in natural scenes seems to be independent of an explicit illuminant cue.

34. Title: Color constancy in natural scenes explained by global image statistics

Author: D.H. Foster, K. Amano, S.M.C.Nascimento, Visual Neuroscience, 23 (2006), pp. 341-349

Illumination: Daylights, 4000- 6700K, 6700- 25000K, Spectral product

Background: 2D natural scenes on monitor, **Same material CI:** 0.69-0.97,

Points of this research: 43% of the variance in constancy index was explained by the log of the mean relative deviation in spatial cone-excitation ratios evaluated globally across the two images of a scene. A further 20% was explained by including the mean chroma of the first image and its difference from that of the second image and a further 7% by the mean difference in hue. Together, all four global color properties accounted for 70% of the variance and provided a good fit to the effects of scene and of illuminant change on color constancy, and, additionally, of changing test-surface position. By contrast, a spatial-frequency analysis of the images showed that the gradient of the luminance amplitude spectrum accounted for only 5% of the variance.

35. Title: Color constancy: Phenomenal or projective?

Author: A.J. Reeves, K. Amano, D.H. Foster, Perception & Psychophysics, 70 (2008), pp. 219-228

Illumination: Daylights, 4000-16000K, Spectral product

Background: 2D multielement(square array) on monitor, **Material appearance CI:** 0.75,

Background: 2D multielement on monitor, **Hue saturation appearance CI:** 0.35,

Background: 2D multielement on monitor, **Same material CI:** 0.77,

Points of this research: Observers seem able to separate phenomenal percepts from their ontological projections of mental appearance onto physical phenomena; thus, even when a chromatic change alters perceived hue and saturation, observers can reliably infer the cause, the constancy of the underlying surface spectral reflectance.

36. Title: Effect of scene dimensionality on colour constancy with real three-dimensional scenes and objects

Author: V.M.N. de Almeida, P.T. Fiadeiro, S.M.C.Nascimento, Perception, 39 (2010), pp. 770-779

Illumination: Daylights, 6700, 25000K, Physical reflection

Background: 3D tableau, illuminated surfaces, **Same material CI:** 0.85,

Background: 2D projection, illuminated surfaces, **Same material CI:** 0.83,

Points of this research: The extent of constancy obtained in the experiment was not influenced by scene dimensionality and varied significantly with the color of the test object. These results suggest that color constancy in the conditions tested here may be determined by local spectral quantities.

1.5 Mathematic models for color constancy

Many potential algorithms have been proposed for the color constancy. There are two main kinds of expected theoretical points: reflectance theoretical color and von Kries theoretical color. Land (1974) has developed the retinex theory of color constancy, then it has been developed to numerous computational approaches, as white-patch retinex algorithm and the gray world assumption, both algorithms assume that the illumination of the scene is uniform. Ebner (2009) has shown the approaches that estimating the illuminant locally by the gray world assumption, and Ebner (2011) also developed a computational model for the color constancy of motion object.

(1) Reflectance theoretical color model

Lambertian reflectance theoretical model is mostly used for color constancy. The apparent brightness of a Lambertian surface to an observer is the same regardless of the observer's angle of view.

$$f(x) = \int\omega \ e(\lambda)\rho k(\lambda)s(x,\lambda)d\lambda, \qquad (1\text{-}1)$$

Where, $e(\lambda)$ is the color of the light source, $s(x,\lambda)$ is de surface reflectance and $\rho k(\lambda)$ is the camera sensitivity function ($k \in \{R,G,B\}$). ω is the visible spectrum, x is the spatial coordinates and λ is the wavelength of the light.

However, the reflectance is much more complexed in the real world. We can divide reflection into three components as ideal diffuse and directional diffuse and ideal specular, as figure1.31 shows. Specular reflection mean that the light is reflected off mostly in a reflection direction.

$$f = f_{\text{ideal diffuse}} + f_{\text{directional diffuse}} + f_{\text{ideal specular}}$$
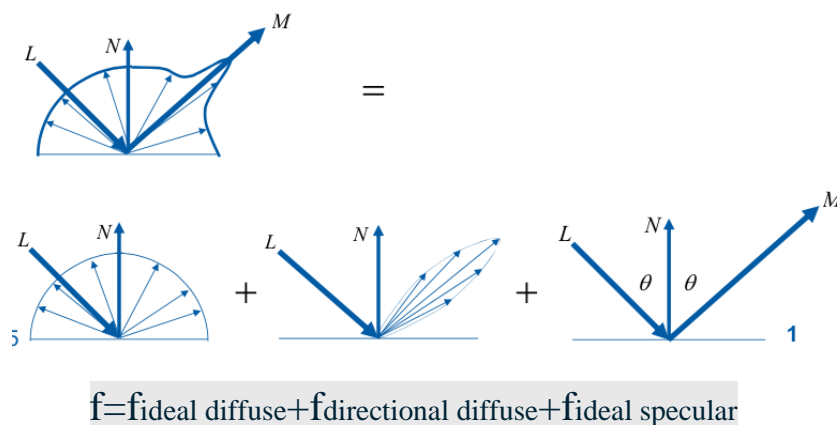
Figure 1. 31 Reflection could be divided into three components as ideal diffuse and directional diffuse and ideal specular.

By the more complex way of reflectance, Fleming(2003) has compared the different appearance of the object as figure1.32 shows. It would involve differences in color constancy.

Figure 1.32 shows the three parameters of the Ward reflectance model. Diffuse reflectance specifies the proportion of incoming light reflected by the diffuse (Lambertian) component. Specular reflectance controls the proportion of incoming light reflected by the specular component, surface roughness controls the spread or blur of the specular reflection.
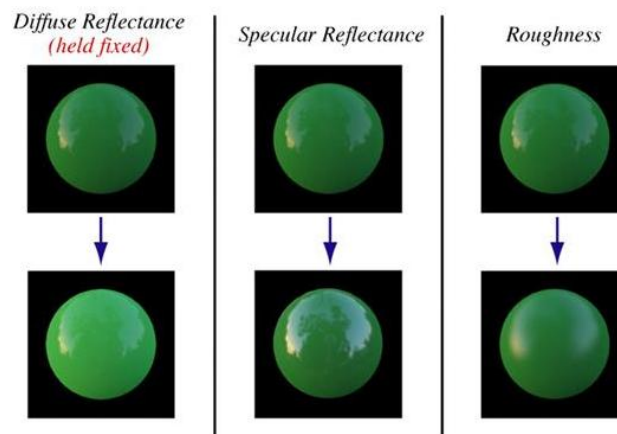
Figure 1. 32 Different appearance of diffuse , specular reflectance and roughness object from Fleming(2003)

(2) Von Kries model

The simple application of the von Kries model assumes that the sensitivity of each cone type would be reduced by adaptation to an illumination. This process is explained in Ma(2016): Reduction under the model is treated as a linear and an independent effect expressed by changes in the coefficient values, which can be used separately to multiply the sensitivity of each cone type, meaning that the influence of each object's surface is not included, in principle. For one patch, the post-adapted L-, M-, and S-cone signals should be the same under the D65 and test illumination; thus, the following equation should hold:

$$
\begin{pmatrix} L_{\text{post-adapted}} \\ M_{\text{post-adapted}} \\ S_{\text{post-adapted}} \end{pmatrix} = \begin{pmatrix} k_{L,T} & 0.0 & 0.0 \\ 0.0 & k_{M,T} & 0.0 \\ 0.0 & 0.0 & k_{S,T} \end{pmatrix} \cdot \begin{pmatrix} L_T \\ M_T \\ S_T \end{pmatrix}
$$
$$
= \begin{pmatrix} k_{L,D65} & 0.0 & 0.0 \\ 0.0 & k_{M,D65} & 0.0 \\ 0.0 & 0.0 & k_{S,D65} \end{pmatrix} \cdot \begin{pmatrix} L_{D65} \\ M_{D65} \\ S_{D65} \end{pmatrix}.
$$

(1-2)

The responses of the post-adapted cones , L post-adapted, M post-adapted, and S post-adapted,

which are the same regardless of the illumination in the von Kries model, can be obtained independently by the constants k_L, k_M, and k_S. L_{D65}, M_{D65}, and S_{D65} are the cone responses of the surface rendered under D65 illumination; L_T, M_T, and S_T are the cone responses for that surface rendered under the test illumination. The constants can be defined as the inverse of the L-, M-, and S-cone responses for a perfect white patch under the D65 illuminant and test illumination, meaning the illumination determines the constants multiplied in each of the three kinds of cones. Thus,

$$\begin{cases} k_{L,T} = 1/L_{W,T} \\ k_{M,T} = 1/M_{W,T}, \\ k_{S,T} = 1/S_{W,T} \end{cases}$$

$$\begin{cases} k_{L,D65} = 1/L_{W,D65} \\ k_{M,D65} = 1/M_{W,D65}. \\ k_{S,D65} = 1/S_{W,D65} \end{cases}$$

(1-3)

$L_{W,D65}$ and $L_{W,T}$ denote the L-cone responses excited by a perfect white patch (100% reflectance in all wavelengths)illuminated by the D65 and test illumination, respectively. $M_{W,D65}$, $M_{W,T}$, $S_{W,D65}$, and $S_{W,T}$ denote the same except the M- and S-cone responses, respectively. From Eqs. (1-2) –(1-3), the cone responses of the theoretical colors under the von Kries model can be predicted from the cone responses under the standard D65 illumination, as follows:

$$\begin{pmatrix} L_T \\ M_T \\ S_T \end{pmatrix} = \begin{pmatrix} k_{L,D65}/k_{L,T} & 0.0 & 0.0 \\ 0.0 & k_{M,D65}/k_{M,T} & 0.0 \\ 0.0 & 0.0 & k_{S,D65}/k_{S,T} \end{pmatrix} \cdot \begin{pmatrix} L_{D65} \\ M_{D65} \\ S_{D65} \end{pmatrix},$$

(1-4)

$$\begin{cases} k_{L,D65}/k_{L,T} = L_{W,T}/L_{W,D65}(= k_{L,\text{trans}}), \\ k_{M,D65}/k_{M,T} = M_{W,T}/M_{W,D65}(= k_{M,\text{trans}}), \\ k_{S,D65}/k_{S,T} = S_{W,T}/S_{W,D65}(= k_{S,\text{trans}}). \end{cases}$$

(1-5)

Figure1.33 shows the example of calibration of the image by Von Kries model.
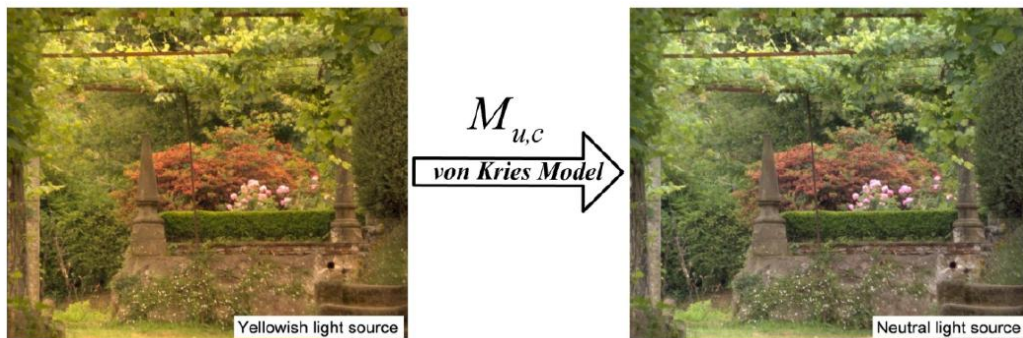
Figure 1. 33 The examples of calibration of the image by Von Kries model. From Gao(2013).

(3) Retinex theory of color constancy

Land (1974) has developed the retinex theory of color perception. It works on assumption that an abrupt change in chromaticity is caused by a change in reflectance properties. This implies that the illuminant smoothly varies across the image and does not change between adjacent or nearby locations. This algorithm partially addresses the issue of varying illumination. White patch retinex and gray world assumption are based under the assumption of under uniform illuminations, these methods do not perform well enough compared to recent more complex methods, because these assumption is violated in real images. Land has later developed center-surround retinex(CSR) model by using convolution method to estimate the illumination, based on the assumption of nonuniform illumination which is more conformed to the performance of human vision. Ebner has developed the local space average color model based on the resistive grid simulation to explain color constancy. Now more complex methods as SSR(Single-Scale retinex), MSR(Multi-Scale Retinex),CNN(Center Neural Networks) has been developed for the computational method for color constancy. These methods are different in the way of illumination estimation. The term illumination estimation refers to estimate the geometry or direction of light , or to estimate the color of light, or to estimate the full spectral power distribution of light. The illumination estimation methods falls into following categories explained by Kulkarni, Seema G.(2014): (1) statistical methods estimates the illuminant for each image based on its statistical properties, as white patch retinex and gray world assumption (2) physics-based methods estimates the illuminant using physical models of image formation, (3) learning-based methods estimates illuminants by a model that is learned from training images, as CNN and (4) gamut based methods compares a canonical gamut and image gamut to estimate the illuminant. We select some of the computational methods to discuss as follows:

➢ **White patch retinex**

The white patch retinex algorithm is basically just a simplified version of the retinex algorithm. This algorithm is based on the assumption that, if there is a white patch in the scene, then this patch reflects the maximum light possible for each band.

input2   White Patch Retinex
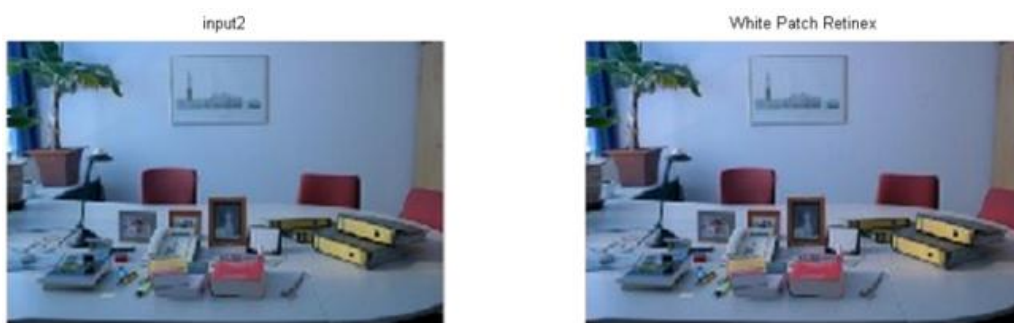
Figure 1. 34 The white patch retinex algorithm is used to perform the color adjustments for the input image, the result is show in the right side. From Ebner(2007).

> ➢ **Gray world assumption**

Buchsbaum(1980) developed the gray world assumption. It estimates the illuminant using the average color of the pixels. This algorithm is based on the assumption that, on the average, the world is gray. Assuming that we have a good distribution of colors in our scene, the average reflected color is assumed to be the color of the light. Therefore, we can estimate the illumination color cast by looking at the average color and comparing it to gray. Gray world algorithm produces an estimate of illumination by computing the mean of each channel of the image. One of the methods of normalization is that the mean of the three components is used as illumination estimate of the image.
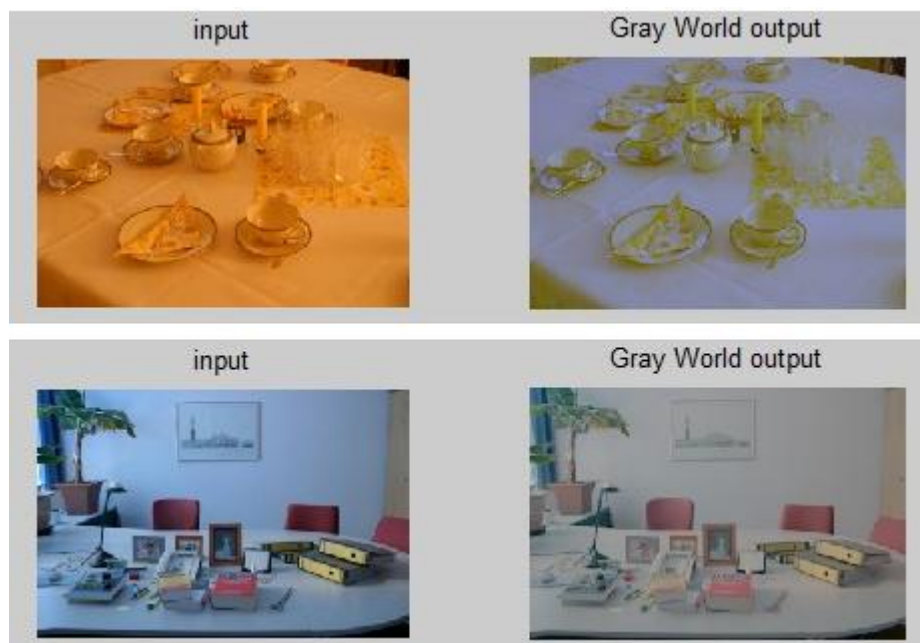
Figure 1. 35 The gray world assumption algorithm is used to perform the color adjustments for the input image, the result is show in the right side. From Ebner(2007).

➢ **Ebner's model of local space average color and color constancy model for motion object**

Ebner's model for motion object is constructed on the Werner's color constancy experiment of motion object, in the model, color stimuli were converted from Luv color space to sRGB space. The three channel RGB system corresponds to the retinal receptors which absorb light in the red, green, and blue parts of the spectrum. The intensity, O_i, retina (x, y) measured by the retinal receptors for three channels of red, green, and blue, $i \in \{r, g, b\}$ at position (x, y) in the image , is given by

$$O_{i\,retina}(x, y) = \log R_i(x, y) + \log L_i(x, y) \tag{1-6}$$

where Ri(x, y) is the reflectance, Li(x, y) is the intensity of the irradiance, here the assumption is that even though the illuminant is non-uniform, it varies smoothly over the image, and the local space average color ai(x,y) is computed as

$$a_i(x, y) = \frac{1}{|N(x, y)|} \sum_{(x', y') \in N(x, y)} a(x', y') \tag{1-7}$$

Let N (x , y) be the set of neurons which are resistively coupled to neuron (x , y).

In the motion condition with the pursuit eye moment, a temporal averaging of local space average color $\tilde{a}(x, y)$ was calculated as

$$\tilde{a}(x, y) := p_t a(x, y) + (1 - p_t)\, \tilde{a}(x, y) \tag{1-8}$$

where p_t=0.1, Figure1.36 shows the same stimuli observed in the aspect of the retinal receptors. The eyes essentially track the test patch maintaining it exactly in the fovea of the retina, and 8 frames were taken to make convolution with Gaussian spatial filter. Then the averaged 8 frames as the temporal and local-space averaged color was obtained as showed in the top of Figure 1.37.
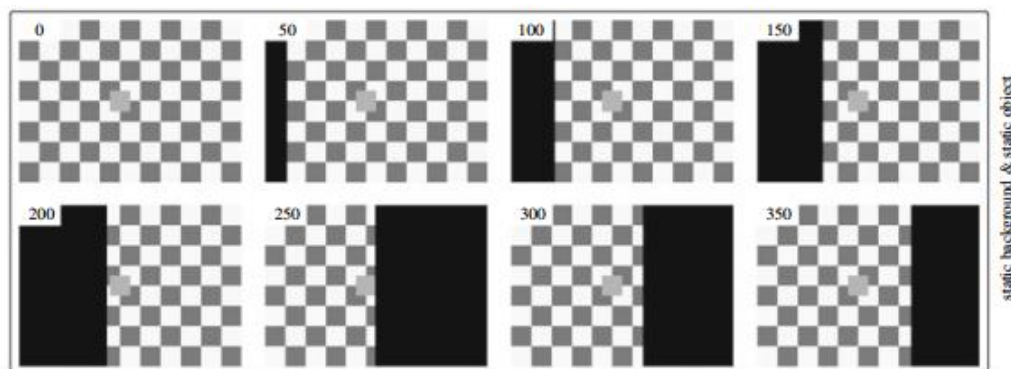
Figure 1. 36 Visual stimulus for experiment as measured by the retinal receptors under motion condition with pursuit eye movement.
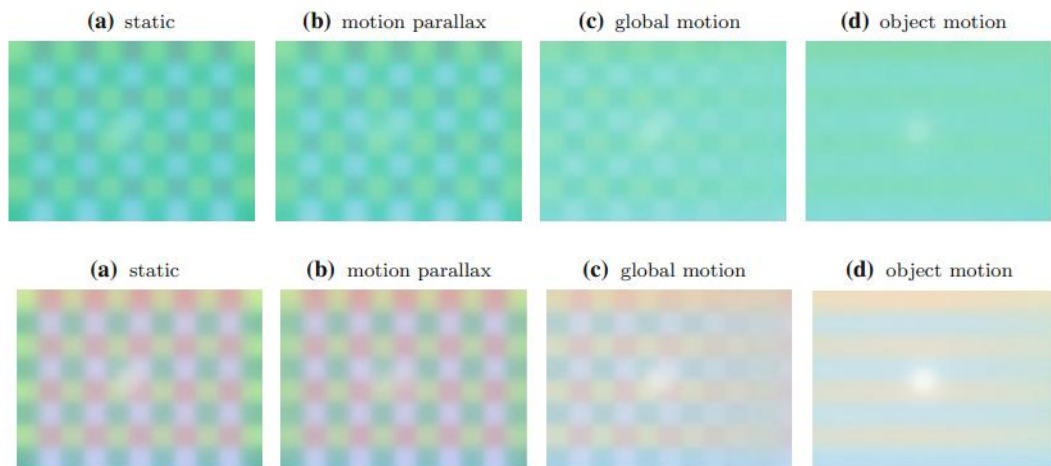
Figure 1. 37 Top figure is Local space averaged color computed by Ebner's mathematical model. Bottom figure is bias with respect to the illuminant for experiments.From Ebner(2011).

The color constancy descriptor Oi, cc (x, y) is computed by essentially subtracting local space averaged color ai(x, y) from the measured color   Oi, retina (x, y). This process is like the process of illumination estimation, which needs to offset the bias color caused by the induction and adaptation.

$$O_{i,cc}(x,y) = O_{i,retina}(x,y) - a_i(x,y) = \log R_i(x,y) + 1 \qquad (1\text{-}9)$$

*
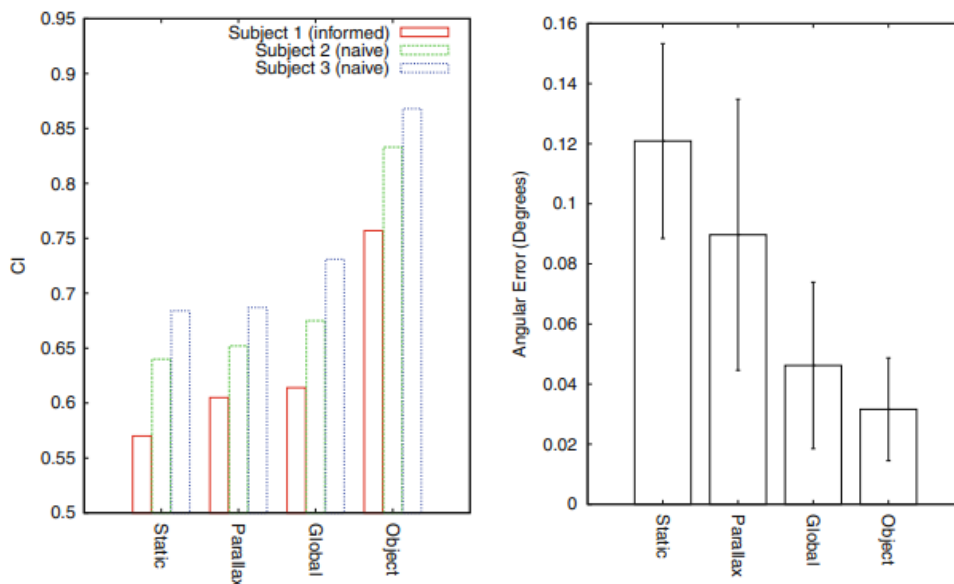
Figure 1. 38 The color constancy descriptor is computed under motion and static condition.From Ebner (2011).

Then apply the inverse of the cube root function to obtain reflectance estimates, $\vec{R}$

$$\vec{R} = (|O_{cc}(x,y) + [k,k,k]|)^3 \qquad (1\text{-}10)$$

The color of the illuminant $\vec{R}$ is estimated by taken the average reflectance estimates over all pixel values of the test patch. Then, the angular error is defined as

$$e = \cos^{-1}\frac{\vec{R_e}\,\vec{R_d}}{|\vec{R_e}|\,|\vec{R_d}|}$$

(1-11)

$\vec{R_d}$ is the estimated reflectance under illuminant D65, $\vec{R_e}$ is the estimate under a non-standard illuminant. Figure1.38 shows the angular error, e between the estimated reflectance under a standard D65 illuminant and a non-standard illuminant obtained from the modified Ebner's model. I have simply the model of Ebner's model and use it to calculation models for our experiment, and I will discuss it again in chapter 5.

(4) Double-opponency color constancy model

The double-opponent (DO) color sensitive cells in the primary visual cortex (V1) of the human visual system have been recognized as one of the important reason for color constancy. Fleet (1985) and Richter(1982) showed a center-surround model by the Difference-of-Gaussian function.
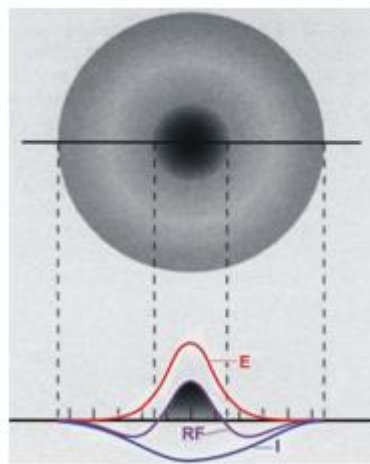
Figure 1. 39 DOG model, from Xiao(2008)

We will discuss in details later in chapter 5. Figure1.38 show some examples of both indoor and outdoor images corrected with the illuminant estimates of various methods from Shao-Bing Gao (2015).

Figure 1. 40 Some examples of indoor and outdoor images from Gehler-Shi dataset corrected with multiple methods. From Gao (2015).

1.6 Research motivations

The adaptation of the cone photoreceptors at the retina and cognitive mechanism occurring at a higher level are considered as two main factors contributing to the color constancy. Ma et al. (2016) mentioned the higher-level mechanism for the color constancy underlying the statistical operation of the scene and illuminant-by-illuminant estimation strategy, which depend on the appearance of the scene. The contribution of these complex mechanisms should be compared to that of the von Kries adaptation mechanism using simple adaptation and/or gain control. In this study, we did not specify the certain mechanism as the higher-level process contributing to the color constancy. Instead, we summarized these mechanisms as the illumination estimation effect.

However, it is not clear whether the utilization of these two types of color constancy mechanisms depend on different observing modes: eye movement and attention. The eye movement, mentioned in this study as the difference between eye fixation and smooth pursuit eye movement, will make different situations of retinal adaptation. Werner (2007) and Ebner (2011) reported that the color constancy improves with an object motion. In these experiments, the color constancy was tested in an achromatic experiment under the situation that observers fixed eyes on the stable objects, or pursued to track the moving objects although the attention was not considered. However, the attention may also have different effects on the retinal adaptation and eye movement combined with the attention state could subsequently influence to the color constancy. Suchow and George (2011) reported that the motion could cause failure to detect changes of color and size, except in the case that the observer attended to the objects and noticed the objects' changes. Golz (2010) found that the viewing behavior also has influences on color constancy; the exploration in the visual field increases the color constancy compared to fixating to the test field.

From these previous researches, I have the following questions:

➢ The achromatic adjustment experiment provides only an estimation of the illumination at that point. Could it be able to represent the color constancy of the other colors?

➢ If the observers pay attention to the surround colors when the target is moving, will it have some influences on color constancy?

Therefore, the main purpose of this study was to investigate about the possible influences of motion and attention controlled by gaze-state to the retinal adaptation. The amount of contribution of the retinal adaptation to the color constancy was estimated with the amount of the overall color constancy; the difference between them would be attributed to the contribution of illumination estimation effect occurred at the higher-level mechanism.

Chapter2

General methods

2.1 Apparatus and calibration

All experiments were performed in a darkened room. The stimuli were presented on 19-in CRT color monitor (Sony, Trinitron G420). Visual stimulus generation (VSG) system (ViSaGe, Cambridge Research Systems (CRS), Inc.) provided 14-bit resolution for each RGB phosphor in 1280×960 resolution under 60 Hz frame rate. A black paper board (90 cm*60 cm) was vertically placed in front of the observer to create a haploscopic presentation in which the left half of the screen was viewed by the left eye and the right half was viewed by the right eye. The observer was situated 90 cm from the CRT monitor, and viewed haploscopicly with his/her head supported by a chin rest. The handheld 6-button box (CB-6, CRS) was used for observer's response of the color adjustment. The gamma correction of the monitor was carried out by the calibration software of the VSG system (VSG-Desktop, CRS) with light measurement instrument (ColorCAL, CRS) and a spectral radiometer (CS-200, Konica-Minolta, Inc.), confirmed that the error of screen presentation was less than 3% in CIE1931 xy chromaticity coordinates, and less than 5% in luminance.
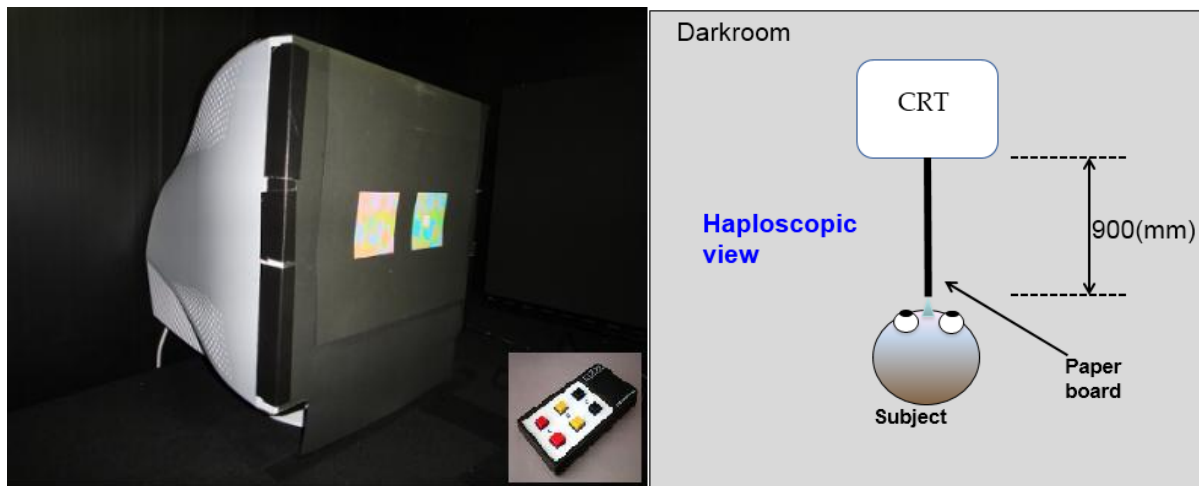
Figure 2. 1 The apparatus of the color constancy experiment.

2.2 Visual Stimulus

Figure 2.2 shows the visual stimulus consisting of 5 deg. square standard pattern virtually illuminated by the standard illumination, D65 (6500 K daylight) and 5 deg. square test pattern virtually illuminated by red, green, blue, yellow test illuminations; the standard and test patterns were presented side by side, separated by a 1 deg., completely-black space made with the black paper board flame covering the entire monitor screen except for those two patterns. Paired patterns had an identical spatial arrangement, consisting of a 1.2 deg. square color patch at the center surrounded by background ellipses. The background of both patterns was composed of 230 superimposed ellipses painted one of eight colors (see below). Each ellipse had a random position and orientation with a random size change between 0.8 and 1.2 deg. in the shorter axis and between 1.6 and 2.0 deg. in the longer axis. These two patterns were observed in a haploscopic view; the left standard pattern was observed by left eye and the right test pattern was observed by right eye; the black paper board was vertically placed from the screen to the eye at the center of two patterns to prevent pattern viewing by the other eye.
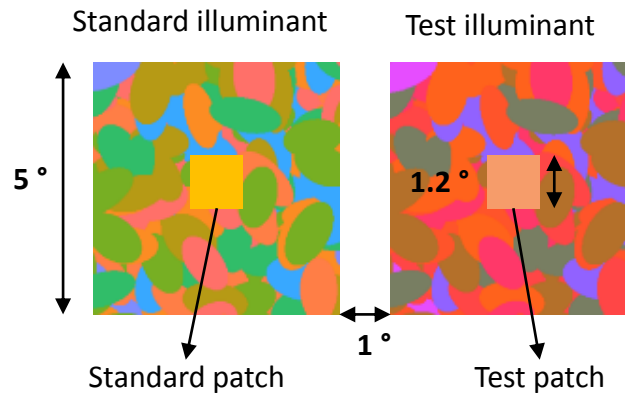
Figure 2. 2 Example of test stimulus for red illumination condition. The standard pattern under D65 illumination (left) and the test pattern under colored illumination (right) were presented haploscopically in each trial. The left and right locations of patterns were changed from session to session.

All colors used in the stimuli were simulations of Munsell matte color surfaces. The colors were calculated using spectral reflectance from the Munsell Book of Color and the spectral radiance of the illumination. The spectral reflectance of the central colored patch was selected from among 12 Munsell surfaces: Munsell 5R5/6, 2.5YR5/6, 10YR5/6, 7.5Y5/6 , 5GY5/6, 2.5G 5/6, 10B5/6, 7.5PB5 /6, 5P5/6, 2.5RP5/6, 10RP5/6, Figure 2.3 shows chromaticity coordinates of these test colors under the D65 llumination.
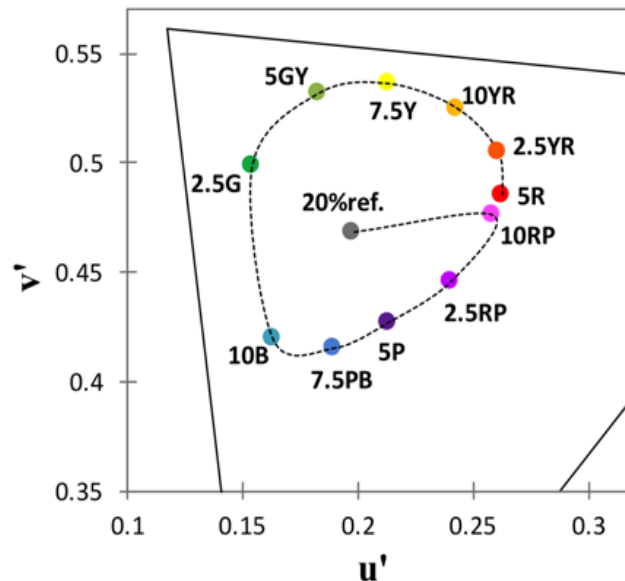
Figure 2. 3 CIE 1976 u'v' chromaticity coordinates of the twelve central colored patches, illuminated by D65 illumination. The label denotes the code in the Munsell color system. The Value and Chroma were 5 and 6.

The reflectance spectra in the background ellipses were composed of eight Munsell surfaces, taken from the Munsell Book of Color with Value 5 and Chroma 6, yielding an angle distance of approximately 45 deg in the hue circle of the Munsell Color System. Considering that the color of

the background surfaces cannot be the same as that of the central patches, in case observers might refer to the background color in the adjustment of the central patch, the Chroma of the background color was changed at random to either 4 or 8 if the randomly selected hue coincided with one of the twelve surfaces used in the central colored patch. The eight surfaces forming one background pattern, different for each of the 6 sessions, were obtained by rotating the Munsell hue circle clockwise.

The standard illuminant was illuminant D65 and invariant in all experiment sessions. The test illuminant was constructed by a linear combination of the daylight spectral basis functions. The color of illuminants were shifted from D65 by the specific color difference defined by CIE 1976 L*u*v*, $\Delta ef_{uv.}$ on equal luminant plane. The color of red and green illuminants were shifted equally by the color difference of 53 $\Delta E*_{uv}$ along (L-M) axis. The color of blue and yellow illuminants were shifted by the color difference of 45 $\Delta E*_{uv}$ along [S-(L+M)] axis. The intensity of each illumination was adjusted to achieve the same luminance on the 20% flat-reflectance surface illuminated to be 25 cd/m2. Table 1 summarizes CIE 1931 xy chromaticity coordinates, Color difference, $\Delta E*_{uv}$ and difference of L- or S-cone excitation for the color illuminants.

The chromaticity coordinates of the Munsell surfaces under D65 and the test illuminations were calculated using CIE 1931 standard color matching functions. Spectra were sampled at 5 nm intervals and integrated from 380 to 780 nm. We used Smith–Pokorny's cone fundamentals and the CIE 1931 color-matching function with the cone matrix by Kaiser and Boynton. Figure 2.4 shows u'v' chromaticity coordinates of 12 colors under red, blue, yellow, green and D65 illuminants. Figure 2.5 shows the stimulus configuration in the haplosocpic appearance under red, green, blue and yellow using the 20% flat-reflectance surface as the contral target.
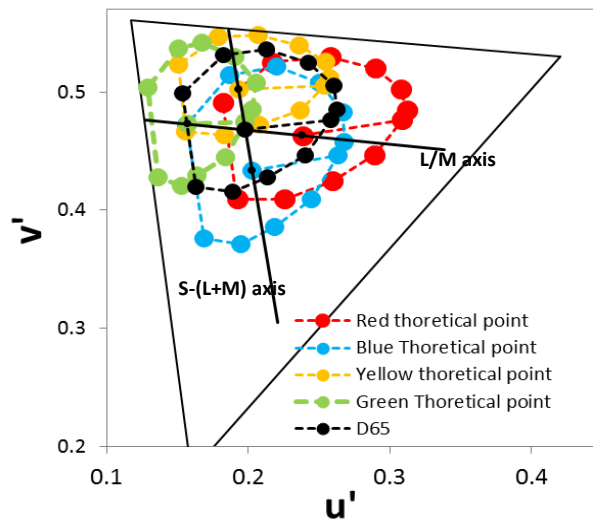
Figure 2. 4 u'v' chromaticity coordinates of 12 test colors under the D65, red, green, blue and yellow illuminants denoted by black, red, green, blue and yellow circles, respectively. Slanted vertical and horizontal black-lines denote S-(L+M) and (L-M) axes, respectively.

Table2.1 Illumination condition (CIE1931 xy chromaticity coordinates, Color difference, ΔE*uv and difference of L- or S-cone excitation)

	X	y	ΔE	ΔL or ΔS
R	0.3562	0.3074	53	+4.9% ΔL
G	0.2635	0.3516	53	-4.8% ΔL
B	0.2907	0.2736	45	-43% ΔS
Y	0.3393	0.3923	45	-37.5% ΔS
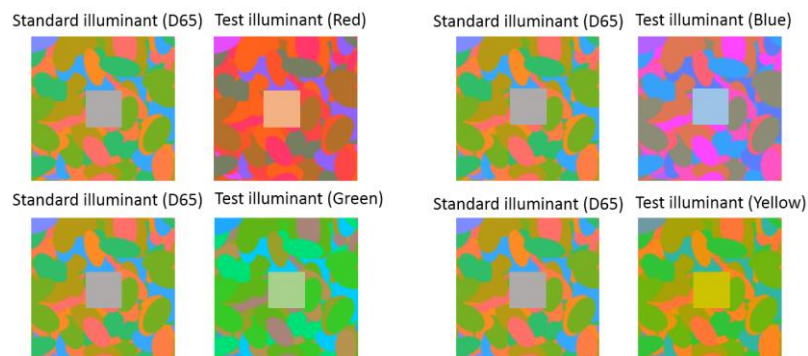
Figure 2. 5 Stimulus configuration under red (top-left), green(bottom-left), blue (top-right) and yellow (bottom-right) test illuminant conditions in Haploscopic view.

2.3 Procedure

In order to control the state of the color constancy measurement, we set two parameters. The first parameter was about the motion of the target: target-static, target-motion, and target-rotation conditions. In the case of the target-static condition, the test-patch stayed at the center of the static background, as shown in Fig. 1. In the target-motion condition, the central test-patch (in right or left) and standard-patch (in left or right) in the paired patterns moved simultaneously from the top to the bottom of the patterns with the speed of the 3 deg./s. This vertical movements were continuously looped along the vertical lines at the horizontal center of each background pattern. In the target-rotation conditions, the test patch rotated counterclockwise in a circular fashion staying within 2 deg. in center of the background.

So as to modulate attention, we additionally set the second parameter about the observation; eye-fixation and eye-free conditions. In the eye-fixation condition, the observer was asked to fixate their eye on the test- and standard-patches. We would like to mention that in the target-motion condition, the eye-fixation means the pursuit eye movement to the moving target and it does not mean that the eye is not moving. In the eye-free condition, the observer was asked to explore the entire stimulus. The observers were instructed before the experiment as follows; in the eye-free condition, "make paper match and explore the screen by looking around the surrounding colors, move your gaze to different parts of the scene." In the eye-fix condition, "Make paper match and fixate your eyes on the test- and standard-patches during the matching task, even if the patches move vertically".

At the beginning of the session, the observer adapted to the D65, 25 cd/m2 white-screen for 5 min with both eyes. Before starting trials, the observer adapted to the backgrounds for 5 min with the colored illumination for one eye and under the D65 illumination in the other eye. After the adaptation, the observer started to conducr the paper match for static targets, motion targets and rotation targets. In the first part of the experiment, the observer was instructed to explore the surround in the eyes-free condition. In the second part, the observer was instructed to fixate eyes on the target in the eye-fixation condition. The one trial continued until the observer completed the matching and the averaged time for one tiral was about 1 min. There were 12 trials performed in pseudo-random order for each condition, corresponding to the 12 different surfaces of the central test-patches. Each matching point was averaged over 6 sessions for one observer. In 3 sessions, the left side was the standard pattern illuminated by D65, and the right side was the test pattern illuminated by the test illumination; the reverse arrangement was used in the other 3 sessions. Each session took about 90 min.
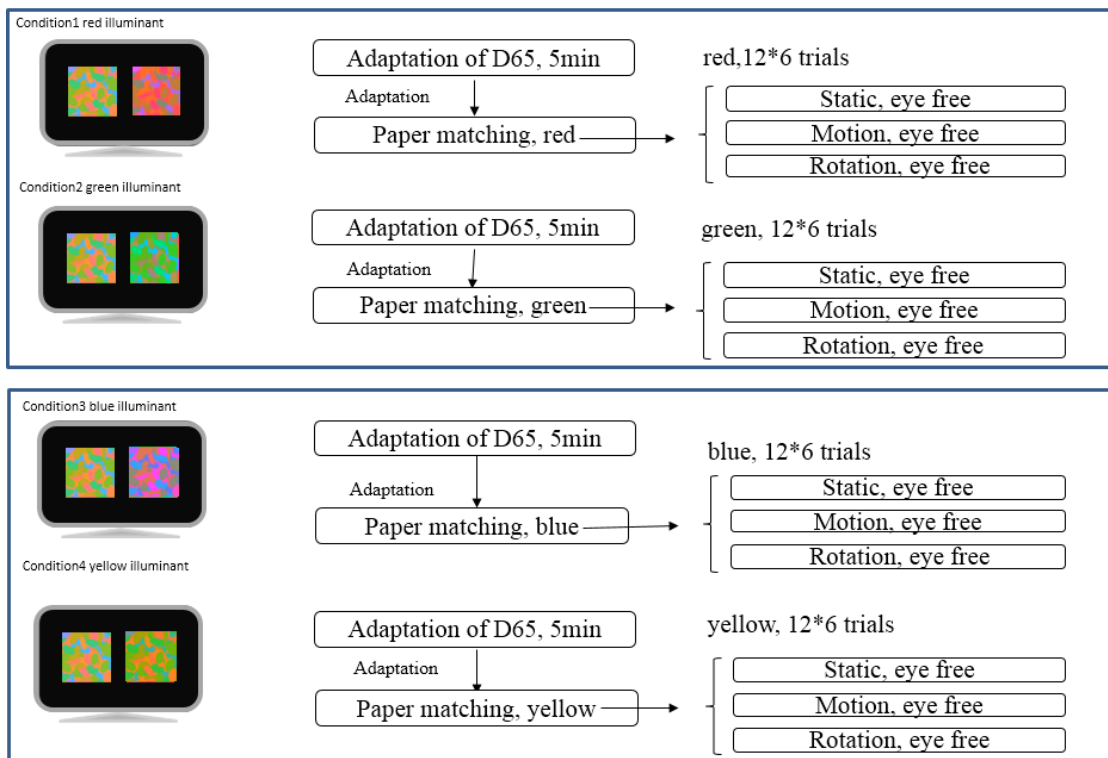
Figure 2. 6 Procedure for the color constancy experiment with eye free
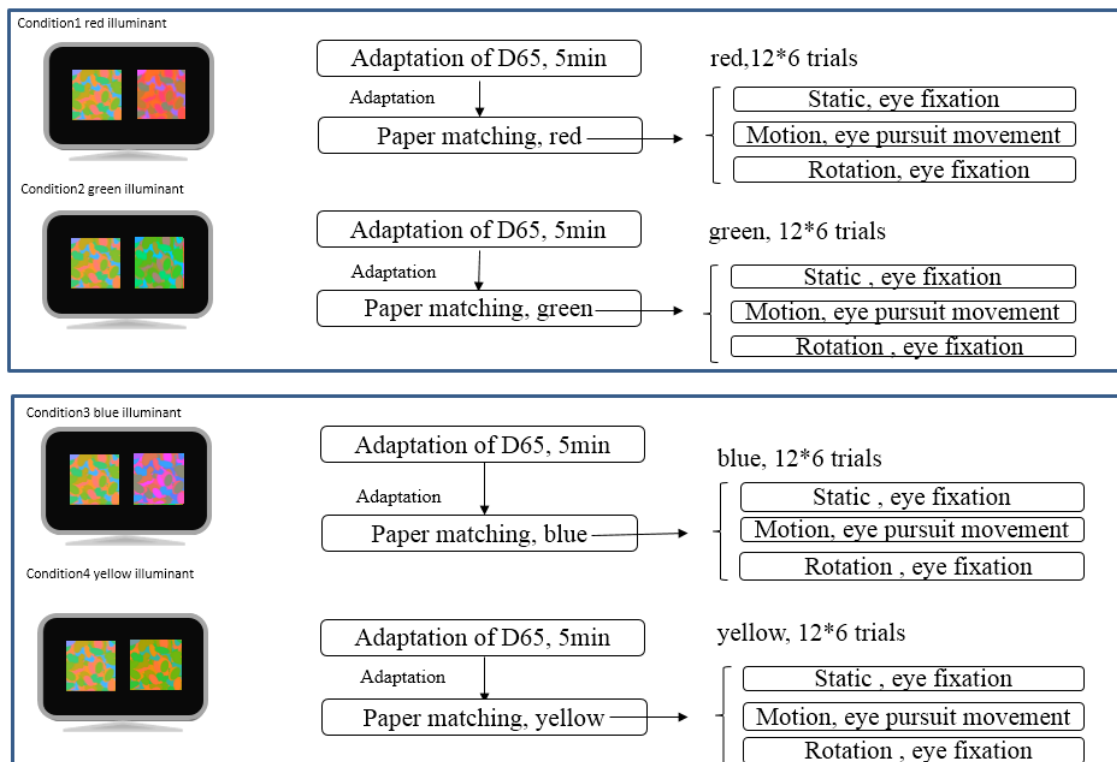
Figure 2. 7 Procedure for the color constancy experiment with eye fixation

2.4 Instruction

Observers were told that the paper arrays of two patterns were identical and illuminated by different or same light sources and one pattern could not be seen simultaneously by two eyes. Observers were instructed to adjust the color and brightness of rectangular patch in the test pattern and make the test patch look as if "it were cut from the same piece of paper as the corresponding patch in the standard pattern". Time was not limited.

2.5 Observers

Six observers (2 male and 4 female) in the age from 21 to 28 years old participated in this study. We confirmed that all observers had normal or corrected-to-normal visual acuity better than 0.6 (1.67 min. of visual angle) and they had normal color vision assessed by Ishihara-plate and D-15 tests. The procedures and experiments conform to the principles expressed in the Declaration of Helsinki and were approved by Kochi University of Technology Research Ethics Committee. Written informed consent was obtained prior to testing.

Chapter3

RESULTS

3.1 Color Constancy Performance

For color normal observers, the color constancy index proposed by Arend was used to quantitatively evaluate the degree of color constancy. The index I, is defined as

$$I = 1 - b/a; \qquad (3-1)$$

Where b denotes the Euclidean distance from the matched point to the theoretical point (the chromaticity coordinates of the patch under test illumination) at which the color constancy would be perfect in the sense of predicting the color appearance of the patch under the test illumination, a denotes the Euclidean distance from the standard point (the chromaticity coordinates of the patch under D65 illumination) to the theoretical point. In this study, the distance was defined in two-dimensional CIE 1976 uvL color space. An index value of 1 indicates perfect color constancy (the matched point would coincide with the theoretical point); an index value of 0 indicates no color constancy.

If cone adaptation/gain control to illuminant plays a prominent role in surface match, the (uvL chromatic shift, luminance or cone responses of twelve matched colors will coincide with those of the von Kries theoretical colors. If theoretically calculated color estimation mechanism plays a key

role, the various values of twelve matched colors will overlap with those of reflectance theoretical colors. The coefficients in the von Kries model here were taken to be the inverse of the L, M and S cone responses for a perfect white patch under standard illuminant D65 or test illuminants. The Smith and Pokorny cone fundamentals (Smith and Pokorny1975) and CIE 1931 color matching function were used to convert match results into cone responses.

Figures 3.1, 3.2, 3.3 and 3.4 show the constancy indices of the color normal observers on twelve color patches under red, green, blue, yellow illuminations. The results indicate that the target motion did not improve the color constancy, it is different with achromatic adjustment experiment of Werner(2004). Each result could be influenced by different situations of cone adaptation and illumination estimation effect.
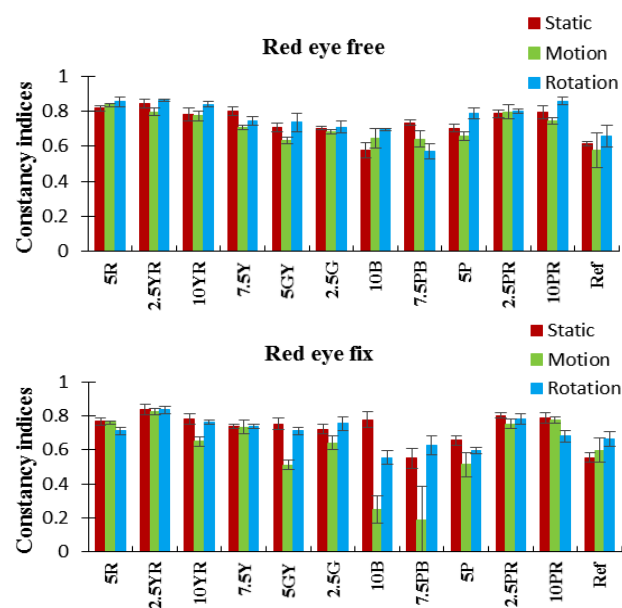
Figure 3. 1 Constancy indices of color normal observers on twelve color patches under the red illumination with eye free conditions and eye fixation conditions. Red, green and blue bars represent target-static, target-motion, and target-rotation conditions. The value for each color patch was averaged over six observers. Error bars represent the ±2SEM.
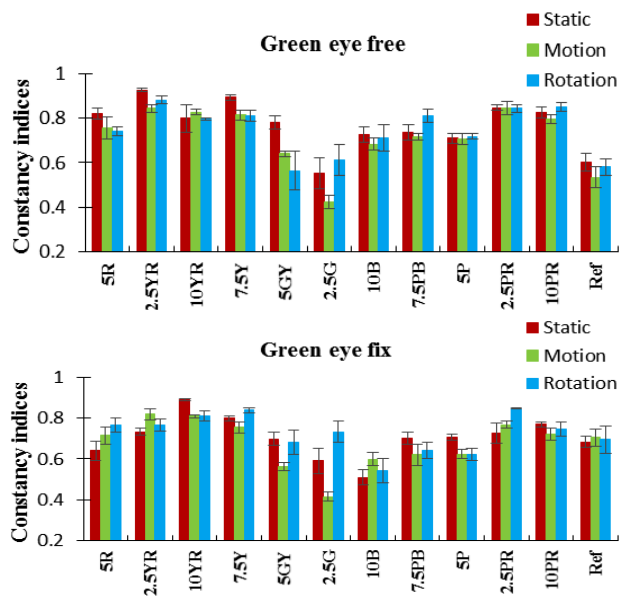
Figure 3. 2 Constancy indices under the green illumination. All other details are the same as in Figure3.1.
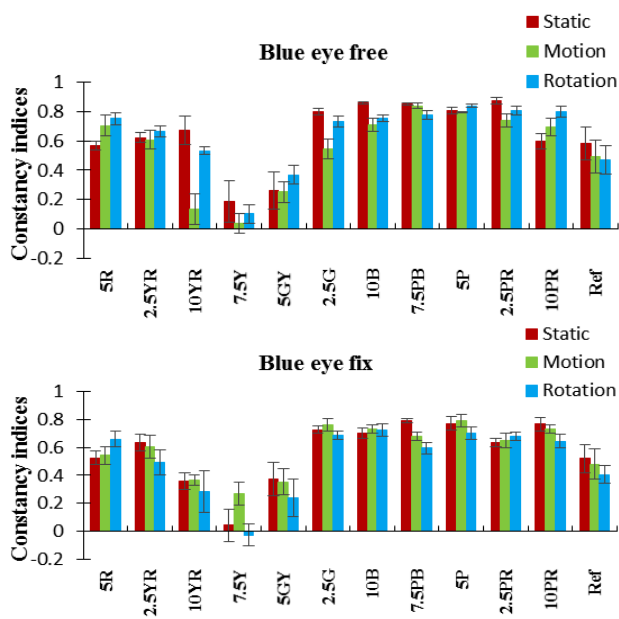
Figure 3. 3 Constancy indices under the blue illumination. All other details are the same as in Figure3.1.
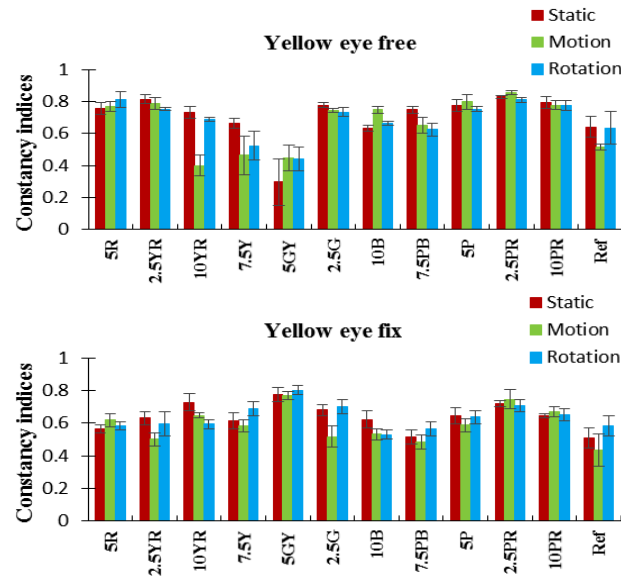
Figure 3. 4 Constancy indices under the yellow illumination. All other details are the same as in Figure3.1.

Figure 3.5 shows Mean constancy indices of six observers and twelve color surfaces with eye-free and eye-fixation conditions under red, green, blue, and yellow illuminations. The tendency of the data will be analyzed in the next subsection
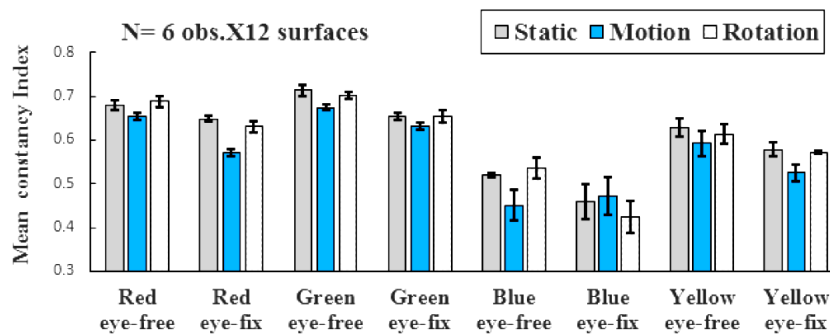
Figure 3. 5 Mean constancy indices of six observers and twelve color surfaces with eye-free and eye-fixation conditions under red, green, blue, and yellow illuminations. Gray bars, blue bars and patterned bars represent target-static, target-motion, and target-rotation conditions, respectively. Error bars denote ±2SEM

3.2 Three-way repeated measures analysis of variance (ANOVA)

We conducted three-way repeated-measures analysis of variance (ANOVA) in parameters of the attention control (eye-free and eye-fixation conditions) and the target motion status (target-static, target-motion, and target-rotation conditions) with test illuminants (red, green, blue, and yellow illuminations) as within-subject factors. We found significant main effects of target motion status was significant (F=11.808, p=0.021<0.05). Attention control by gaze-state was not significant (F=5.203, p=0.071>0.05). Test illuminants was not siginificant (F=6.043, p=0.087>0.05). Note that there was no significant interaction.

Multiple comparison by Bonferroni's correction (significance level: 0.05) revealed that the color constant indices, *CIs* were significantly higher for the static and rotation conditions than those for the motion conditions. The color constancy of four illuminations were in the order of green > red > yellow > blue, and there were significant differences between red & blue, green & blue, and green & yellow illuminant comparisons. Statistical analysis were summarized in Table 3.1.

Table 3.1 Multiple comparison by Bonferroni's correction (significance level: 0.05)

Compare conditions	Mean difference ΔCI	sig
static- motion	0.039	0.009**
rotation- motion	0.031	0.037*
static-rotation	0.008	0.97
Compare conditions	**Mean difference ΔCI**	**sig**
red- blue	0.169	0.031*
green- blue	0.195	0.035*
yellow-blue	0.108	0.171
red-yellow	0.061	0.073
green-yellow	0.087	0.033*
green-red	0.026	0.178
Compare conditions	**Mean difference ΔCI**	**sig**
eye free- eye fix	0.053	0.071

3.3 L, M, S cone response and Luminance

Figure 3.6 shows the L,M,S cone responses and luminance matches under red illuminant. Standard colors are denoted by black symbols; matched colors under static conditions by red symbols; matched colors under motion conditions by green symbols; matched colors under rotation conditions by blue symbols; von Kries predicted color by orange symbols and reflectance predicted color by gray symbols.

From figure 3.6 under red illuminant,

1) L cone responses of matched colors are mostly larger than those of von Kries predicted colors, and close to theoretical reflectance data. It indicates the observers use some high level cognitive strategies to do the illumination estimation. However, the color patch of 10PR and ref made the matched color curve seems that it follows the shape of von kries model, it indicates that adaptation also plays an important role under red illumination, too. Compare with eye free and eye fix condition, Lcone response are more closer to reflectance data under eye free conditions than eye fix conditions. It implys that eye fix could reduce the high level cognitive ability, involves less illumination estimation, and more influenced by cone adaptation. It is very easy to imagine that when observers fixed their eyes, they could not pay attantion to the surrounding colors and they could not calculate colors as beter as when they explored surrounding areas.

2) M cones response are mostly closely to those of von Kries predicted colors. Because of the von Kries model and theoretical model are similar to each other, so I could not say whether the M cone response is more influenced by adaptation or by illumination estimation. Compare with eye free and eye fix condition, M cone response are more closer to reflectance data under eye free conditions than eye fix conditions, this is same with L cones.

3) The S cone responses predicted by von Kries or reflectance model show that the illuminant change from D65 to red illuminant does not produce noticeable S cone stimulation changes. S cone responses of matched colors appear to correspond well to those of standard colors and theoretical colors, except those of color chips (10B5/6), (7.5PB5/6), (5P5/6) in blue region, especially under the eye fix condition, matched colors of motion condition are much more larger than rotation and static condition. Why S cone has such a large change in blue regions when target motion and fixation eyes?

4) Luminance is determined by L and M cone responses, by considering the luminance matches and corresponding L, M cone responses together,it is expected that the luminance of matched colors is

not only contributed by cone adaptation/gain control, but also determined by a high level cognitive strategy. This result reveals that von Kries rule has limitations to explain the lightness constancy(Kulikowski et al.2012).
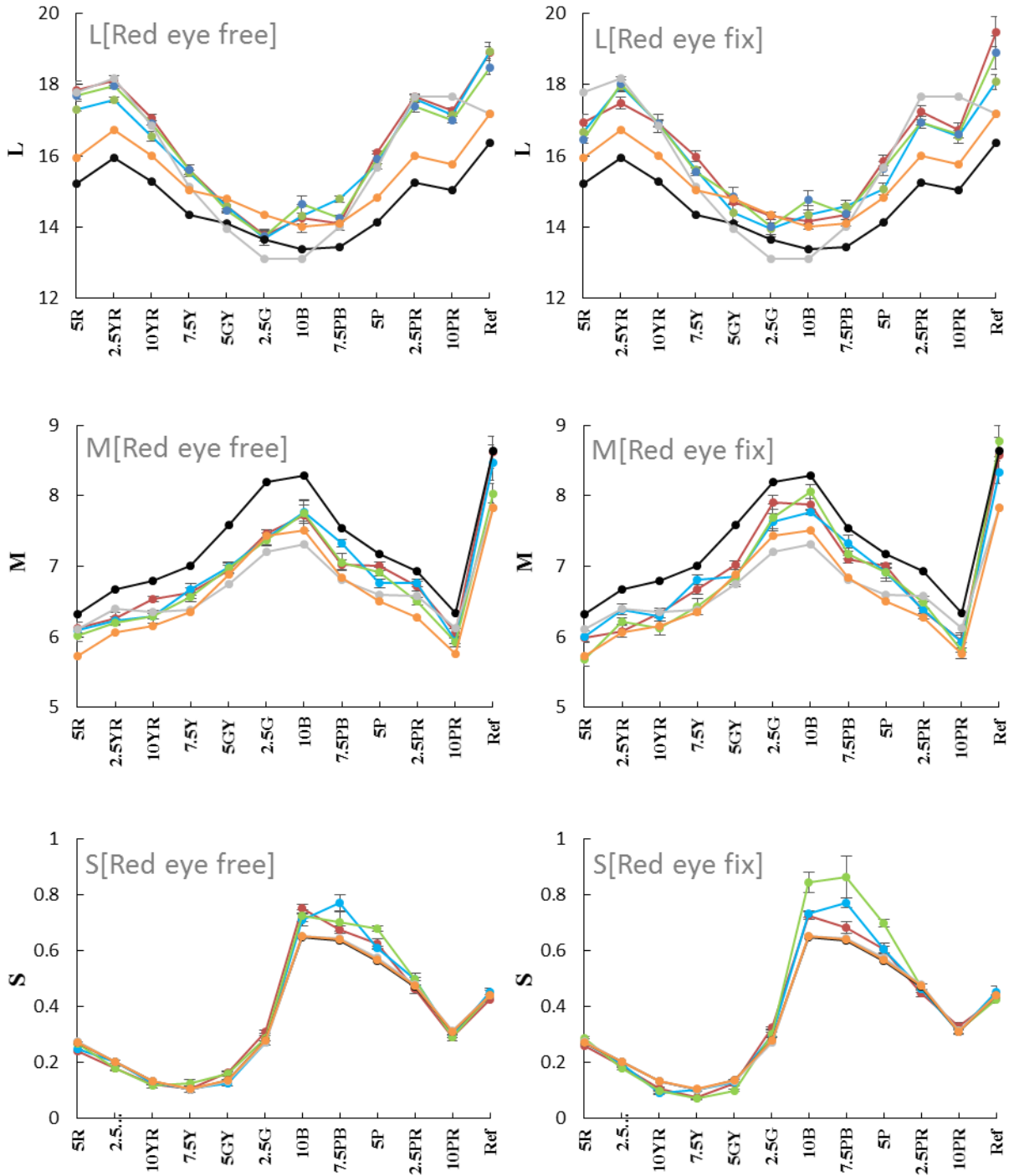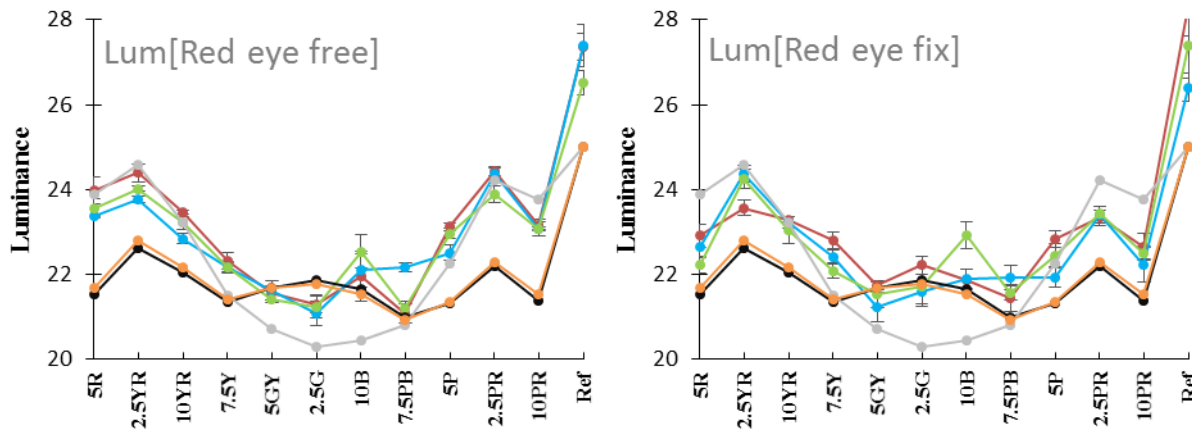
Figure 3. 6 luminance comparison and LMS cone responses for twelve patches under static,motion,rotation conditions with eyefree(left) and eyefix(right) under red illuminant. The data was averaged over 6 color normal observers. The central patch numbers 1 to 12 correspond to color chips: Mun-sell 5R5/6, 2.5YR5/6, 10YR5/6, 7.5Y5/6, 5GY5/6, 2.5G5/6, 10B5/6, 7.5PB5/6, 5P5/6, 2.5RP5/6, 10RP5/6, and 20% flat-reflectance surface. Error bars indicate standard error of the mean (± 2 SEM). L, M, S cone responses and luminance value of standard colors (black), matched colors (red line is the matched color of static condition, green line is motion, blue line is rotation), von Kries predicted colors (orange) and reflectance predicted colors (gray).

Figure 3.7 shows that under green illuminant,

1) L cone responses of matched colors are between von Kries predicted colors and reflectance colors. and close to theoretical reflectance data under eye free condition. It indicates the observers use some high level cognitive strategies to do the illumination estimation. And adaptation also plays an important role under green illumination, too. Compare with eye free and eye fix condition, Lcone response are more closer to reflectance data under eye free conditions than eye fix conditions, and L cone response are more closer to von Kries model under eye fixation. It implys that eye fix could reduce the high level cognitive ability, involves less illumination estimation, and more influenced by cone adaptation. It is very easy to imagine that when observers fixed their eyes, they could not pay attantion to the surrounding colors and they could not calculate colors as beter as when they explored surrounding areas.

2) M cones response are mostly closely to those of von Kries predicted colors. Because of the von Kries model and theoretical model are similar to each other, so I could not say whether the M cone response is more influenced mostly by adaptation or by illumination estimation.

3) The S cone responses predicted by von Kries or reflectance model show that the illuminant change from D65 to red illuminant does not produce noticeable S cone stimulation changes. S cone responses of matched colors appear to correspond well to those of standard colors and theoretical colors, except those of color chips (10B5/6), (7.5PB5/6), (5P5/6) in blue region and (2.5PR5/6), especially under the eye fix condition, matched colors of static condition are larger than rotation and

motion condition.

4) Luminance is determined by L and M cone responses, by considering the luminance matches and corresponding L, M cone responses together,it is expected that the luminance of matched colors is not only contributed by cone adaptation/gain control, but also determined by a high level cognitive strategy. This result reveals that von Kries rule has limitations to explain the lightness constancy(Kulikowski et al.2012).
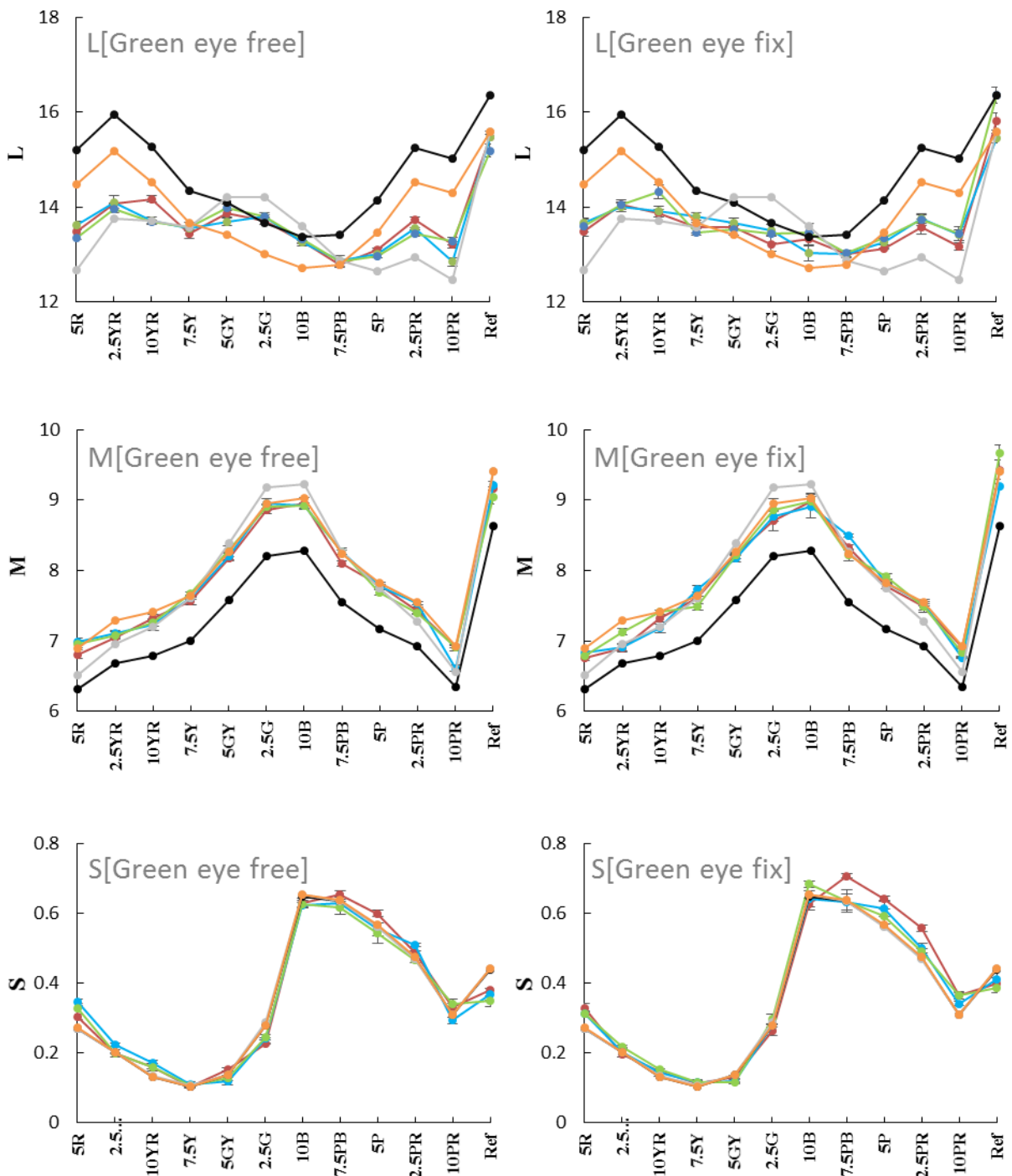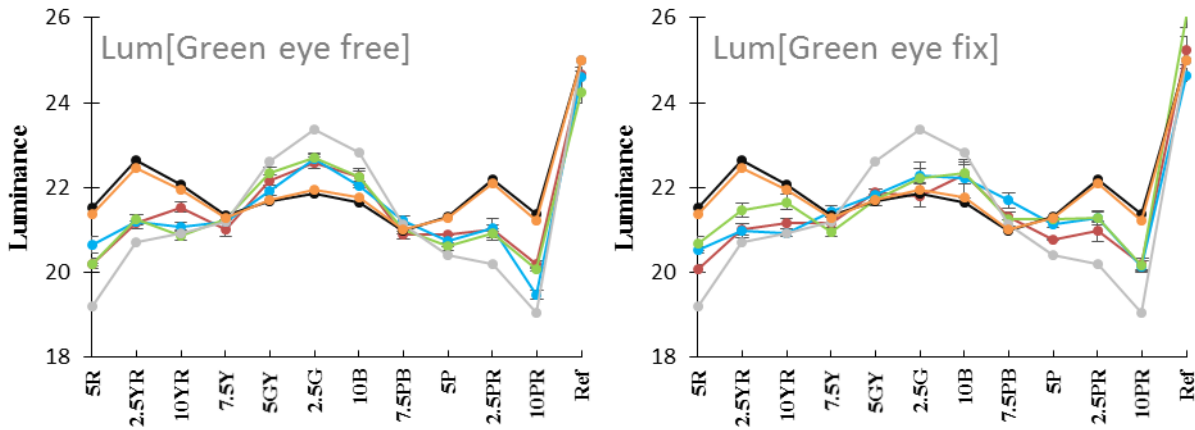
Figure 3. 7 luminance comparison and LMS cone responses for twelve patches under static,motion,rotation conditions with eyefree(left) and eyefix(right) under green illuminant. All other details are the same as in Figure3.6.

Under blue illuminant, the von Kries and reflectance model predicted value does not have large difference. And blue illuminant does not induce large changes of L and M cone: the von Kries predicted L and M cone responses overlapped with the reflectance model predicted and those of standard colors.

Figure 3.8 shows that under blue illuminant, The L and M cone responses of matched colors have a small deviation from those of von Krie theoretical colors/standard colors/reflectance colors. S cone responses appear to correspond well to von Kries predictions and reflectance colors.
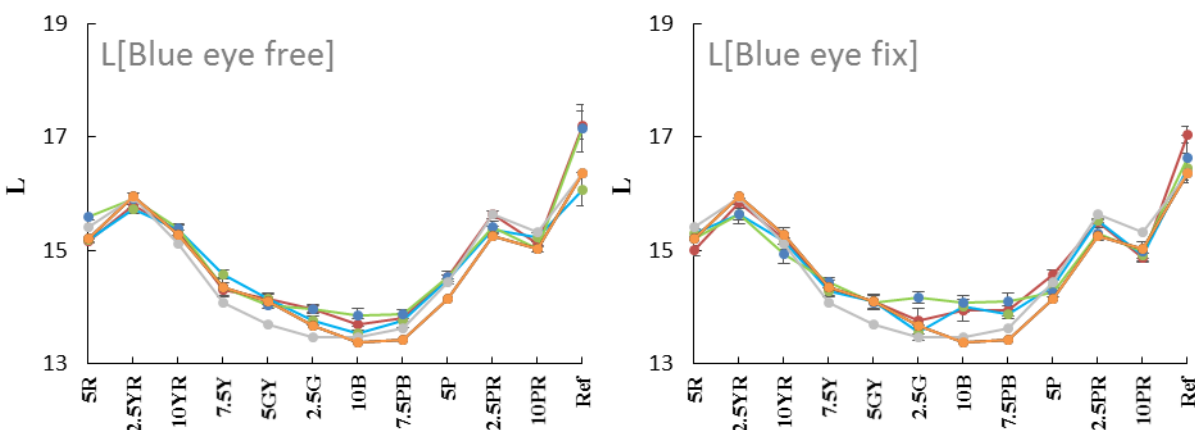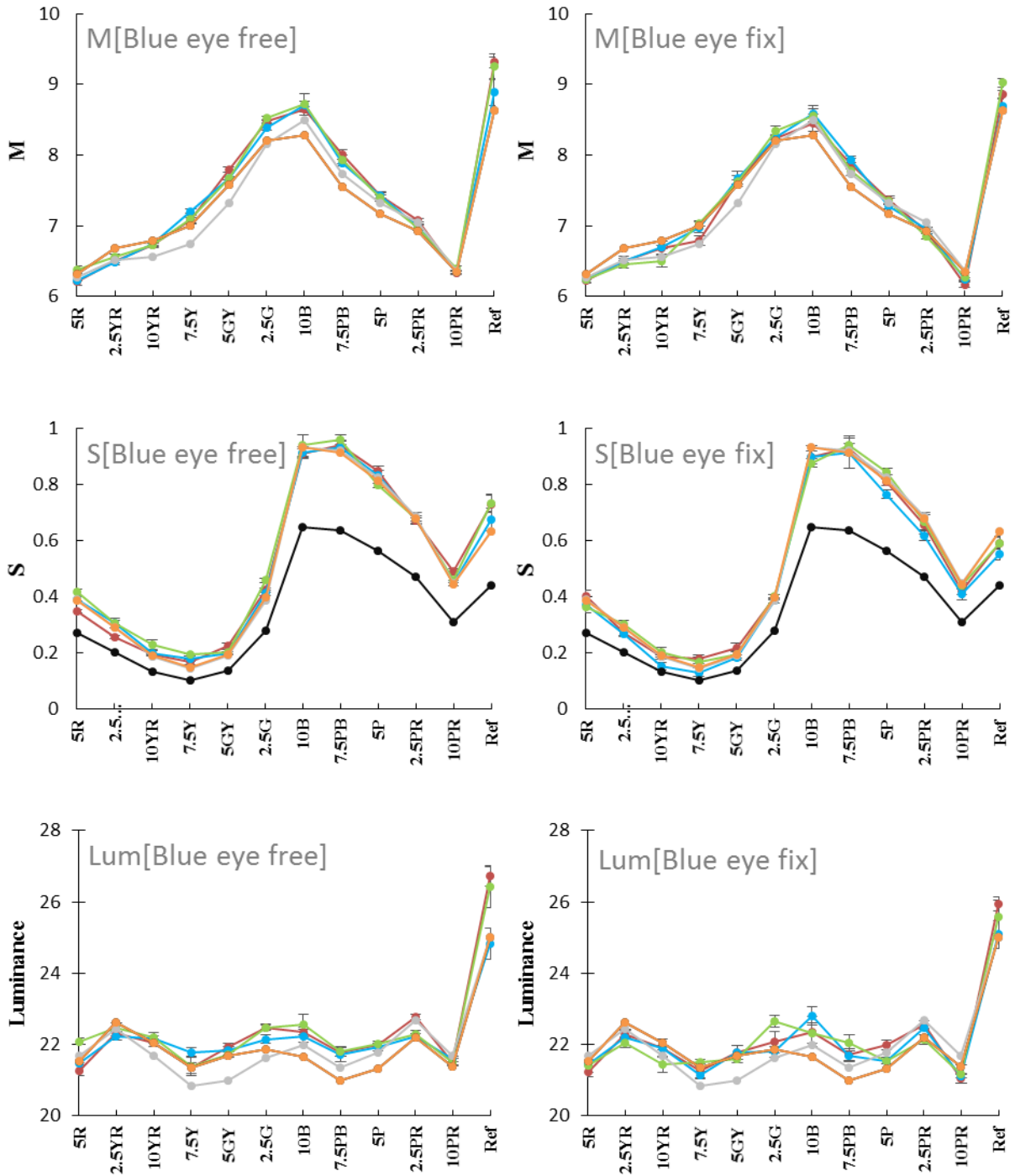
Figure 3. 8 luminance comparison and LMS cone responses for twelve patches under static,motion,rotation conditions with eyefree(left) and eyefix(right) under blue illuminant. All other details are the same as in Figure3.6.

Under yellow illuminant, the von Kries and reflectance model predicted value does not have large difference. And yellow illuminant does not induce large changes of L and M cone: the von Kries predicted L and M cone responses overlapped with the reflectance model predicted and those of standard colors. Figure 3.9 shows that under yellow illuminant, The L and M cone responses of matched colors have a small deviation from those of von Krie theoretical colors. S cone responses

appear to correspond between von Kries predictions and standard colors.
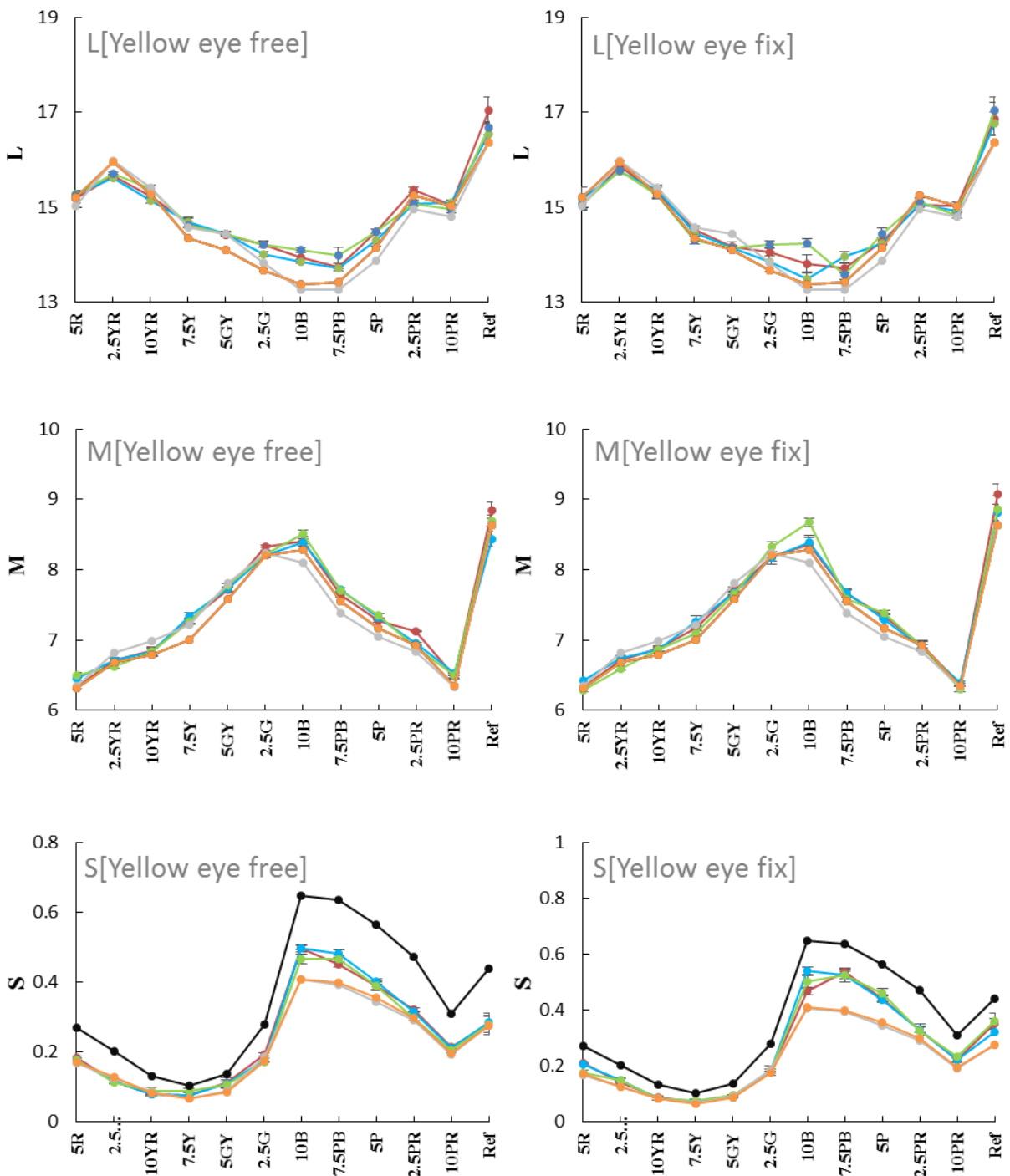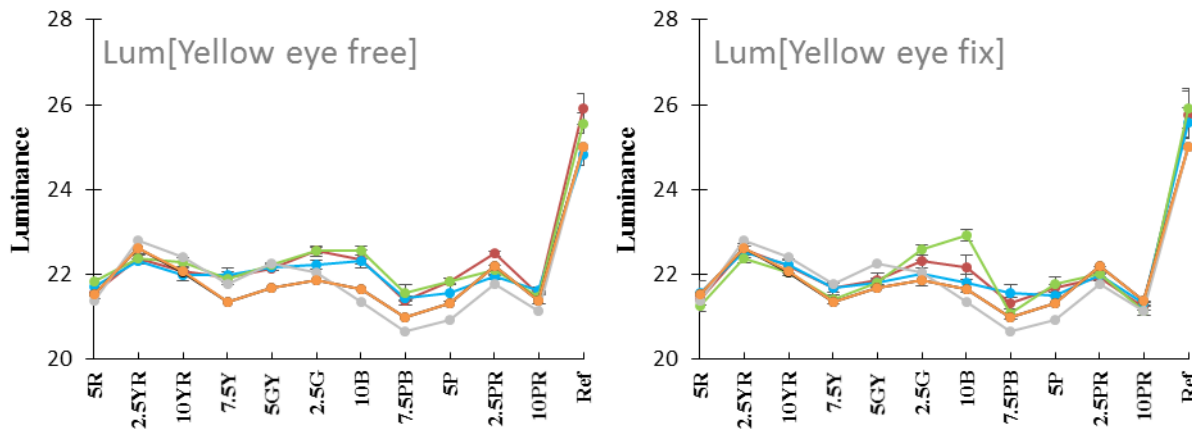
Figure 3. 9 luminance comparison and LMS cone responses for twelve patches under static,motion,rotation conditions with eyefree(left) and eyefix(right) under yellow illuminant. All other details are the same as in Figure3.6.

3.4 Von Kries Model Prediction at the Photoreceptoral Stage:

We compare the performance of static, motion, rotation target with eye free and fixation conditions by using the von Kries model, calculate the prediction L, M, S cone response at the photoreceptoral stage, the details is explained in our previous study Ma(2016). Figures 3.10, 3.11, and 3.12 show the comparison of L-, M- and S-cone responses on twelve color patches matched by the color-normal observers and those predicted by the von Kries model under red, green, blue and yellow illuminations. In Figure3.10, 3.11 and 3.12, the prediction under D65 (denoted by solid black lines) and that of the perfect adaptation line (denoted by diagonal dotted lines) were also presented. If the matched cone responses in the color constancy task could be perfectly predicted by the von Kries model, the data points would be on the diagonal line; In some conditions, the cone responses were influenced little by changes of illumination from D65 to test illuminations, as shown in the cases where the slopes of the black lines (no constancy) were close to the diagonal line (perfect adaptation). The response predicted by the von Kries model and those under D65 illumination overlapped, and the diagonal line indicates both perfect adaptation and no adaptation, explaination details in Ma(2016). The fitted lines (denoted by the red lines for targe-static condition, green lines for targe-motion condition, blue lines for target-rotation condition) to the data points were obtained by multiplying the von Kries model prediction by the constant coefficient to minimize the sum of the squared error between the prediction and the match. The slope k and coefficient of determination R^2 for the fitted line in each panel are shown in Table 3. It is well know that the von Kries-type adaptation is often modest under certain experimental conditions for a variety of reasons, meaning the adaptation effect is not necessarily of perfect strength (100%). Thus, the slope coefficient k of the fitted line, which can reflect the strength of the von Kries-type adaptation, can vary between the slope of the no adaptation line, that is the prediction under D65 and that of the perfect adaptation line.

Figure 3. 10, 3.11 and 3.12 and Table 3.2 show that, in the red illuminant, the L-cone response could not be explained even qualitatively by the simply application of the von Kries model alone, however, the color constancy was reasonably good and the matched points were sufficiently close to the reflectance model data, meaning that the observers were good at illumination estimation. The comparison the results between eye-fixation and eye-free conditions, M- and S-cone response were substantially higher in the eye-fixation condition than those matched results in the eye-free condition. It indicates that the eye-fixation might cause the inceasement of M- and S-cone responses; one reason for this may be explained by the adaptation. The adaptation response of L cones could be suppressed under the red illuminant, but M cones could be just excited. Interestingly, the deviation of the S-cone matching was mainly caused by the strong S-cone stimulation in some of the color patches (5P5/6, 7.5PB5/6 and 10B5/6): this phenominon agrees with those of previous studies as Kuriki(1996), Nieves(2000), Bäuml(1999), Kulikowski(2012) and Ma(2014), and this deviation increases especially in the target-motion condition with the eye-fixation.

In the green illuminant, the L-cone response could not be explained even qualitatively by the simply application of the von Kries model alone. However, the color constancy performance calculated by the *CI* as presented in Figure3.5 was even better than that in other illumination; one possible explantion for this is that observers performed better illumination estimation. In comparison between eye-fixation and eye-free condition, L- and S-cone responses were substantially higher in the eye-fixation condition than those in the eye-free condition. It indicates that the gaze-state of eye fixation increased the L- and S-cone responses in the matched points; it also may cause the adaptation effect stronger. In the green illuminant, the adaptation response of M-cone was suppressed but L-cone iresponses was more excited.

In the blue illumination, the matched L-, M- and S-cone responses approached to the diagonal lines and M-cone response had a slightly- upward deviation; this deviation was smaller in the eye-fix condition than that in the eye-free condition. In the yellow illumination, the matched L, M, S cone responses approach the diagonal lines, S cone response has a slight upward deviation, and this deviation is smaller in eye-free condition than eye-fix condition.

In the analysis of cone responses, the influence of the motion to the color constancy was small regardless of cone types illumiantion color and gaze-state.
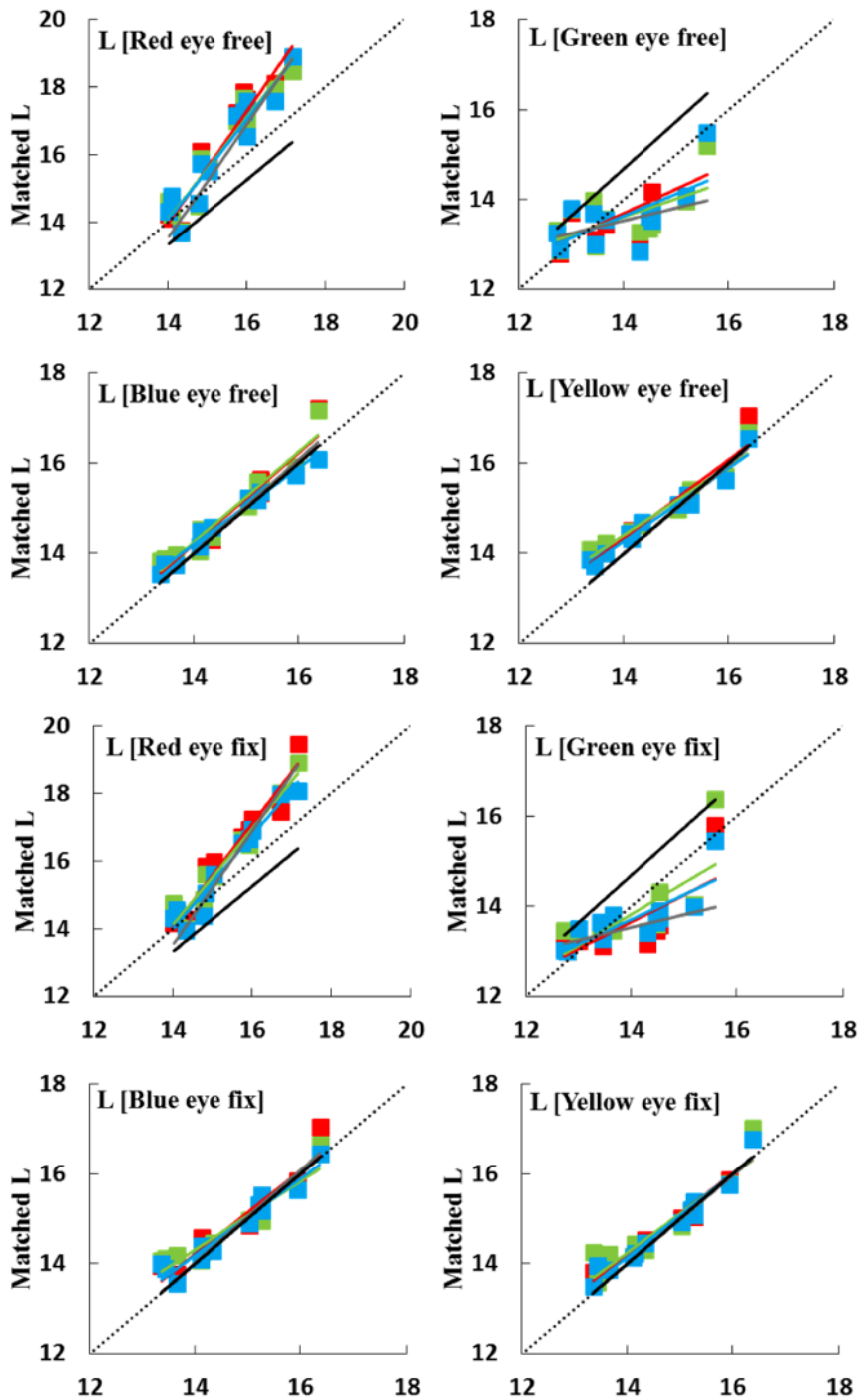
Figure 3. 10 Comparison of the L-cone matched results by observers (ordinate) with those predicted by the von Kries model (abscissa) for twelve color patches. The data of the red, green, blue and yellow illuminations in eye free condition (top four panels) and eye fixation condition (bottom four panels). Diagonal dotted black-lines indicate perfect von Kries-type adaptation. The red, green and blue squares are matched result of target-static, target-motion and target-rotation conditions, respectively. The red, green and blue lines denote the best fits of target-static, target-motion and target-rotation conditions, respectively. Each data point was averaged over six observers and six sessions. Black lines denote the prediction under D65 (see text for details).
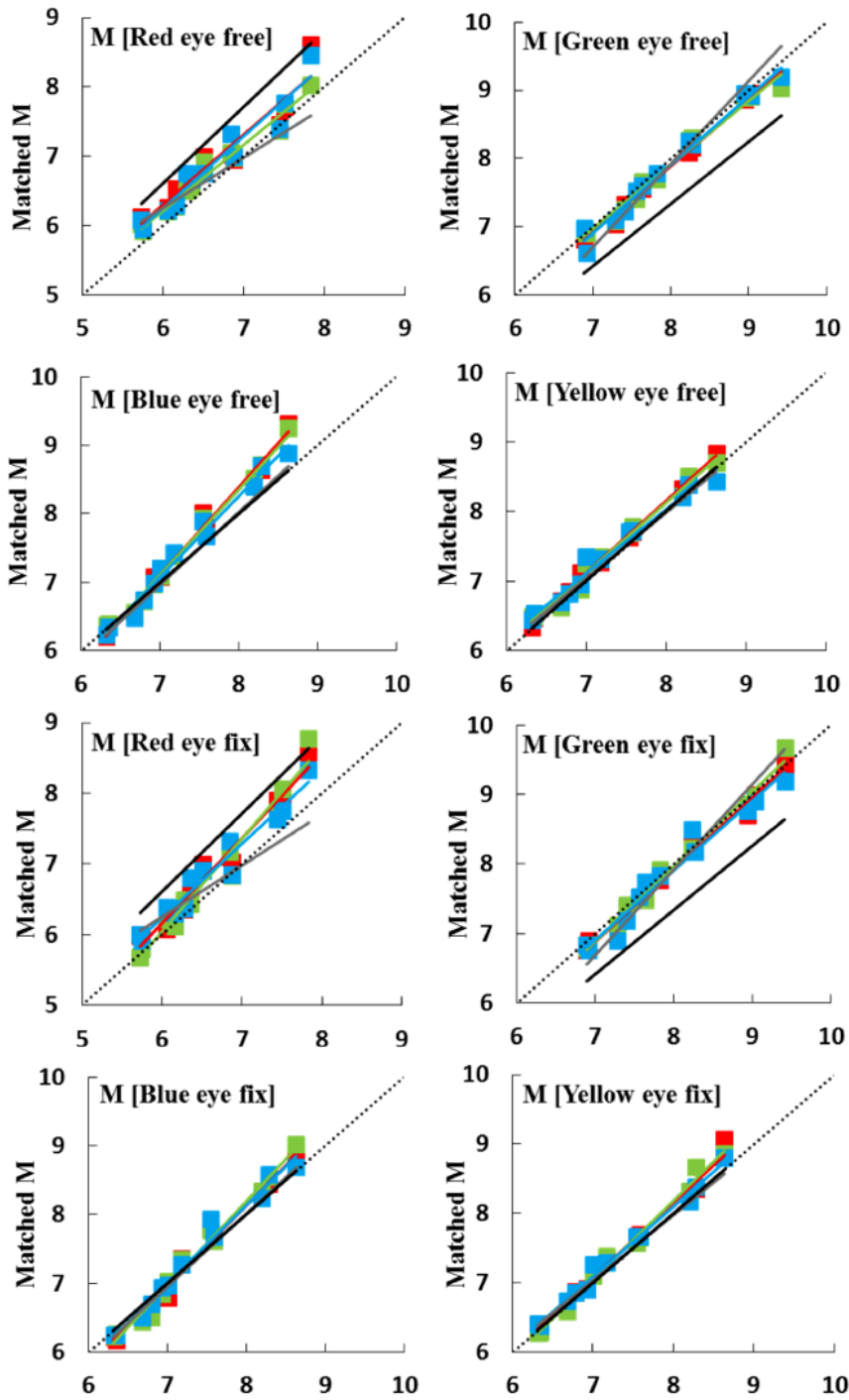
Figure 3. 11 Comparison of the M-cone matched results (ordinate) with those predicted by the von Kries model (abscissa). All other details are the same as in Figure3.10.
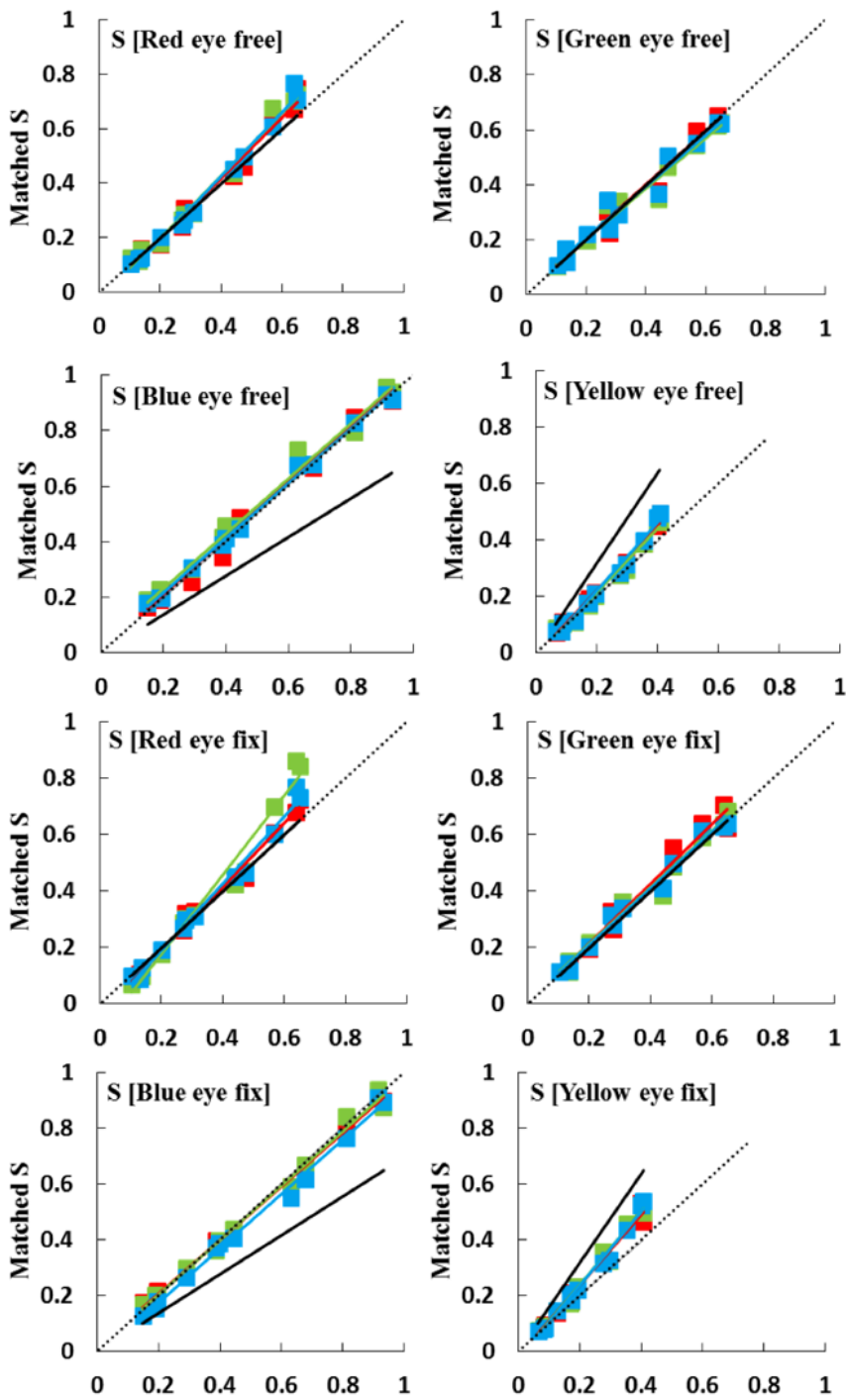
Figure 3. 12 Comparison of the S-cone matched results (ordinate) with those predicted by the von Kries model (abscissa). All other details are the same as in Figure3.10.

Table3.2 Slope Coefficient k and Coefficient of Determination R2 for Fitted Lines in Figures3.10, 3.11, and 3.12.

		Red illuminant			
		Eye free		Eye fix	
		k	R2	k	R2
	L	1.657	0.916	1.507	0.932
Static	M	1.013	0.914	1.206	0.969
	S	1.115	0.978	1.124	0.987
	L	1.492	0.894	1.407	0.945
Motion	M	0.959	0.971	1.323	0.956
	S	1.147	0.982	1.4	0.969
	L	1.48	0.883	1.37	0.939
Rotation	M	1.044	0.933	1.054	0.948
	S	1.171	0.986	1.187	0.984
		Green illuminant			
		Eye free		Eye fix	
		k	R2	k	R2
	L	0.54	0.489	0.595	0.513
Static	M	0.97	0.992	1.031	0.979
	S	0.981	0.972	1.057	0.96
	L	0.405	0.325	0.689	0.506
Motion	M	0.937	0.976	1.074	0.988
	S	0.917	0.964	0.997	0.977
	L	0.497	0.381	0.546	0.61
Rotation	M	1.004	0.979	0.998	0.957
	S	0.935	0.958	0.996	0.984

		Blue illuminant			
		Eye free		**Eye fix**	
		k	R2	k	R2
	L	1.005	0.922	0.926	0.891
Static	M	1.287	0.984	1.163	0.978
	S	1.015	0.981	0.964	0.994
	L	0.998	0.928	0.765	0.899
Motion	M	1.251	0.986	1.22	0.983
	S	0.984	0.986	0.975	0.991
	L	0.848	0.975	0.856	0.924
Rotation	M	1.18	0.98	1.134	0.976
	S	0.987	0.997	0.976	0.993

		Yelow illuminant			
		Eye free		**Eye fix**	
		k	R2	K	R2
	L	0.871	0.905	0.907	0.938
Static	M	1.036	0.992	1.084	0.983
	S	1.16	0.983	1.274	0.979
	L	0.761	0.928	0.868	0.851
Motion	M	1.009	0.981	1.138	0.989
	S	1.129	0.981	1.321	0.984
	L	0.81	0.954	0.925	0.947
Rotation	M	0.917	0.972	1.014	0.989
	S	1.208	0.983	1.338	0.987

3.5 von Kries Model Prediction at the Post-receptoral Stage

In the next step, we considered the von Kries type of adaptaion in the post-receptoral stage. We calculated the predictions in the red-green chromatically-opponnet channel response represented by (L-2M) and the blue-yellow chromatically-opponent channel response represented by [S-(u_n)*(L+M)] at the postreceptoral stage by using the von Kries model. In the blue-yellow response, we introduced a constant coefficient for neutralization to white, u_n to make the balance of blue-yellow equivalence. In this study, u_n was set to 0.0175 for all illumination conditions.; the more details were explained in Ma(2014). We compared the color constancy performance of the target in static, motion and rotation conditions with eye-free and eye-fixation conditions.

Figure 3.13 shows the comparison between the matched points by observers in the response of L-2M (ordinate) with the von Kries model prediction of L-2M (ordinate). If the changing of opponent color signals would be described in terms of the simple adaptation on each cone type separately, the data points would fall on the diagonal lines as explained in the previous section. In Figure3. 13, we also calculaed the prediction by the perfect illumination estimation effect as denoted by gray lines. In red and green illuminants, the data points almost conform to the diagonal line with just a small deviation from the diagonal line, even the no adaptation prediction (denoted by black lines) was different to the perfect adaptaion prediction. Although the difference was not sufficiently large, in red illuminant, the matched points were on the gray line rather than on the diagonal line in both eye-freen and eye-fix conditions. It indicates that the effect of illumination estimation must contrivute to the color constancy; it also means that the red-green opponent signal matched by the observers tended not to follow the von Kries model adaptation, but more reflecting to the reflectance model. This result is consistent with the result reported in the literature of K.-H. Bäuml(1999). In blue and yellow illuminations, the reflectance data overlapped on the diagonal line, meaning that is is impossible to seperete the mechanism between the von Kries model dataptation and illuminantion esitimation effect.

Figure3.14 shows the mean matched blue-yellow opponent color response for twelve color patches. The color patches of 5P5/6, 7.5PB5/6, and 10B5/6 in eye-fixation condition have much larger deviation from the diagonal line than other chips and all chips in the eye-free condition in red, green and yellow illuminations. Except these three patthces, the matched data for all observers under all illumination conditions could be fitted by the von Kries model well, meaning that the blue-yellow opponent responses can be predicted well by the von Kries model; this result is consistent with the Ma's study (2014).

In the analysis of the post-receptoral responses, the influence of the motion to the color constancy was still small regardless of cone types illumiantion color and gaze-state. It may suggest that the effect of target motion is small to the von Kries type of adaptaion. However, it still remains the possibity that the color constancy in this stimulus configuration is mainly determined by the illumination estimation effect like the reflectance

model but the effect of motion to the adaptation and to the illumination estimation tends to cancel each other. This possibility will be discussed in later part.
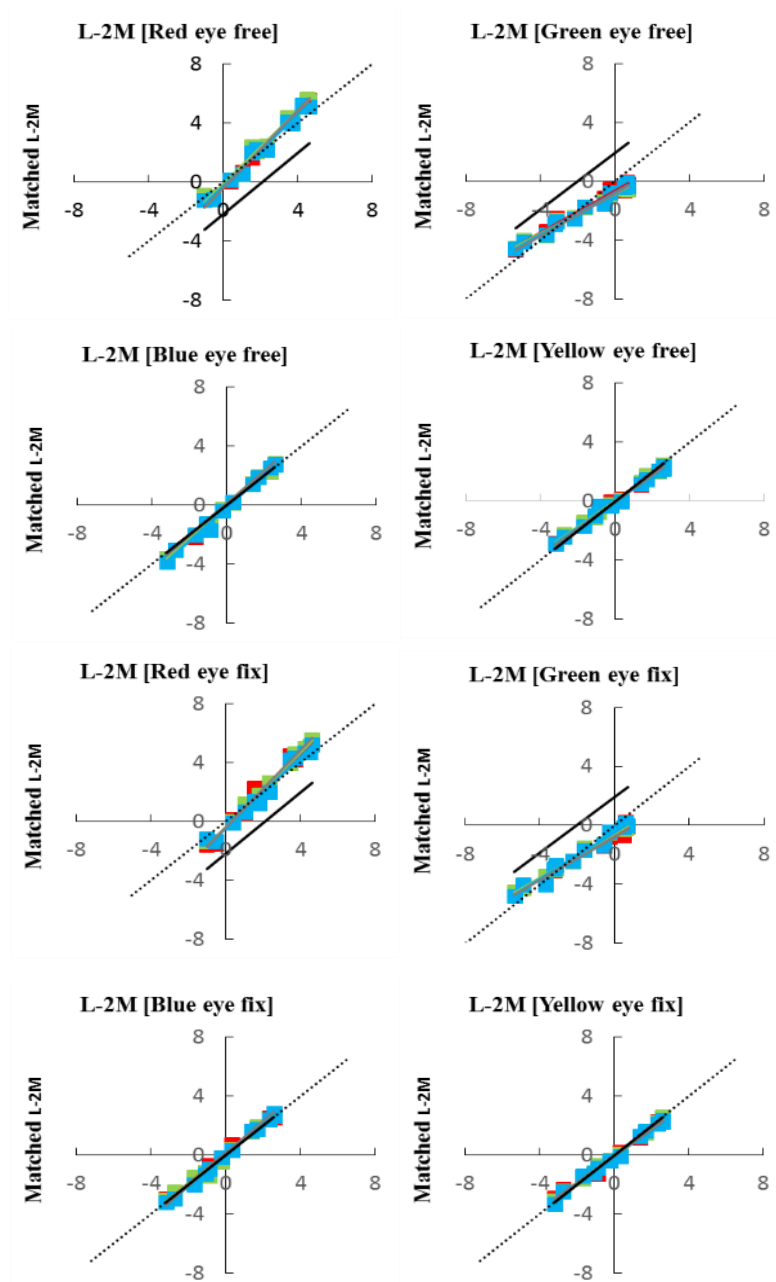
Figure 3. 13 Comparison of the matched L-2M response by observers (ordinate) and the von Kries model predictions (abscissa) for red, green, blue, and yellow illuminations with eye-free and eye-fixation conditions. Diagonal dotted black lines indicate perfect von Kries-type adaptation. The red, green and blue squares are the matched result of static, motion and rotation conditions, respectively. The red, green and blue lines denote the best fits of static, motion and rotation conditions. Black lines denote the prediction under D65 and gray lines denote the prediction by perfect illumination estimation effect (see text for details). Each data point was averaged over six observers and six sessions.
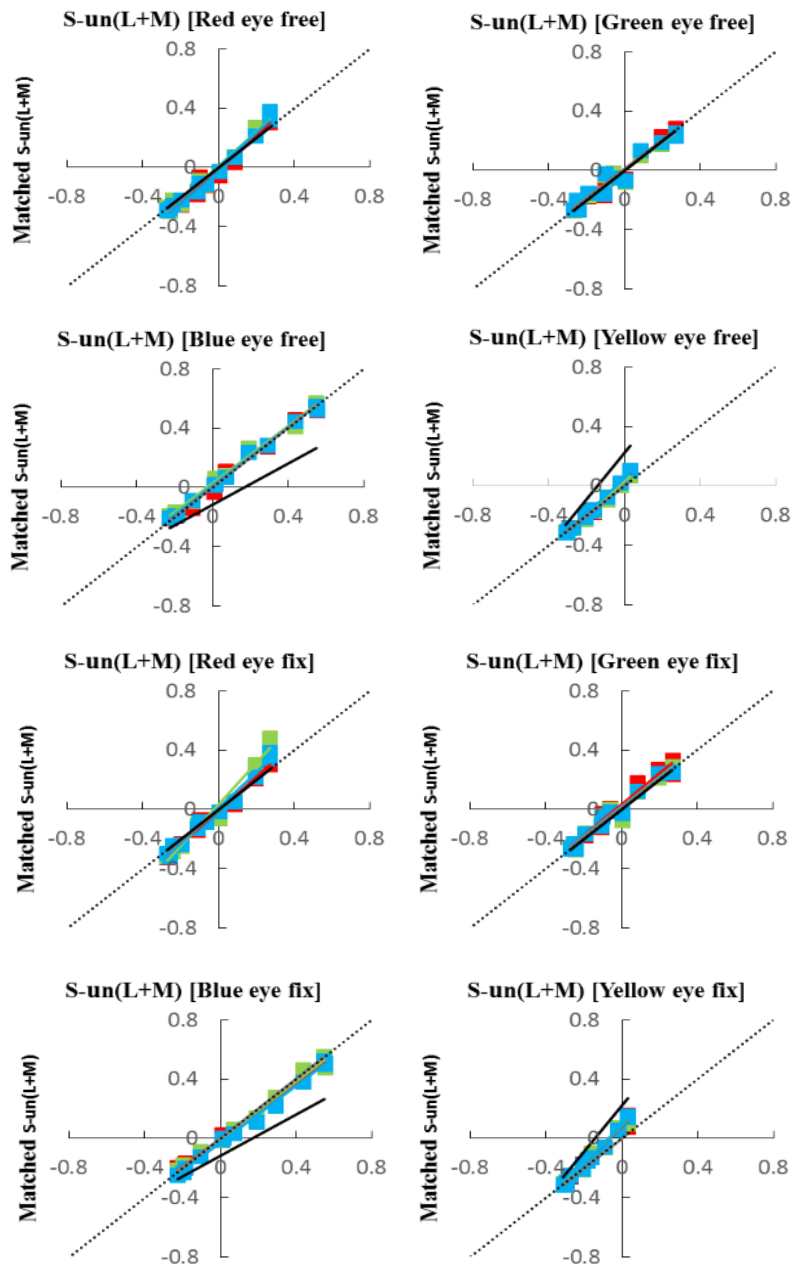
Figure 3. 14 Comparison of the matched blue-yellow [S-u$_n$(L+M)] response (ordinate) and the von Kries model predictions (abscissa). All other details are the same as in Figure3.13 except gray lines were not shown.

3.6 Correlation to von Kries model and reflectance model

As we know, von Kries model is used to explain the adaptation to the photoreceptors (cones) and/or post-receptoral process (R-G and Y-B opponet channels) at the retina and the earlier part of the color process (i.e. LGN and the primary visual cortex) and reflectance model is used to explain cognitive and/or computational mechanism occurring at a higher level; these two strategies are considered as two main factors contributing to the color constancy.

Our experiments were set up to investigate whether the motion and the attention would influence the contribution to the retinal adaptation and high level cognitive mechanism in the color constancy. Thus, we compared the distance of the matched points of the results to the predicted points by the reflectance model to the distance to the predited points by the von Kries model. We calculating the distance, Dvon Kries which is from matched points to the von Kries model predition points and the distance, Dreflectance which is from the matched points to the reflectance model prediction points,

$$D_{von\,Kries} = \frac{1}{N} \sum_{i=1}^{N} \sqrt{\left(L_{i,Match} - L_{i,vK}\right)^2 + \left(M_{i,Match} - M_{i,vK}\right)^2 + \left(S_{i,Match} - S_{i,vK}\right)^2}$$

(2)

$$D_{reflectance} = \frac{1}{N} \sum_{i=1}^{N} \sqrt{\left(L_{i,Match} - L_{i,Ref.}\right)^2 + \left(M_{i,Match} - M_{i,Ref.}\right)^2 + \left(S_{i,Match} - S_{i,Ref.}\right)^2}$$

(3)

where N=12; Li, Match, Mi, Match and Si, Match are the matched results, Li, vK, Mi, vK and Si, vK are the predicted points by the von Kries model, Li, Ref., Mi, Ref. and Si, Ref. are the predicted points by the reflectance model data, i represents the 12 test color patches. The results are shown in Figure3.15.

Figure3.15 shows that, in the red and green illuminants, the matched points were much closer to the reflectance model prediction points in the eye-free condition. Concersely, the matched points in the target-motion and target-rotation conditions were closer to the von Kries model prediction points in the eye-fixation condition. in the blue and yellow illuminations, the matched points were closer to the von Kries model prediction points in both eye-free and eye-fixation condtions. It can be implied that since the blue and yellow illuminants along the daylight locus were familiar to the observers, the color constancy by the adaptation could be reasonably surficient and the observers felt the color appearance of the right and left sides were close to each other. Thus, the observers weakly conducted the illumination estimation, causing the matched points were closer to the von Kries model prediction points. This result is conforming to the previous study which points out that the illumination changes along the daylight locus are primarily mediated in the S-cone responses, the

human color system may have developed a higher sensitivity along the blue/yellow dimension, referenced by Foster(2011).

However, in the eye-free condition with the red and green illuminants, which are not along the daylight locus, the observers felt the color appearance of right side and left side are much more different, thus, the observers needed more illumination estimation which involves the higher-level mechanism. The observers had to make matches in the color illuminations that would mainly reflect possible mechanisms of the statistical operation of the scene, which is reported by Golz (2002,2008) or the illuminant-by-illuminant estimation strategy from Dalahunt (2004), Uchikawa (2012)and Uchikawa (2017). It caused that the matched points were closer to the reflectance model prediction points.
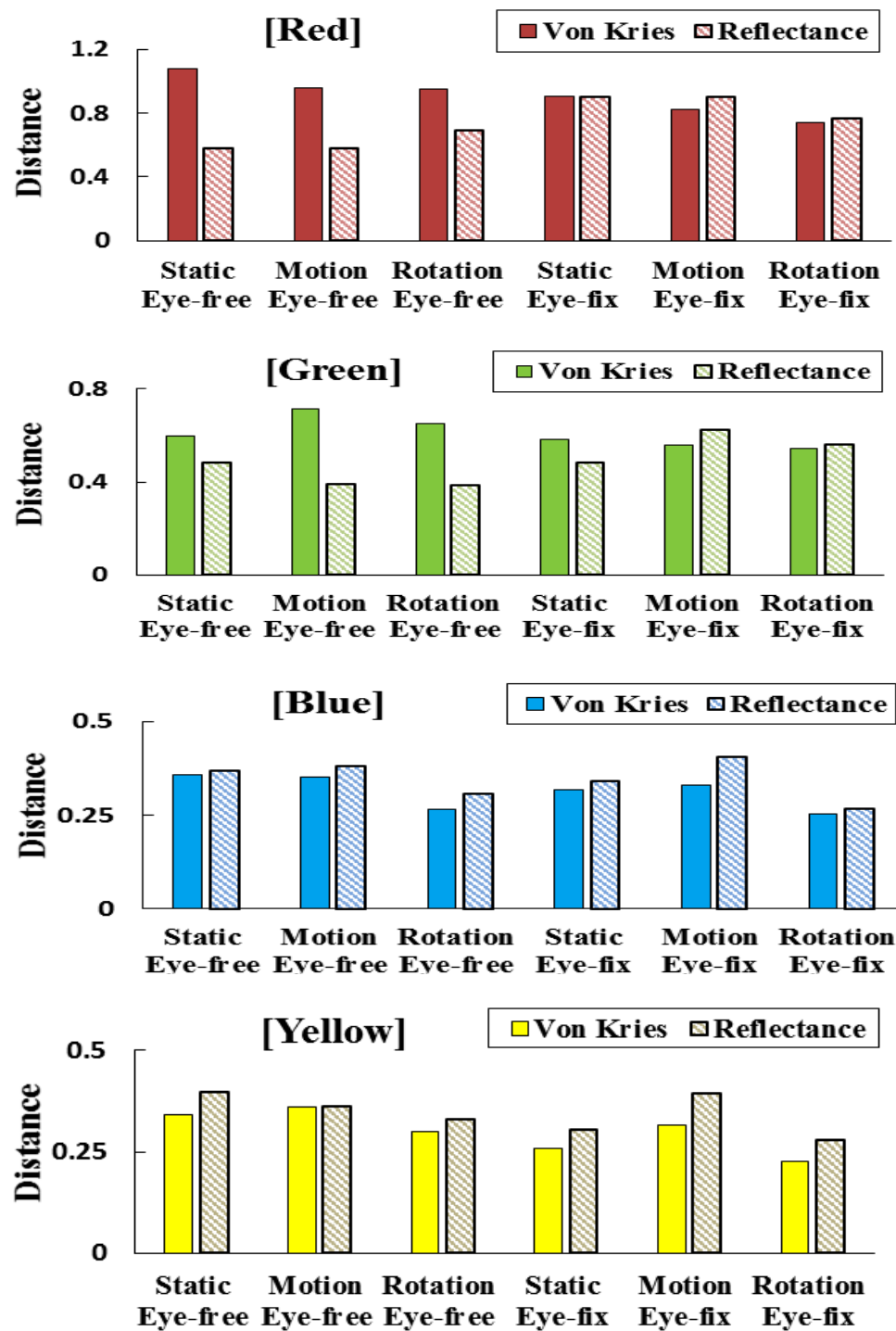
Figure 3. 15 Distance of matched points to the predicted points by reflectance model and von Kries model in four illuminations. Color bars denote the distance between matched points to the von Kries model predictions. Patterned bars denote the distance between matched points to the reflectance model predictions. The red, green, blue and yellow bars denote red, green, blue and yellow illumination conditions, respectively.

3.7 Correlation coefficient to von Kries model and reflectance model

The correlation coefficients of L, M, S, Luminance to Von Kries model and relectance model was calculated here, table 3.3 show the result of 2-tailed Pearson correlation test. coef is the correlation coefficient, sig is the significance level.

Table 3.3 shows that under red illuminant observers's match result has a higher correlation coefficient to Vonkries model in Eye fixation condition than eye free condition. It indicates that observers are more influenced by adaptation whey they fix their eyes under red illuminant. Under red illuminant, L cone has a higher correlation coefficient to Vonkries models than reflectance models, means L cones response are more conformed to Von kries model than reflectance model.

Under green illumination, L, M, Luminance has a higher correlation coefficient to reflectance model than Von kries model with eye free. It indicates that observers are more good at illumination estimation whey their their eyes are free under green illuminant. And the result shows that L cones and Luminance has a higher correlation coefficient to Vonkries model under Eye fixation condition than eye free condition under green illuminant, also implys that adaptation have more effect on L cones when eyes are fixated than free.

Under blue illuminant, observers's match result has a higher correlation coefficient to Vonkries model than reflectance model. It indicates that observers are more influenced by adaptation whey they under blue illuminant. S cones has higher correlation coefficient under eyefix condition than eye free condtion, means S cones are more influenced by adaptation when eye are fixed under blue illuminant.

Under yellow illuminant, observers's L cone and Luminance match result has a higher correlation coefficient to Vonkries model in Eye fixation condition than eye free condition under yellow illuminant. It indicates L cones are more influenced by adaptation whey they fix their eyes under yellow illuminant. L cone, M cone and Luminance has a higher correlation coefficient to Vonkries models than reflectance models, means under yellow illuminant, observers' match results are more conformed to Von kries model than reflectance model.

Table3.3 Correlation coefficient to Vonkries model and reflectance model

		Red illuminant and Static condition			
		Eyefree		**Eyefix**	
		coef	Sig	coef	Sig
Correlation to Vonkries	L	0.961	0	0.968	0
	M	0.96	0	0.986	0
	S	0.99	0	0.994	0
	Lum	0.878	0	0.955	0
Correlation to Reflectance	L	0.955	0	0.865	0
	M	0.984	0	0.971	0
	S	0.989	0	0.993	0
	Lum	0.898	0	0.71	0

		Green illuminant and Static condition			
		Eyefree		**Eyefix**	
		coef	Sig	Coef	Sig
Correlation to Vonkries	L	0.732	0.007	0.747	0.01
	M	0.996	0	0.99	0
	S	0.987	0	0.982	0
	Lum	0.848	0	0.861	0
Correlation to Reflectance	L	0.847	0.001	0.794	0.002
	M	0.997	0	0.986	0
	S	0.985	0	0.979	0
	Lum	0.956	0	0.919	0

		Blue illuminant and Static condition			
		Eyefree		**Eyefix**	
		coef	Sig	coef	Sig
Correlation to Vonkries	L	0.964	0	0.949	0
	M	0.993	0	0.99	0
	S	0.991	0	0.997	0
	Lum	0.946	0	0.933	0

		coef	Sig		Coef	Sig
Correlation to Reflectance	L	0.954	0		0.943	0
	M	0.986	0		0.99	0
	S	0.991	0		0.997	0
	Lum	0.935	0		0.935	0

Yellow illuminant and Static condition

		Eyefree			**Eyefix**	
		coef	Sig		Coef	Sig
Correlation to Vonkries	L	0.956	0		0.971	0
	M	0.996	0		0.992	0
	S	0.992	0		0.99	0
	Lum	0.962	0		0.973	0
Correlation to Reflectance	L	0.942	0		0.962	0
	M	0.981	0		0.979	0
	S	0.993	0		0.988	0
	Lum	0.915	0		0.933	0

Chapter4

DISCUSSION

4.1 mathematical model comparison

During the experiments, the observers reported that the color difference of the two-side patterns was not the same between the static and motion conditions in the eye-fixation condition. Figure 4.1 shows the conceptual simulation of the perceived appearance in the haploscopic view. In the static and eye-fix condition (left side), the observers felt the color of the two sides were more different since the fixation to the static target and the background caused less modulation in the retinotopic (local) adaptation and rather caused more attention to the background colors; the adaptation effect became weaker but the illumination estimation effect could be stronger and dominant, causing the better color constancy in total. On the contrary, in the motion and eye-fixation condition (pursuit eye movement) (right side), the observers reported that they felt the color of the two side patterns was almost the same, since more modulation of the retinotopic adaptation by the spatio-temporal averaging and the background color was less attended; the adaptation effect could be stronger but the illumination estimation effect was weaker, causing the poor color constancy in total. According to the phenomenon that the observers perceived and the results of the color constancy shown clearly in Figure 3.15 as the difference between eye-free and eye-fix condtions, we conducted the model analysis so as to explain the influence of the eye movement. In this study, we compared performances of the Ebner's computational model and double opponency models here.
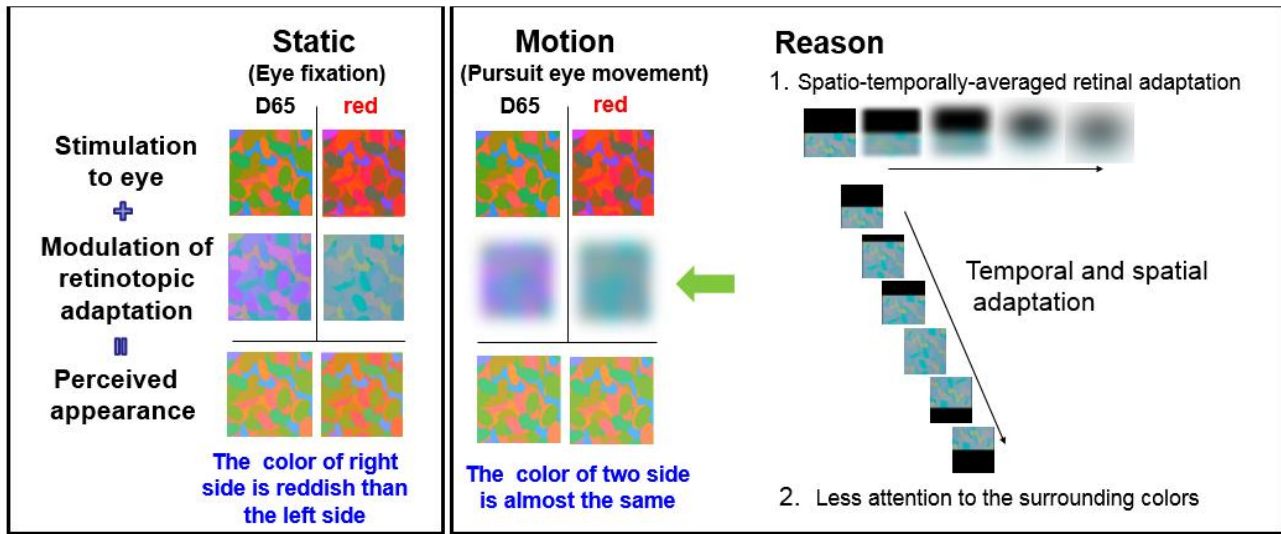
Figure 4. 1 Perceived appearance under haploscopic view in static and motion conditions.

4.1.1. Ebner's computational model

Many potential algorithms have been proposed for the color constancy. Land (1974) has developed the retinex theory of color constancy, then it has been developed to numerous computational approaches, as white-patch retinex algorithm and the gray world assumption, both algorithms assume that the illumination of the scene is uniform. Ebner (2009) has shown the approaches that estimating the illuminant locally by the gray world assumption, and Ebner (2011) also developed a computational model for the color constancy of motion object. In this subsection, Ebner's model is used to simulate the color constancy of the static and motion conditions in four colored illuminations.

In the model, color stimuli were converted from Luv color space to RGB space. The three channel RGB system corresponds to the retinal receptors which absorb light in the red, green, and blue parts of the spectrum. The intensity, O_i, retina (x, y) measured by the retinal receptors for three channels of red, green, and blue, $i \in \{r, g, b\}$ at position (x, y) in the image , is given by

$$O_{i,retina}(x,y) = \log R_i(x,y) + \log L_i(x,y) \tag{4-1}$$

where Ri(x, y) is the reflectance, Li(x, y) is the intensity of the irradiance, here the assumption is that even though the illuminant is non-uniform, it varies smoothly over the image, and the local space average color ai(x,y) is computed by convolution with a kernel function;

$$a_i(x,y) = k \iint O_{i,retina}(x,y)\, g(x-x', y-y') dx' dy' \tag{4-2}$$

The constant k is used to normalizing the result. Here the kernel function is a normalized two-

dimensional Gaussian,

$$g(x, y) = \frac{1}{2\pi\delta^2} e^{-\frac{x^2+y^2}{2\delta^2}} \quad (\delta = 30).$$

(4-3)

In the motion condition with the pursuit eye moment, a temporal averaging of local space average color was calculated. Figure 4.2 shows the same stimuli observed in the aspect of the retinal receptors. The eyes essentially track the test patch maintaining it exactly in the fovea of the retina, and 7 frames were taken to make convolution with Gaussian spatial filter. Then the averaged 7 frames as the temporal and local-space averaged color was obtained as showed in Figure 4.3. The color bias of induction and adaptation may be explained by the local space averaged color in the Ebner's mathematic model.
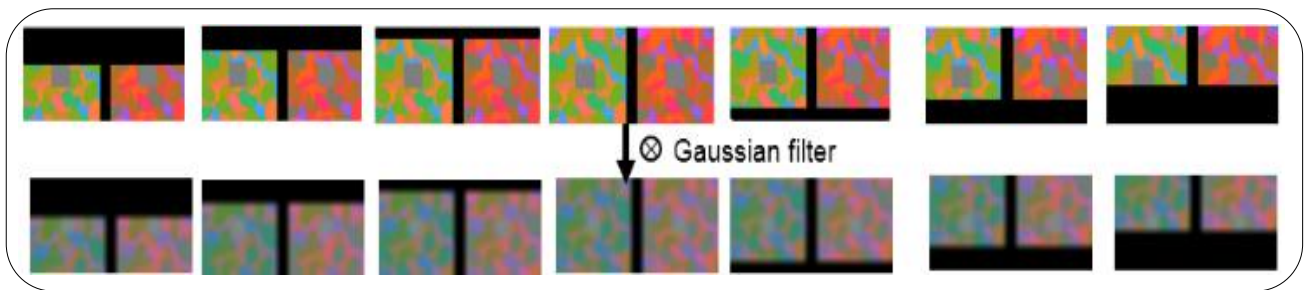
Figure 4. 2 Visual stimulus for experiment as measured by the retinal receptors under motion condition with pursuit eye movement and the result of convolution with Gaussian spatial filter.
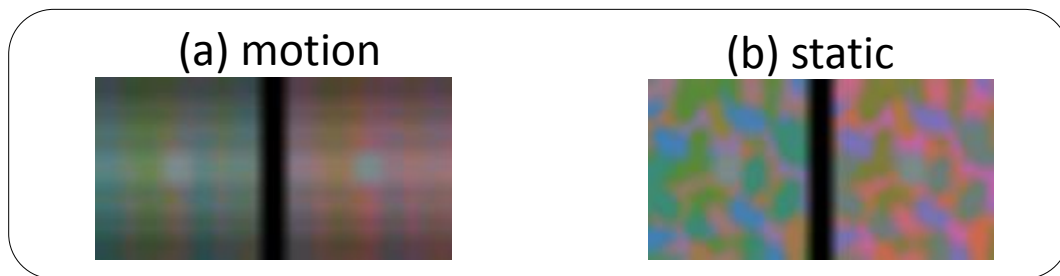
Figure 4. 3 Local space averaged color computed by Ebner's mathematical model.

The color constancy descriptor Oi, cc (x, y) is computed by essentially subtracting local space averaged color ai(x, y) from the measured color Oi, retina (x, y) , as explained in Figure 4.4. This process is like the process of illumination estimation, which needs to offset the bias color caused by the induction and adaptation.

$$O_{i,cc}(x, y) = O_{i,retina}(x, y) - a_i(x, y) = \log R_i(x, y) + 1$$

(4-4)

$O_{i,retina}(x,y)$ $a_i(x,y)$ $O_{i,cc}(x,y)$
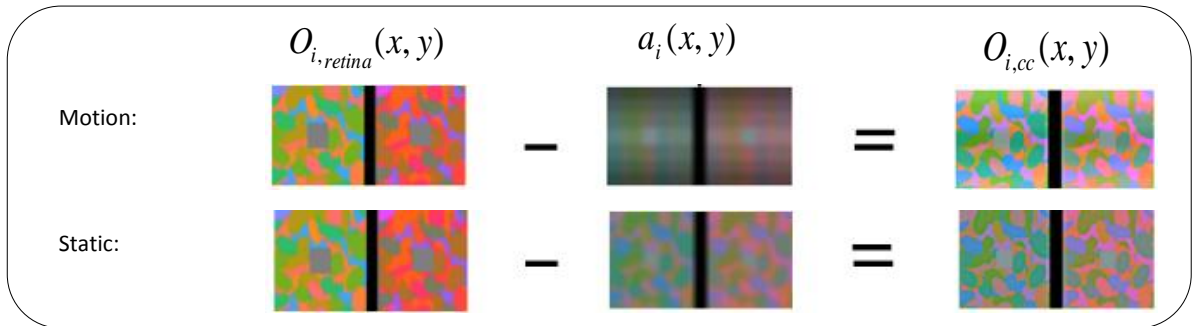
Motion:

Static:

Figure 4. 4 The color constancy descriptor is computed under motion and static condition.

Then apply the inverse of the cube root function to obtain reflectance estimates, $\vec{R}$

$$\vec{R} = \left(O_{cc}(x,y)\right)^3 \tag{4-5}$$

The color of the illuminant $\vec{R}$ is estimated by taken the average reflectance estimates over all pixel values of the test patch. Then, the angular error is defined as

$$e = \cos^{-1}\frac{\vec{R_e}\,\vec{R_d}}{|\vec{R_e}|\,|\vec{R_d}|} \tag{4-6}$$

$\vec{R_d}$ is the estimated reflectance under illuminant D65, $\vec{R_e}$ is the estimate under a non-standard illuminant. Figure 4.5 shows the angular error, e between the estimated reflectance under a standard D65 illuminant and a non-standard illuminant obtained from the modified Ebner's model. From this simulation result, the angular error of motion is smaller than static condition, and angular error of Blue < Yellow < Red < Green. This computational model result conforms to our experiment results shown in Figure3.5. The Ebner's model suggests the better color constancy in the blue and yellow illuminants compared that in the red and green illumiants.
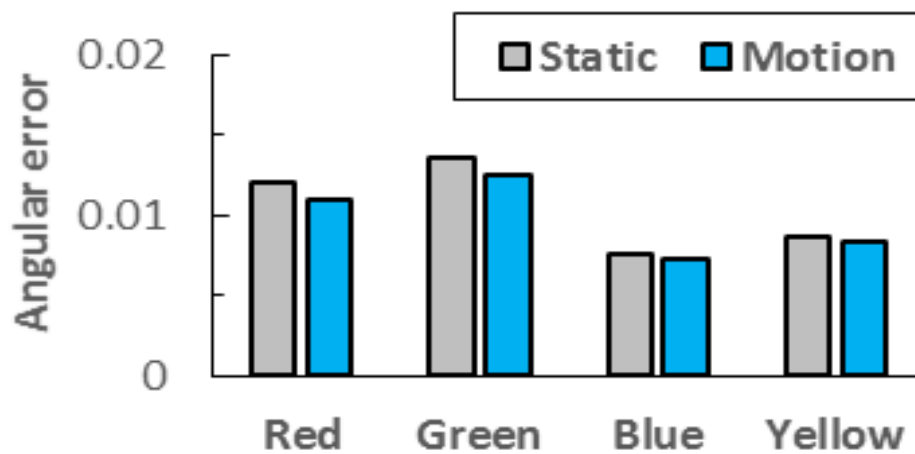
Figure 4. 5 Angular error calculated by Ebner's model. Gray bars and blue bars denote static and motion conditions, respectively.

4.1.2 Double-opponency model

The double-opponent (DO) color sensitive cells in the primary visual cortex (V1) of the human visual system have been recognized as one of the important reason for color constancy. The hypothesis is based on that the responses of DO cells to the color –biased images provide clear information about the scene illuminant. Thus, we use the double opponency model by Gao (2015) to simulate this experiment.
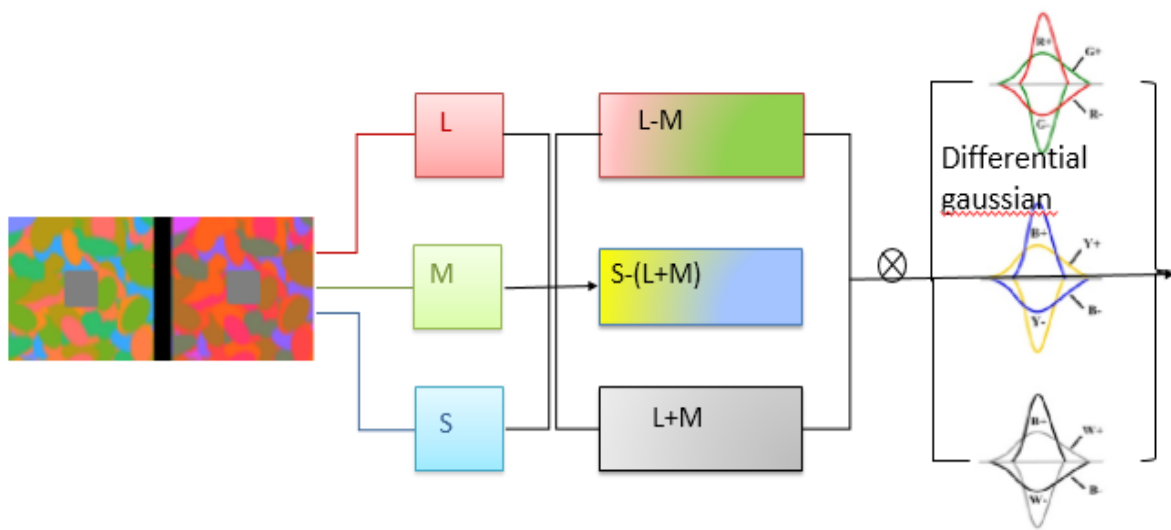
Figure 4. 6 Double opponency model for color constancy. First, the stimuli transfer from LMS-cone to ganglion layer and LGN as red-green (L-M), blue-yellow(L+M-S) and luminance (L+M) channels, and then propagated to double-opponent cell in V1 by convolution with a Difference-of-Gaussian function.

The color information received by the retina first transfer to L-, M- and S-cones in a trichromatic way, and then propagated to the retinal ganglion layer and LGN via single-opponent neurons, then responds in V1 by double-opponent neurons. We simulated this process by using double-opponency model: the image is first transformed to cone's LMS space. Then, the signal transformed from LMS space to the L-M (red-green), L+M-S (blue-yellow) and L+M (luminance) channels , we call it the Single-Opponent (SO) space.

$$\begin{bmatrix} o_{lm} \\ o_{ys} \\ o_{b+} \end{bmatrix} = \begin{bmatrix} 1 & -1 & 0 \\ 1 & 1 & -1 \\ 1 & 1 & 0 \end{bmatrix} \begin{bmatrix} l \\ m \\ s \end{bmatrix}, \begin{bmatrix} o_{ml} \\ o_{sy} \\ o_{b-} \end{bmatrix} = - \begin{bmatrix} o_{lm} \\ o_{ys} \\ o_{b+} \end{bmatrix} \qquad (4\text{-}7)$$

The Single-Opponent (SO) cell was found in ganglion layer and LGN and responds at the lowest spatial frequencies by Johnson(2008). The SO codes the color information within their receptive fields (RFs) in the way of red-green, blue-yellow and black-white opponency, although recently black and white are not considered as color opponent from the literature written by

Shinomori(1994,1997). The RF spatial structure of each component of a type-II SO cell is described as a gaussian function,

$$RF(x, y, \delta) = \frac{1}{2\pi\delta^2} e^{\frac{x^2+y^2}{2\delta^2}}$$

(4-8)

For example, the response of SO cell with red-on/green-off (L+M-) opponency is given by SOl+m-(x, y; δ):

$$SO_{l+m-}(x, y; \delta) = O_{lm}(x, y) \otimes RF(x, y; \delta)$$

(4-9)

where $\otimes$ denotes the convolution, SOm+l-(x, y; λδ) is computed for green-on/red-off SO cells, and SOs+y-(x, y; δ) and SOy+s-(x, y; λδ) for the response of blue-yellow SO sells, SOb+(x, y; δ) and SOb-(x, y; λδ) for the response of brightness-sensitive cells, and the signs, '+' and '-' denote the excitation and inhibition, respectively.

In V1 layer, most Double-opponent (DO) cells are found orientation-selective for both achromatic and chromatic stimuli, and they would be approximated as a Difference-of-Gaussian function, Shapley (2011). The response of a double opponent cell (DO) is computed as

$$DO_{lm}(x, y) = SO_{l+m-}(x, y; \delta) + k1 \cdot SO_{m+l-}(x, y; \lambda\delta)$$

(4-10)

$$DO_{sy}(x, y) = SO_{s+y-}(x, y; \delta) + k2 \cdot SO_{y+s-}(x, y; \lambda\delta)$$

(4-11)

$$DO_b(x, y) = SO_{b+}(x, y; \delta) + k3 \cdot SO_{b-}(x, y; \lambda\delta)$$

(4-12)

The size of RF surround is roughly 3 times larger than the RF center, so here we set λ =3, δ =10, k1, k2 and k3 are the reletive cone weights that control the contribution of the RF surround, here 0<k1, k2 ,k3 <0.1 Then obtain reflectance estimates, $\vec{R}$ as

$$\vec{R} = \begin{bmatrix} DO_{lm} \\ DO_{sy} \\ DO_b \end{bmatrix}$$

(4-13)

The angular error is defined as Eq. (9), Rd is the estimated reflectance under illuminant D65, Re is the estimate under a non-standard illuminant. Figure 4.7 shows the angular error, e between the estimated reflectance under a standard D65 illuminant and a non-standard illuminant obtained from the modified Double opponency model. From this simulation result, the angular error of the motion is smaller than that in the static condition, and the order of the angular error is Blue ≒ Yellow < Red ≒ Green. Although the color constancy in the motion is better than that in the static condition, the difference is still small. The adaptation effect to the color constancy itself cannot explain the entire results. The difference of the color constancy in this study should mainly be ascribed to the illumination estimation effect.
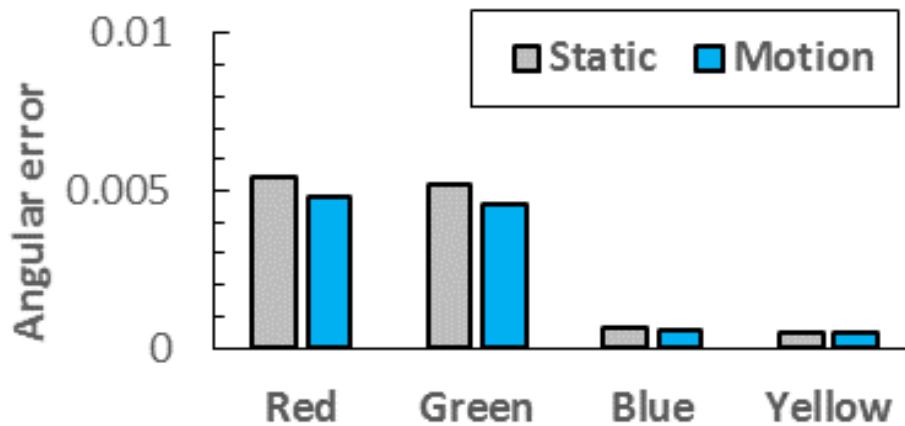
Figure 4. 7 Angular error for Double opponency model. Gray bars, blue bars represent target-static, target-motion conditions, respectively

4.2 Effect of motion to color constancy

The results of this asymmetric color matching experiment indicate that the motion of the target could not improve the color constancy, rather the motion averagely decreased the color constancy. The free eye movement increased the color constancy by the better attention, which is conform to the previous studies Golz(2010), but the difference was not statistically significant. The comparison of the results between eye-fixation and eye-free conditions indicates that in eye-free condition, the observers could pay more attention to the colors of the surround and the color constancty was determined more dominantly by the illumination estimation. Thus, the color constancy in the eye-free condition was better than that in the eye-fixation condition. There are several studies shows that the color constancy in the paper match is better than that in the appearance match reported by Bäuml (1999), Arend and Reeves(1986,2001); the possible reason is that the illumination estimation effect is stronger in the paper match and the appearance match is more influenced by the induction and adaptation with the weaker illumination estimation effect. The amount of the color constancy in four illuminations was in the order of green > red > yellow > blue. The difference of the illumination were significant between red & blue, green & blue, and green & yellow illuminants.

The results in this study have some potential association with the result of previous studies from Werner (2007) and Hurlbert (2004) and Pearce and Hurlbert (2014). Werner (2007) found that the color constancy was improved when the object moved in the achromatic adjustment experiment. The result might be caused that such kind of experiment involved less memory contribution and the

illumination estimation effect was little required in the task; thus, the main effect contributing to the color constancy could be the induction and adaptation.

Hurlbert (2004) reported that the induction of the moving target is stronger than that in the stationary condition. However, in the simultaneous asymmetric matching experiment in this study, the observers could see the two illuminant background simulteniously; it means that the observer had a very accurate memory of the color in different illuminations, causing that the observers could use more the illuminant estimation strategy in this situation. In addition, as descibed in the previous subsection, the target in the motion could have the stronger induction and adaptation; it could increase the color bias of the test target. Hurlbert (2004) also found that the strength of contrast induction was weakened in the order of blue > yellow > red > green substantially, and the induction of a blue-yellow texture is stronger than a red-green texture. Conversly, in this study, the observer needed to estimate illumination and had to offset the bias color caused by the induction and adaptation; it means that the illumination with high induction and adaptation may involve the poorer color constancy.

As reported by Pearce and Hurlbert (2014), the ability to discriminate highly-chromatic illuminations may involve strong estimation effect. The results in this study also correspond to the result in the previous study from Pearce and Hurlbert (2014) showing that chromatic illumination discrimination ability of blue is poorest and green is best .

In our study, the color constancy depends on both the illumination estimation effect and the von Kries type adaptation effect; the difference of influences between conditions could be explained by stronger contribution of the illumination estimate/ion effect to the color constancy. However, in the most of natural environments, the color constancy is more influenced by the adaptation and induction effect with less contribution of the illumination estimation effect. Thus, the human color constancy is optimised for blue daylight illumination (Pearce and Hurlbert ,2014) except in the situation that the observers retain good memory and can do better illumination estimation.

4.3 Limitation of this study

In this study, the experiments were conducted in the two-dimensional multi-element background, and the result has some differences with the previous literature of Delahunt(2004), which was performed in the three-dimensional background; the three dimensional background may involve some more information to contribute to the color constancy. The second limitation of this study is the limited color range of the color gamut of the CRT monitor. Because the color difference of the four

illuminations to D65 was limited, the difference of the matched points predicted by the reflectance model and obtained just by the D65 background (no color constancy) were not obviously different especially in the blue and yellow illuminants. It may cause the matched points conforming to the von Kries model or to no color constancy; if we will increase the color difference of the illumiants in the simulation, the observers will have to conduct the illumination estimation for the matching. These limitations have to be investigated in the future.

Chapter5

ipRGC experiment

5.1 Introduction

As we know, there are two systems detecting light in mammals and humans. The first one is the classical visual system responsible for image formation, and the second one is the non-image-forming (NIF) system which detects environmental irradiance and contributes to modulation of many fundamental functions (review of Daneault,2016). Human retinas contain four types of classical photoreceptors for image forming or visual processing, including rods, short-wavelength-sensitive (S-) cones, middle-wavelength-sensitive (M-) cones, and longwavelength-sensitive (L-) cones. At photopic light levels, rods are saturated, and visual perception is mediated by S-, M-, and L-cones. There are at least three physiologically and anatomically distinct pathways in primate vision, include a magnocellular pathway which is fast, high-contrast sensitivity, low-spatial resolution; and a chromatic parvocellular pathway which is slower, high-spatial resolution; a koniocellular pathway which is color-opponent and slow, with poor spatial resolution. Overlaid onto the organization of these pathways are conveyed through ON and OFF pathways, which provide excitatory responses to light increments and decrements, respectively (Schiller,1992). A number of psychophysical studies has been investigated about rod and cone TCSFs（temporal contrast sensitivity functions）, Dingcai Cao(2007) has made a summary of rod and cone TCSFs and two-pulse summation studies, as table 5.1shows.

Table 5.1 A summary of rod and cone TCSFs and two-pulse summation studies, from Cao(2007)

Study	Receptor type	Method	Adaptation level[a]	Spatial extent	Surround	Retinal locus	Pulse duration (ms)
Hess and Nordby (1986)	Rod	TCSF	0.003–130 ST	10 × 15° (0.3 cpd grating)	N/A	4°–5°	
Nygaard and Frumkes (1985)	Rod	TCSF	0.025–0.4 ST	2°	No	7°	
Smith (1973)	Rod	TCSF	0.005–50 ST	7° (0.3 cpd grating)	N/A	7°	
van den Berg and Spekreijse (1977)	Rod	TCSF	0.13 ST	5°	No	10°	
de Lange (1958)	Cone	TCSF	4.3–430 PT	2°	Yes	Fovea	
Keesey (1970)	Cone	TCSF	26–260 PT	1°	Yes	Fovea	
Kelly (1959)	Cone	TCSF	1000 PT	2°	Yes	Fovea	
Roufs (1972)	Cone	TCSF	2–525 PT	1°	No	Fovea	
Swanson et al. (1987)	Cone	TCSF	0.9–900 PT	2°	No	Fovea	
van der Gon/van der Tweel (1961)	Cone	TCSF	2–200 PT	0.37°	No	Fovea	
van Nes et al. (1967)	Cone	TCSF	0.85–850 PT	0.64 cpd grating	N/A	Fovea	
Burr and Morrone (1993)	Cone	2 Pulse	163 PT	6.25° (1 cpd grating)	N/A	Fovea	8
Herrick (1972)	Cone	2 Pulse	5.0–210 PT	1.1°	No	Fovea	5
Ikeda (1965)	Cone	2 Pulse	61.2 & 328 PT	0.5°	Yes	Fovea	12.5
Meijer et al. (1978)	Cone	2 Pulse	120 PT	1.6°	No	3.5°	10
Roufs (1973)	Cone	2 Pulse	1–120 PT	1°	No	Fovea	2–3
Shinomori and Werner (2003)	Cone	2 Pulse	49 PT	2.26° (Gaussian patch)	N/A	Fovea	1.2
Uchikawa and Yoshizawa (1993)	Cone	2 Pulse	10 PT	1.5°	No	Fovea	10
Uetsuki and Ikeda (1970)	Cone	2 Pulse	1–300 PT	0.5°	Yes	Fovea	10

[a] ST, scotopic Td; PT, photopic Td.

More recently, a new type of photoreceptor, called intrinsically photosensitive retinal ganglion cells (ipRGCs), was discovered in mammalian inner retinas (Berson, Dunn, & Takao, 2002; Hattar, Liao, Takao,Berson, & Yau, 2002). ipRGCs can potentially combine the inputs from S-, M-, and L-cones, rods and melanopsin at some light levels(Dacey,2005), and support various accessory visual functions including circadian photo entrainment (Hattar,2003; Ruby, 2002) and pupillary reflexes(Clarke,2003; Lucas 2003). Melanopsin ipRGC have a low spatial resolution and long latencies as compared to cone and rod responses, and they show the ability integrate photic energy over long periods of time(Provencio,2000;Panda,2002;Hattar,2002;Berson 2002). ipRGC play a role in conscious perception of spatial brightness and speed motion (Zhao,2014; Dacey,2005; Esteves,2012; Storchi,2015). Tsujimura (2010) reported that the ipRGC signals contribute to the pupillary response by a factor of three times more than the classic photoreceptor cells. Rao (2016) derived a formular for pupil size according to the linear summation of cirtopic and photopic luminance. ipRGC cells interacted with rods and cones, which provide inputs to the postreceptoral visual pathways, contribute to the classical visual system (Zhao,2014; Brown,2010; Schmidt,2011; Esteves,2012).

To study these photoreceptors for vision processing, scientists developed several kinds of systems such as three-primary color displays(Brainard, Pelli, & Robson, 2002), DLP projectors, (Packer et al., 2001),which is based on the trichromatic theory, LED-based four-primary(Tsujimura,2010,show in

figure 5.2), LED-based five-primary photostimulator system(Ding cai Cao, 2015, show in figure 5.3), the problem is that these systems did not isolate ipRGC, or could not show special shape of stimulus. So a new method is required to study photopic vision.
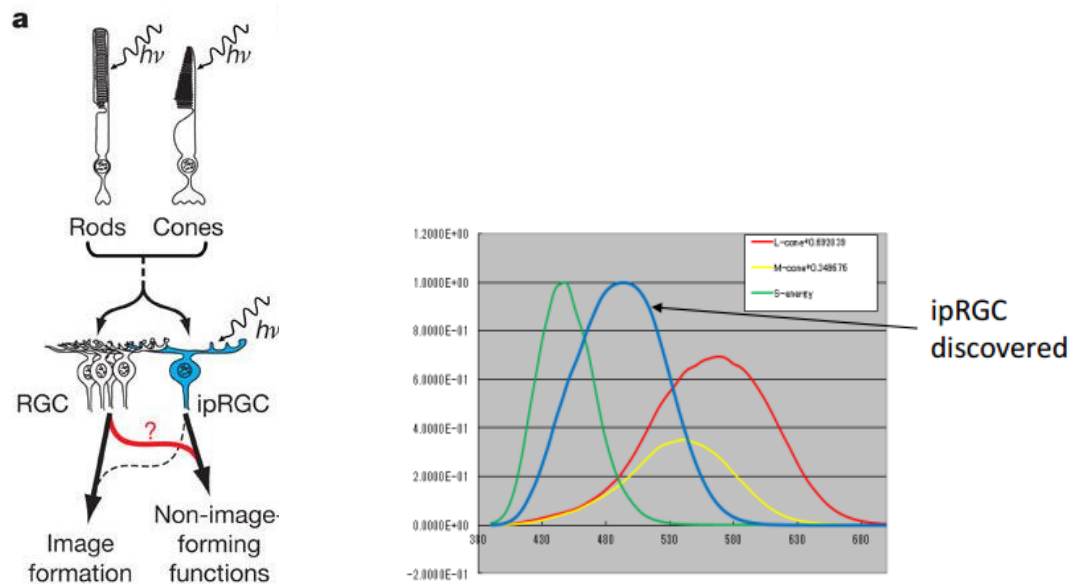
Figure 5. 1 Left figure is rod–cone signalling through conventional RGCs or ipRGCs contributes to NIF functions. From Ali(2008). Right figure is ipRGC,L,M,S sensitive response spectrum.
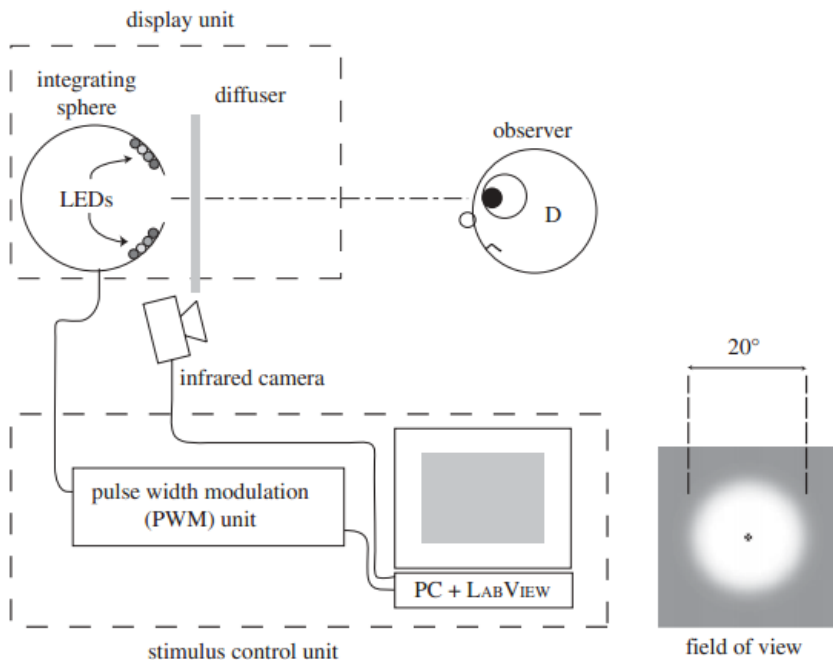
Figure 5. 2 A personal computer and an interface board controlled a four-primary illumination system from Tsujimura(2010). The illumination system consisted of an optical diffuser and an integrating sphere which presented a 20 8 circular field onto the optical diffuser. The luminance output of each LED was controlled by analogue pulse width modulation (PWM) units by adjusting a duty cycle of pulse train.

Dingcai Cao (2015) showed that the S-cone input to pupil responses was antagonistic to the L-, M-

or melanopsin inputs, consistent with an S-OFF and (L + M)-ON response property of primate ipRGCs (Dacey et al., 2005). In addition, the melanopsin-mediated TCSF had a distinctive pattern compared with L+M or S-cone mediated TCSF, they used an LED-based five-primary photostimulator that can control the excitations of rods, S-, M-, L-cones, and melanopsin-containing ipRGCs in humans at constant background photoreceptor excitation levels.

(a)　　　　　　　　　　　　　　　　(b)

(c)
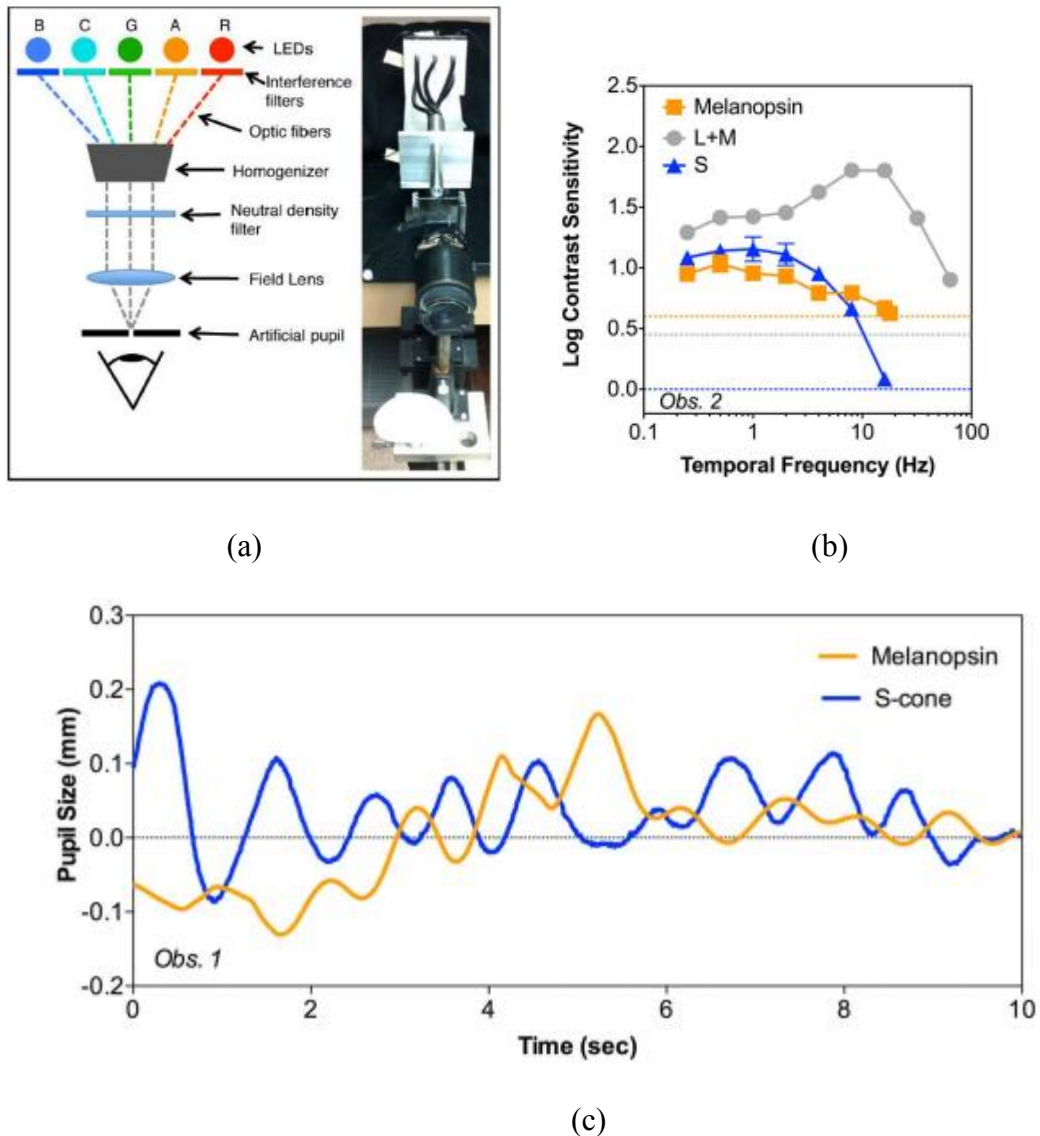
Figure 5. 3 (a)The optical layout and picture of the five-primary photostimulator (Ding cai Cao, 2015)(b) Temporal contrast sensitivity functions (TCSFs) for the melanopsin (orange symbols), L+M (gray symbols), or S-cone (blue symbols) modulation at 2000 Td for one observer (Obs. 2).The error bars, which are typically smaller than the symbol sizes, represent the SEMs from three measurements. The orange, gray, and blue dashed lines indicate the instrument gamuts for the melanopsin, L+M, an d S contrast sensitivities, respectively, meaning for a specific modulation.(c) Representative pupil traces during the first 10 s with the S-cone (blue line) and melanopsin (yellow line) modulations (16% Michelson contrast, 200 Td) recorded during the same session from one observer (Obs. 1), after removing the steady pupil size (4 mm).

　　Later, Barrionuevo (2016) reported that Melanopsin activation combined linearly with luminance, S-cone, and rod inputs, suggesting the locus of integration with MC and KC signals was retina, the

melanopsin contribution to phasic pupil responses was lower than luminance contributions, but much higher than S-cone contributions.

So the TCSF of ipRGC still need to be investigated. Here, we used a four-primary photostimulating method by using three projectors that allows control of the stimulation of ipRGC and of the three types of cones independently at the same chromaticity, retinal locus, and light level，and its theoretical basis is silent substitution to ensure the isolation of each photoreceptor class. The silent-substitution technique used as selective stimulation of each photoreceptor type is required, although selectivity is difficult when spectral sensitivity curves for each photoreceptor overlap. Projectors are a good choice to use as visual stimulation light sources because it can display any special shape of stimulus for image forming system.

In this chapter, temporal impulse response functions (IRFs) were measured to investigate the temporal characteristics of contrast detection of ipRGC in human vision. The IRFs were estimated using models from sequential double-pulse thresholds measured by the staircase method.

5.2 General methods

5.2.1 Apparatus and calibration

All experiments were performed in a darkened room. Stimuli were presented by the four primaries system. This four primaries system is built up by three projectors provided 12-bit resolution for each RGB channel in 1024×768 resolution under 60 Hz frame rate, controlled by a computer with the software made of Microsoft Visual Studio 2013 and OpenGL. Three kinds of narrow-band interference filters (the transmittance of the light spectrum band is nm- nm, nm- nm, nm- nm respectively) of green and yellow and the color of mixture of red and blue, were fixed in front of the lens of the three projectors respectively, the lights of the stimuli projected from the three projectors focus on the same space of an diffuser plate, The observer was situated 30 cm from the diffuser plate, and viewed with his/her head supported by a chin rest. The handheld 4-button box was used for observer's response.
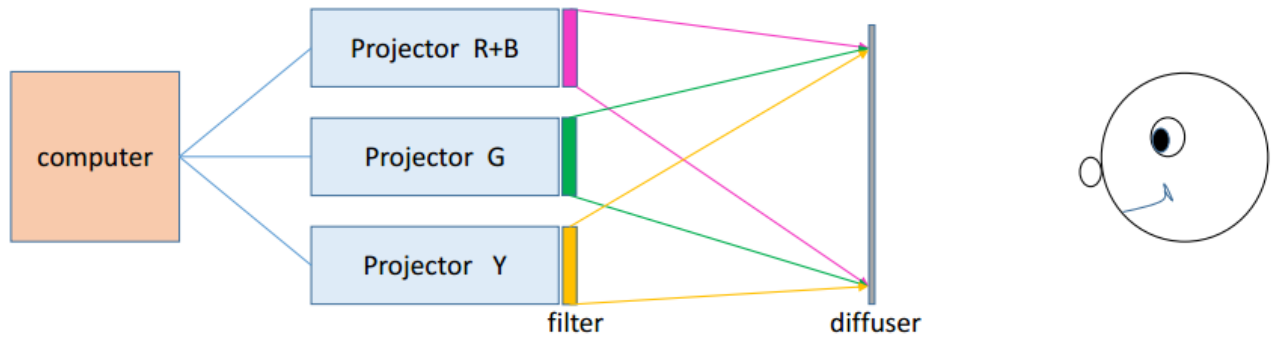
Figure 5. 4 the system of four-primary syetem

The spectral distribution of each projector combined with the interference filter was measured with the CA-2000 spectroradiometer. A 4*4 matrix which can transform R, G, B, Y to L, M, S, ipRGC was calculated. The linearization function for each projector was obtained through spectrum radiance measurements for 4096 digital levels and for each projector by CA-2000, confirmed that the error of screen presentation was less than 3% in CIE1931 xy chromaticity coordinates, and less than 5% in luminance. The luminance of the each pixel on the projected screen was also calibrated by a CCD spectrometer, confirmed that the error of each pixel was less than 5% in luminance. For periodic stimuli, the maximal Michelson contrast of S-, M-, L-cone, and melanopsin modulation was 18%, 9%, 11%, 30%, respectively.

Rise and fall times of the projectors were measured using a pin 10 silicon photodiode (Radiometer/Photometer Model 550, EG&G Gamma Scientific Inc.) connected to a digital oscilloscope. Intensity increments and decrements were approximately 1.2 ms for all phosphors. Since the diameter of the Gaussian patch at 1 SD was 45 pixels on a 512*384 pixel display, the decay of the test stimulus at the vertical scan frequency was less than 1.5 ms from the maximum. The peak-to-peak timing error of the ISI was less than 3%.

5.2.2 Visual Stimulus

The stimuli in the present study had a circular shaper with a 2-D Gaussian shape, two kind of contrasts used to simulate the high contrast and the low contast ipRGC, as defined in the following equation:

$$ipRGC_{low}(x,y)=G(x,y)*M_{lowcontrast} \qquad (5\text{-}1)$$

$$ipRGC_{high}(x,y)=G(x,y)*M_{highcontrast} \qquad (5\text{-}2)$$

$M_{lowcontrast}$ and $M_{highcontrast}$ is the amplitude of the Gaussian function, it was adjusted between 0 and 1 for the contrast stimuli of ipRGC, and $M_{lowcontrast} < M_{highcontrast}$. High contrast ipRGC of double-pulse stimuli $ipRGC_{high}$ (x,y)were presented in one of four quadrants defined by a central fixation

cross on a background. And low contrast ipRGC of double-pulse stimuli ipRGC$_{low(x,y)}$were presented in other three of four quadrants.

Backgound stimuli is sinusoidal modulated temperal Gaussion function constructed by L,M,S cone contrast together, as defined in the following equation:

$$L= G(x,y)*sin(i-Pi/2)*a$$
$$M= G(x,y)*sin(i-Pi/2)*b \qquad (5\text{-}3)$$
$$S= G(x,y)*sin(i-Pi/2)*c$$

Here i is the frame number of the temperal Gaussion function, Pi is ratio of circumference to diameter. a, b, c is a constant parameter to make the background the same chromaticity as the stimulus (equal-energy-white). The background stimuli were presented in each four quadrants overlapped with the ipRGC stimuli. G (x, y) is a 2-D normal distribution (Gaussian distribution) function with a ±3SD in visual angle. Stimulus signals are illustrated in Figure5. 5.

Both the width and height of the center cross were 2 dgree in visual angle. The four stimuli were alternately located 0.71° to one side or the other and 0.71° above or below the center of the fixation cross. The background was approximately 11 ° in width and 8 ° in height. In double-pulse method, the contrast threshold is commonly measured as the detection threshold. Figure 5.5 shows the sinusoidal modulated temperal background luminance contrast and ipRGC in high level and low level contrast stimuli.
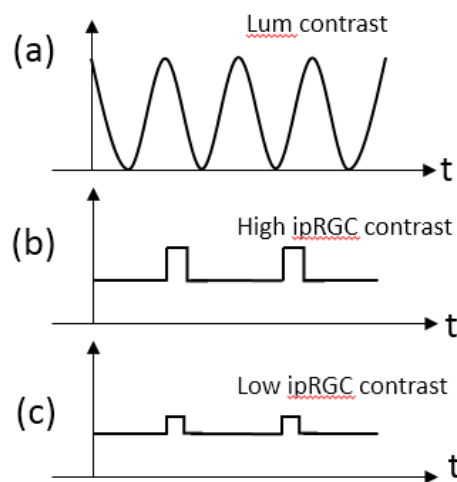
Figure 5. 5 (a) Sinusoidal modulated temperal background stimuli (b) High level contrast of double impulse ipRGC (c) Low level contrast of double impulse ipRGC

5.2.3 Procedure

We tested contrast stimulus configurations as show in figure5.6. Each configuration included

stimuli with 7 different ipRGC contrast. (10%,30%,50%, 70%, 80%, 90%, 100%). Each contrast condition included 14 ISIs:16.7, 33.4, 50.1, 66.8, 83.5, 100.2, 116.9, 133.6, 150.3, 167, 217.1, 267.2, 334, and 417.5 ms (in terms of the number of frames, 1, 2, 3, 4, 5, 6, 7, 8, 9, 10, 13, 16, 20, and 25 frames (16.7 ms/frame)). These ISI settings were presented in pseudo-random order. For each ISI, the detection threshold in the log contrast energy was determined by the staircase method. The staircase method is a classic method to measure threshold. The two-down-one-up (2d1u) staircase method is used here. From an initial intensity value above the preset threshold value, decrease the intensity value of stimulus with certain step after two correct answers and increase the intensity value after one incorrect answer. The step is usually big at initial trials and is small at later trials. The point where the intensity changes direction is called the turning point (see Figure 5.6). After achieving a certain number (e.g. 6) of turning point, the procedure will finish. The estimated threshold value is the mean of last four turning point.

Figure 5. 6 The staircase procedure. The abscissa is the number of trials and the ordinate is the intensity of stimulus. The lled circles indicate correct answers and the empty circles indicate incorrect answers. Points marked by red circles are the turning points.

Figure 5. 7 Frame sequence of one trial. The gray rectangles indicate frames displayed. From left to right, the first, third, and fifth frames are background frames, and the second and fourth frames are stimulus of ipRGC frames. Two beeps were presented to alert participants at the beginning of a trial, and a single be ep provided feedback

5.2.4 Instruction

A four-alternative forced-choice procedure with feedback was used. The observer was asked to present one of four buttons corresponding to the quadrant in which the stimulus of high contrast ipRGC was detected.

5.2.5 Observers

Six observers (male and female) in the age from to years old participated in this study. We confirmed that all observers had normal or corrected-to-normal visual acuity better than 0.6 (1.67 min. of visual angle) and they had normal color vision assessed by Ishihara-plate and D-15 tests. The procedures and experiments conform to the principles expressed in the Declaration of Helsinki and were approved by Kochi University of Technology Research Ethics Committee. Written informed consent was obtained prior to testing.

Appendix

A. Differences of observers

There are two groups of observers : one group is Golden white dress group, the other group is Black blue dress group.
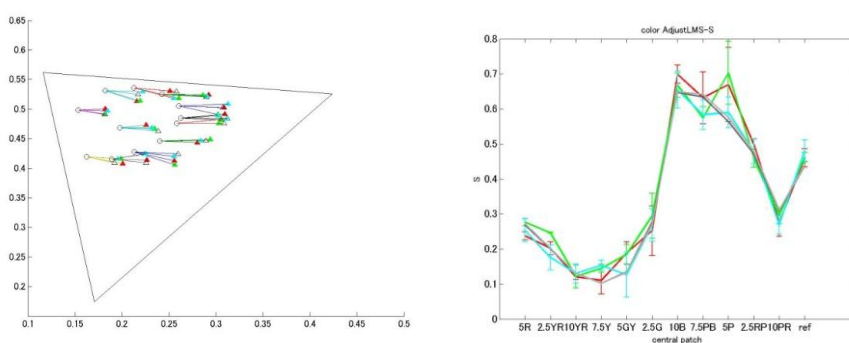
Figure A.1 Match data from Shaou, left side is1976 u'v' data. Right side is reponse of S cone.
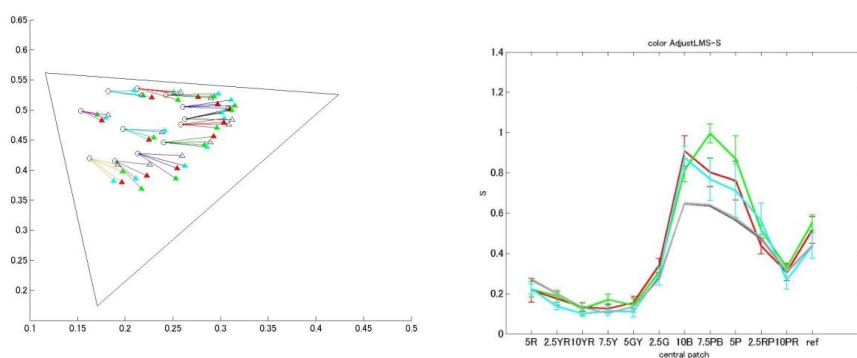
Figure A.2 Match data from Liuli, left side is1976 u'v' data. Right side is reponse of S cone.

B. Adaptation and induction experiment

Motion objects can change the retinal adaptation, this study aims to investigate about the adaptation color on the motion objects. In this experiment, a 1.5*4 deg base color rectangular (one of 12 colors) at center surrounded by random positioned background ellipses. Five illuminations were used for the background, which is red, green, blue, yellow and D65. A motion objects with gray color travels from right side to left side and passed through the base color rectangular in cycles. Observers were asked to fixed their eyes on a gray color square of 1.5 deg which is above on the base color rectangular and make a color appearance match, adjust its color the same to the motion objects when the motion objects passed through the base color rectangular. The color and luminance of the base color rectangular has been changed in the experiments. In the match process, the cones response to the base color rectangular first and then response to the gray color of the motion object, and the adaptation and induction color could be seen on the motion objects. The match results indicate that the L, M, S cone responses of the adaptation color decreased linearly when the L, M, S cone responses of the base color rectangular has increased linearly, and the L, M, S cone response of adaptation color increased linearly when the responses of motion target has increased linearly, this result could explain von kries model. And under different illuminations, all the adaptation colors have a bias to the complementary direction of the illumination colors, it is a reason for color constancy. The results also show that the adaptation modulation of S cone was larger than M and L cone, this could help to explain the reason that constancy and adaptation is better under blue illuminants rather than other colors.
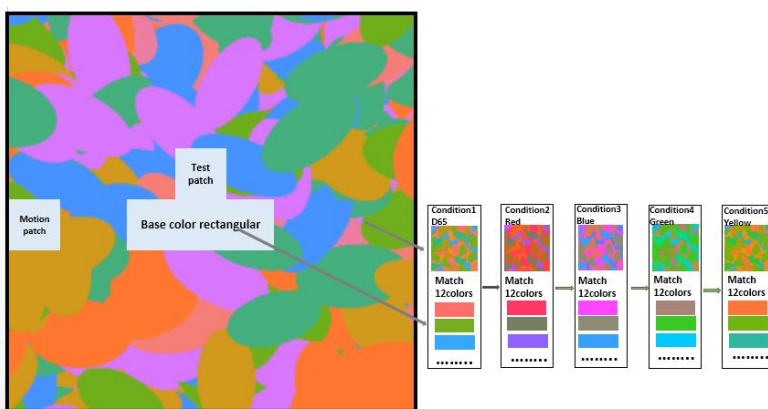
Figure B.1 Stimuli
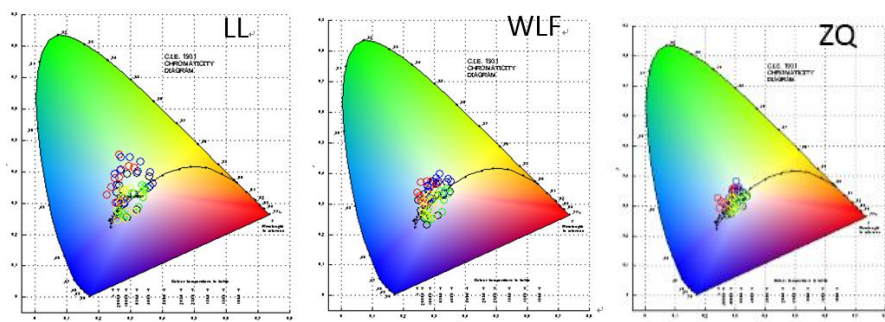
Figure B.2 Match result of x,y coordinate show in CIE.

Figure B.3 Original test colors(upside) and adaptation result(bottom).
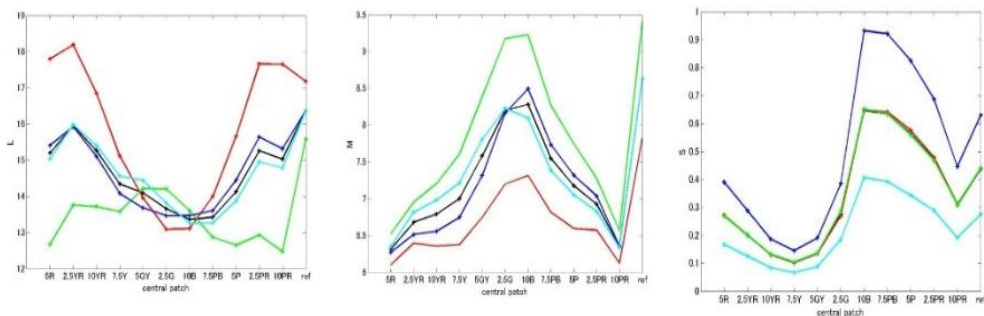
Figure B.4   L,M,S cone response of standard color

L cone response of matched color

M cone response of matched color

S cone response of matched color

L cone response of matched color divided by theory color

Mcone response of matched color divided by theory color

S cone response of matched color divided by theory color
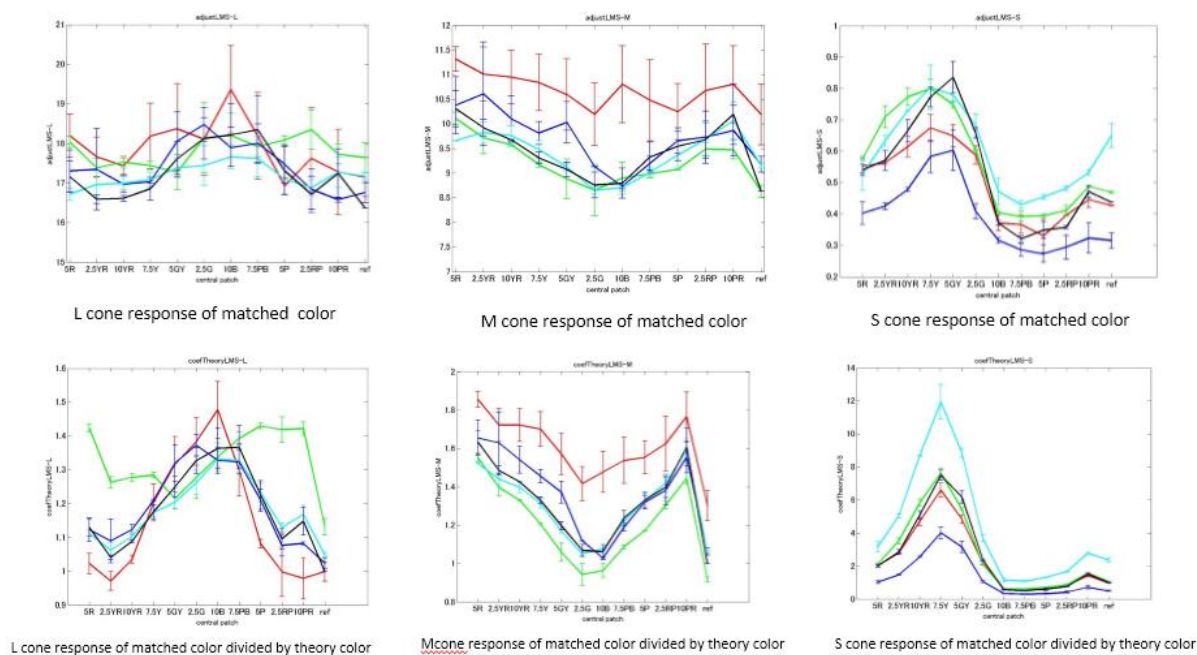
Figure B.5 Up figure shows match result of L, M, S cones.Bottom figure show the L, M, S cone response of matched color divided by theory color.
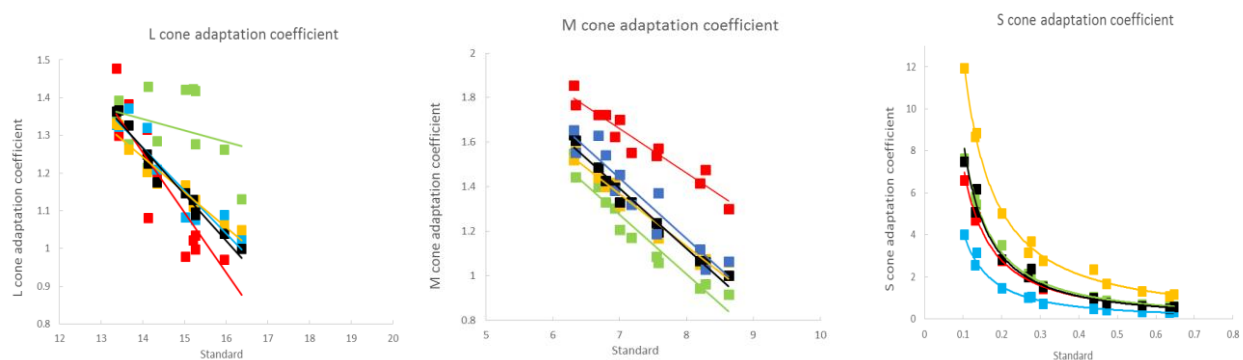
Figure B.6 show the L, M, S cone response of matched color divided by theory color.

Bibliography

Allen, E. C., Beilock, S. L., and Shevell, S. K. (2012). Individual differences in simultaneous color constancy are related to working memory.J. Opt. Soc. Am. A, 29(2):A52–A59.

Amano, K., Foster, D., and Nascimento, S. (2003). Red-green colour deficiency and colour constancy under orthogonal-daylight changes.

Amano, K., Foster, D. H., and Nascimento, S. M. C. (2006). Color constancy in natural scenes with and without an explicit illuminant cue.Visual Neuroscience, 23:351–356.

Arend, L. E. and Reeves, A. (1986). Simultaneous color constancy.J. Opt. Soc. Am. A, 3(10):1743–1751.

Arend, L. E., Reeves, A., Schirillo, J., and Goldstein, R. (1991). Simultaneous color constancy: papers with diverse munsell values.J. Opt. Soc. Am. A, 8(4):661–672.

An,X.,(2012).Distinct Functional Organizations for Processing Different Motion Signals in V1, V2, and V4 of Macaque. The journal of Neuroscience,32(39),13363-13379.

Baraas, R. C., Foster, D. H., Amano, K., and Nascimento, S. M. C. (2004). Protanopic observer-s show nearly normal color constancy with natural reflectance spectra. Visual Neuroscience,21:347–351.

Baraas, R. C., Foster, D. H., Amano, K., and Nascimento, S. M. C. (2006). Anomalous trichromats' judgments of surface color in natural scenes under different daylights. Visual Neuroscience, 23:629–635.102

Baraas, R. C., Foster, D. H., Amano, K., and Nascimento, S. M. C. (2010). Color constancy of red-green dichromats and anomalous trichromats. Investigative Ophthalmology & Visual Science,51(4):2286–2293.

Bäuml, K. (1999a). Color constancy: the role of image surfaces in illuminant adjustment.J. Opt.Soc. Am. A, 16(7):1521–1530.

Bäuml, K. (1999b). Simultaneous color constancy: how surface color perception varies with the illuminant. Vision Research, 39(8):1531 − 1550.

Brainard, D. and Wandell, B. (1992). Asymmetric color matching: how color appearance depends on the illuminant.J. Opt. Soc. Am. A, 9(9):1433–1448.

Brainard, D. H. (1998). Color constancy in the nearly natural image. 2. achromatic loci.J. Opt.Soc.

Am. A, 15(2):307–325.

Brainard, D. H., Brunt, W. A., and Speigle, J. M. (1997). Color constancy in the nearly natural image. 1. asymmetric matches. J. Opt. Soc. Am. A, 14(9):2091–2110.

Breneman, E. (1987). Corresponding chromaticities for different states of adaptation to complex visual fields.J. Opt. Soc. Am. A, 4(6):1115–1129.

Burnham, R. W., Evans, R. M., and Newhall, S. M. (1957). Prediction of color appearance with different adaptation illuminations.J. Opt. Soc. Am., 47(1):35–42.

Buchsbaum, G. (1980). A spatial processor model for object colour perception. Journal of the Franklin Institute,310, 1-26.

Chichilnisky, E. J. and Wandell, B. A. (1995). Photoreceptor sensitivity changes explain color appearance shifts induced by large uniform backgrounds in dichoptic matching.Vision Research, 35(2):239 – 254.

C.Cavina-Pratesi.(2009).Seperate processing of texture and form in the ventral stream: evidence from fMRI and visual agnosia.Cerebral Cortex 20:433-466.

Delahunt, P. B. and Brainard, D. H. (2004a). Color constancy under changes in reflected illumination. Journal of Vision, 4(9).

Delahunt, P. B. and Brainard, D. H. (2004b). Does human color constancy incorporate the statistical regularity of natural daylight? Journal of Vision, 4(2).

David J. Fleet，Peter E. Hallett，Allan D. Jepson．Spatiotemporal inseparability in early visual processing[J]．Biological Cybernetics，1985，52（3）：153-164

Ebner, M. (2011). On the effect of scene motion on color constancy. Biol. Cybern. 105, 319–330.

Ebner, M. (2009) .Color constancy based on local space average color. Mach Vis Appl J 20,283-301.

Ebner, M. (2007).Color constancy. Wiley, 30-31.

Fairchild, M. D. and Lennie, P. (1992). Chromatic adaptation to natural and incandescent illuminants.Vision Research, 32:2077–85.

Fairchild, M. D. and Reniff, L. (1995). Time course of chromatic adaptation for color-appearance judgments. J. Opt. Soc. Am. A, 12(5):824–833.

Foster, D., Amano, K., and Nascimento, S. (2001a). How temporal cues can aid color constancy. Color Research and Application, 26:S180–S185.

Foster, D. H., Amano, K., and Nascimento, S. (2001b). Colour constancy from temporal cues:

better matches with less variability under fast illuminant changes.Vision Research, 41(3):285 –293.

Foster, D. H., Amano, K., and Nascimento, S. M. C. (2006). Color constancy in natural scenes explained by global image statistics.Visual Neuroscience, 23:341–349.

Foster, D. H. and Nascimento, S. M. C. (1994). Relational colour constancy from invariant cone-excitation ratios. Proceedings of the Royal Society of London. Series B: Biological Sciences, 257(1349):115–121.

Foster, D. H., (2011). Review: color constancy, Vis. Res. 51, 674 –700.

Funt, B. , Barnard, K. , Martin, L. (1998) .Is machine colour constancy good enough. In: H. Burkhardt, B. Neumann (eds), Fifth European Conference on Computer Vision(ECCV'98), Freiburg, Germany, Springer-Verlag, Berlin, pp445-459 .

Fleming, Roland W., Dror, Ron O.,(2003) Real-world illumination and the perception of surface reflectance properties. Journal of vision,3(5):347-368

Gao, S. B. (2015). Color constancy using double-opponency. IEEE Transactions on Pattern Analysis and Machine Intelligence,37, 1973-1985.

Goddard, E., Solomon, S., and Clifford, C. (2010). Adaptable mechanisms sensitive to surface color in human vision.Journal of Vision, 10(9).

Golz, J. (2008). The role of chromatic scene statistics in color constancy: Spatial integration. Journal of Vision, 8(13).

Golz, J. and MacLeod, D. I. A. (2002). Influence of scene statistics on colour constancy.Nature, 415:637–640.

Golz, J. (2010). Colour constancy: Influence of viewing behaviour on grey settings. Percept. 39, 606–619.

Granzier, J. J. M., Brenner, E., Cornelissen, F. W., and Smeets, J. B. J. (2005). Luminance-color correlation is not used to estimate the color of the illumination.Journal of Vision, 5(1).

Granzier, J. J. M., Brenner, E., and Smeets, J. B. J. (2009). Can illumination estimates provide the basis for color constancy?Journal of Vision, 9(3).

Gao Shaobing. Visual Mechanisms based color constancy model and its application image processing. Master Thesis of University of Electronic Science and Technology of China.(2013).

Hansen, T., Walter, S., and Gegenfurtner, K. R. (2007). Effects of spatial and temporal context on color categories and color constancy.Journal of Vision, 7(4).

Hedrich, M., Bloj, M., and Ruppertsberg, A. I. (2009). Color constancy improves for real 3d objects.Journal of Vision, 9(4).

Hurlbert, A. (2004). Color contrast: a contributory mechanism to color constancy. Prog. Brain Res. 144, 147-160.

Johnson, E.N. (2008). The orientation selectivity of color-responsive neurons in Macaque V1. The Journal of Neuroscience, 28, 8096-8106.

Jin, E. W. and Shevell, S. K. (1996). Color memory and color constancy. J. Opt. Soc. Am. A, 13(10):1981–1991.

Jacob Richter ，Shimon Ullman．A Model for the Temporal Organization of X-and Y-Type Receptive Fields in the Primate Retina[J]．Biological Cybernetics，1982 ，43（2）：127-145

Judd, D. B., MacAdam, D. L. and Wyszecki, G. (1964). Spectral distribution of typical daylight as a function of correlated color temperature. J. Opt. Soc. Am. 54, 1031 –1040.

Kaiser, P. K. and Boynton, R. M. (1996). *Human Color Vision*, 2nd ed. (Optical Society of America), p. 557.

Kraft, J. M. and Brainard, D. H. (1999). Mechanisms of color constancy under nearly natural viewing.Proceedings of the National Academy of Sciences, 96(1):307–312.

Kulikowski, J., Daugirdiene, A., Panorgias, A., Stanikunas, R., Vaitkevicius, H., and Murray, I.(2012). Systematic violations of von kries rule reveal its limitations for explaining color and lightness constancy. J. Opt. Soc. Am. A Opt Image Sci Vis, 29(2):A275–89.

Kuriki, I. (2006). The loci of achromatic points in a real environment under various illuminant chromaticities.Vision Research, 46(19):3055–3066.

Kuriki, I. and Uchikawa, K. (1996). Limitations of surface-color and apparent-color constancy.J.Opt. Soc. Am. A, 13(8):1622–1636.

Kulkarni, Seema G.(2014).Color constancy techniques. International Journal of Engineering and Computer Science. 3(11):9147–9150

Land. E. H. (1974) Smitty Stevens' Test of Retinex Theory. Sensation and Measurement, 363-368.

Lee, R. and Smithson, H. (2012). Context-dependent judgments of color that might allow color constancy in scenes with multiple regions of illumination.J. Opt. Soc. Am. A, 29(2):A247–A257.

Lucassen, M. P. and Walraven, J. (1996). Color constancy under natural and artificial illumination. Vision Research, 36(17):2699 – 2711.

Liao Ningfang. Digital image management technology.(2009)

Ma, R., Kawamoto, K. , and Shinomori, K., (2016). Color constancy of color-deficient observers under illuminations defined by individual color discrimination ellipsoids. J. Opt. Soc. Am. A 33, A283–A299.

McCann, John J.(2017) Retinex at 50: color theory and spatial algorithms, a review. J. Electron. Imaging 26(3) :1-14.

Munsell Color Corporation, Munsell Book of Color—Matte Finish Collection (Munsell Color Corp., 1976)

Martinovic, J., Mordal, J., and Wuerger, S. M. (2011). Event-related potentials reveal an early advantage for luminance contours in the processing of objects.Journal of Vision, 11(7).

Murray, I. J., Daugirdiene, A., Vaitkevicius, H., Kulikowski, J. J., and Stanikunas, R. (2006). Almost complete colour constancy achieved with full-field adaptation. Vision Research, 46(19):3067 − 3078.

Morimoto,T., Fukuda,K. and Uchikawa,K.(2016).Effects of surrounding stimulus properties on color constancy based on luminance balance. Journal of the Optical Society of America A,33(3):214–227

Nascimento, S. M. C., P., F. F., and Foster, D. H. (2002). Statistics of spatial cone-excitation ratios in natural scenes. J. Opt. Soc. Am. A, 19(8):1484–1490.

Nieves, J. L., García-Beltrán, A., and Romero, J. (2000). Response of the human visual system to variable illuminant conditions: An analysis of opponent-colour mechanisms in colour constancy. Ophthalmic and Physiological Optics, 20(1):44 − 58.

Olkkonen, M., Hansen, T., and Gegenfurtner, K. R. (2008). Color appearance of familiar objects: Effects of object shape, texture, and illumination changes.Journal of Vision, 8(5).

Parkkinen, J. P. S. , Hallikainen, J.,and Jaaskelainen, T. (1989). Characteristic spectra of Munsell colors. J. Opt. Soc. Am. A 6, 318 –322.

Pearce, B. , Hurlbert, A. (2014). Chromatic illumination discrimination ability reveals that human color constancy is optimised for blue daylight illuminations. Plos one 9,1-10.

Rinner, O. and Gegenfurtner, K. R. (2002). Cone contributions to color constancy.Perception, 31(6):733– 746.

Rüttiger, L., Mayser, H., Srey, L., and Sharpe, L. T. (2001). The color constancy of the red-green color blind.Color Research and Application, 26:S209–S213.

Sabbah,S.,(2013).Feedback from Horizontal Cells to Cones Mediates Color Induction and May Facilitate Color Constancy in Rainbow Trout. Plos One,8(6),1-11.

Shinomori, K. , Nakano, Y. and Uchikawa, K. (1994). Influence of the illuminance and spectral composition of surround fields on spatially induced blackness. J. Opt. Soc. Am. A 11, 2383-2388.

Shinomori, K. , Schefrin, B. E. and Werner, J. S. (1997). Spectral mechanisms of spatially induced blackness: Data and quantitative model. J. Opt. Soc. Am. A 14, 372-387.

Shapley, R., Hawken, M.J. (2011). Color in the cortex: single- and double-opponent cells. Vision Research, 51, 701-717.

Suchow, J. W. and George, A. A. (2011). Motion Silences Awareness of Visual Change. Current Biol. 21,140–143.

Smith, V. C. and Pokorny, J. (1975). Spectral sensitivity of the foveal cone photopigments between 400 and 500 nm.Vision Research, 15(2):161 – 171.

Smithson, H. and Zaidi, Q. (2004). Colour constancy in context: Roles for local adaptation and levels of reference. Journal of Vision, 4(9).

Sobagaki, H., Yamanaka, T., Takahama, K., and Nayatani, N. (1974). Chromatic-adaptation study by subjective-estimation method.J. Opt. Soc. Am. A, 64(6):743–9.

Troost, J. M., Li, W., and De Weert, C. M. M. (1992). Binocular measurements of chromatic adaptation.Vision Research, 32(10):1987 – 1997.

Troost, J. M. and Weert, C. M. M. (1991). Naming versus matching in color constancy.Perception and Psychophysics, 50:591–602.

Uchikawa, K., Fukuda, K., Kitazawa, Y., and MacLeod, D. I. A. (2012). Estimating illuminant color based on luminance balance of surfaces.J. Opt. Soc. Am. A, 29(2):A133–A143.

Uchikawa, K. , Morimoto, T. and Matsumoto, T(2017). Understanding individual differences in color appearance of "#TheDress" based on the optimal color hypothesis. J. Vis. 17(8), Article Number 10, 1-14.

Von Kries, J., (1970) .Chromatic adaptation. In Sources of Color Science ,D. L. MacAdam, ed., pp. 145–148.

Webster, M. A. and Mollon, J. D. (1995). Colour constancy influenced by contrast adaptation. Nature, 373(23):694 – 698.

Werner, J. S. and Walraven, J. (1982). Effect of chromatic adaptation on the achromatic locus: The role of contrast, luminance and background color. Vision Research, 22(8):929 – 943.

Werner, A. (2007). Color constancy improves, when an object moves: High-level motion influences color perception. J. Vis. 7(14):19, 1 – 14.

Wyszecki, G. and Stiles, W. S. (Wiley, 1982)*Color Science: Concepts and Methods, Quantitative Data and Formulae*.

Xiao Manjun. Human visual characteristics based realistic image rendition algorithms and assessment.2008. Doctoral thesis of Beijing institute of Technology.

Yang, J. N. and Maloney, L. T. (2001). Illuminant cues in surface color perception: tests of three candidate cues.Vision Research, 41(20):2581 – 2600.

Yang, J. N. and Shevell, S. K. (2003). Surface color perception under two illuminants: The second illuminant reduces color constancy. Journal of Vision, 3(5).

Zaidi, Q., Spehar, B., and DeBonet, J. (1997). Color constancy in variegated scenes: role of low-level mechanisms in discounting illumination changes. J. Opt. Soc. Am. A, 14(10):2608–2621.

ipRGC Reference

Altimus CM, Guler AD, Villa KL, McNeill DS, Legates TA, Hattar S. Rods-cones and melanopsin detect light and dark to modulate sleep independent of image formation. Proc Natl Acad Sci U S A. 2008;105(50):19998–20003.

Ali D.Guler. (2008) Melanopsin cells are the principal conduits for rod-cone input to non image forming vision. Nature 453,102-105.

Brown TM, Gias C, Hatori M, Keding SR, Semo M, Coffey PJ, Gigg J, Piggins HD, Panda S, Lucas RJ. Melanopsin contributions to irradiance coding in the thalamo-cortical visual system. PLoS Biol. 2010;8(12):e1000558.

Barrionuevo, P. A., & Cao, D. (2014). Contributions of rhodopsin, cone opsins, and melanopsin to post-receptoral pathways inferred from natural image statistics. Journal of the Optical Society of America A , 31(4), A131–A139, doi:10.1364/JOSAA.31. 00A131.

Barrionuevo, P. A., Nicandro, N., McAnany, J. J., Zele, A. J., Gamlin, P., & Cao, D. (2014). Assessing rod, cone, and melanopsin contributions to human pupil flicker responses. Investigative Ophthalmology & Visual Science, 55(2), 719–727.

Cao, D., Lee, B. B., & Sun, H. (2010). Combination of rod and cone inputs in parasol ganglion cells of the magnocellular pathway.Journal of Vision, 10(11):4,1–15, doi:10.1167/10.11.4 .

Cao, D., Nicandro, N., & Barrionuevo, P. A. (2015). A five-primary photostimulator suitable for studying intrinsically photosensitive retinal ganglion cell functions in humans. Journal of Vision, 15(1):27, 1–3, doi:10.1167/15.1.27 .

Corie Lok.(2011). Vision science: Seeing without seeing. Nature469,284-285.

Dacey DM, Liao HW, Peterson BB, Robinson FR, Smith VC, Pokorny J, Yau KW, Gamlin PD. et al. Melanopsin-expressing ganglion cells in primate retina signal colour and irradiance and project to the LGN. Nature. 2005;433(7027): 749– 54.

Ecker JL, Dumitrescu ON, Wong KY, Alam NM, Chen SK, LeGates T, Renna JM, Prusky GT, Berson DM, Hattar S. Melanopsin-expressing retinal ganglion-cell photoreceptors: cellular diversity and role in pattern vision. Neuron,2010;67(1):49–60.

Estevez ME, Fogerson PM, Ilardi MC, Borghuis BG, Chan E, Weng S, Auferkorte ON, Demb JB, Berson DM, et al. Form and function of the M4 cell, an intrinsically photosensitive retinal ganglion cell type contributing to geniculocortical vision. J Neurosci. 2012;32(39):13608– 20.

Est é vez, O., & Spekreijse, H. (1982). The ''silent substitution'' method in visual research. Vision Research , 22(6), 681–691.

Hattar S, Liao HW, Takao M, Berson DM, Yau KW. Melanopsin-containing retinal ganglion cells: architecture, projections, and intrinsic photosensitivity. Science. 2002;295(5557):1065 – 70.

Lucas RJ, Hattar S, Takao M, Berson DM, Foster RG, Yau KW. Diminished pupillary light reflex at high irradiances in melanopsin-knockout mice. Science. 2003;299(5604):245– 7.

Lucas RJ, Peirson SN, Berson DM, Brown TM, Cooper HM, Czeisler CA, Figueiro MG, Gamlin DP, Lockley SW, O ' Hagan JB, Price LL, Provencio I, Skene DJ, et al. Measuring and using light in the melanopsin age. Trends Neurosci. 2014;37(1):1–9.

Provencio I, Rodriguez IR, Jiang G, Hayes WP, Moreira EF, Rollag MD. A novel human opsin in the inner retina. J Neurosci. 2000;20(2):600 – 5.

Panda S, Sato TK, Castrucci AM, Rollag MD, DeGrip WJ, Hogenesch JB, Provencio I, Kay SA. Melanopsin (Opn4) requirement for normal light-induced circadian phase shifting. Science. 2002;298(5601):2213– 6.

Schmidt TM, Chen SK, Hattar S. Intrinsically photosensitive retinal ganglion cells: many subtypes, diverse functions. Trends Neurosci. 2011;34(11):572 –80

Schmidt TM, Do MT, Dacey D, Lucas R, Hattar S, Matynia A. Melanopsin-positive intrinsically photosensitive retinal ganglion cells: from form to function. J Neurosci. 2011;31(45):16094 – 101.

Storchi R, Milosavljevic N,   Eleftheriou CG, Martial FP, Orlowska-Feuer P, Bedford RA, Brown TM, Montemurro MA, Petersen RS, Lucas RJ, et al. Melanopsin-driven increases in maintained activity enhance thalamic visual response reliability across a simulated dawn. Proc Natl Acad Sci U S A. 2015; 112(42):E5734– 574

Tsujimura, S., Ukai, K., Ohama, D., Nuruki, A., & Yunokuchi, K. (2010). Contribution of human melanopsin retinal ganglion cells to steady state pupil responses. Proceedings of the Royal Society B, 277, 2485–2492 .

Zhao X, Stafford BK, Godin AL, King WM, Wong KY. Photoresponse diversity among the five types of intrinsically photosensitive retinal ganglion cells. J Physiol. 2014;592(Pt 7):1619 –36.